AN INTERNATIONAL FORUM FOR THE RAPID PUBLICATION OF ORIGINAL SCIENTIFIC ARTICLES DEALING WITH CHEMISTRY AND RELATED INTERDISCIPLINARY AREAS

SOUTHERN BRAZILIAN JOURNAL OF CHEMISTRY

ESTABLISHED IN 1993

VOLUME TWENTY-NINE, NUMBER THIRTY-ONE

Printed ISSN: 0104-5431 - E-ISSN: 2674-6891

DECEMBER – 2021

SOUTHERN BRAZILIAN JOURNAL OF CHEMISTRY

Volume 29 Number 31 – 2021 ISSN 0104-5431

International Cataloging Data on Publication (CIP)

SOUTHERN BRAZILIAN JOURNAL OF CHEMISTRY: órgão de divulgação científica e informativa [recurso eletrônico] / SOUTHERN BRAZILIAN JOURNAL OF CHEMISTRY – Vol. 29, n. 31 (Dec. 2021)- . – Porto Alegre: T Tchê Associated Editors, 2021 - Semestral.
Sistema requerido: Adobe Acrobat Reader.
Modo de acesso: World Wide Web:
<http://www.sbjchem.com>

Descrição baseada em: Vol. 29, n. 31 (Dec. 2021).
ISSN 0104-5431
1. Química. I. SOUTHERN BRAZILIAN JOURNAL OF CHEMISTRY.

CDD 500

Logo design by Up Logos
<https://uplogos.com.br/>

SOUTHERN BRAZILIAN JOURNAL OF CHEMISTRY

Volume 29 Number 31 – 2021 ISSN 0104-5431

SOUTHERN BRAZILIAN JOURNAL OF CHEMISTRY

ISSN - 0104-5431 (Print)
ISSN – 2674-6891 (Eletronic)
DOI: 10.48141/SBJCHEM
Digital preservation: Portico

Available at

http://www.sbjchem.com

Mission

The **SOUTHERN BRAZILIAN JOURNAL OF CHEMISTRY** is a double-blind peer review, open access, **interdisciplinary** journal dedicated to publishing high-quality content and is intended to fill a gap in terms of scientific information for Southern Brazil. We have set high standards for the articles to be published by ensuring strong but fair refereeing by at least two reviewers. The Journal publishes original research articles in all the fields of Engineering, Mathematics, Physics, Chemistry, Biology, Agriculture, Natural resource management, Pharmacy, Medicine, and others.

Occasionally the journal will include review papers, interviews, and other types of communications. It will be published mainly in English, and at present, there are no page charges.

We hope that this journal will provide a forum for the dissemination of high-quality research in Science and are open to any questions and suggestions.

The responsibility for the articles is exclusive to the authors.

Subjects List

Chemistry – All fields
Interdisciplinariry: Mathematics; Physics; Biology; Engineering; Medical Sciences; Agronomic sciences Pharmaceutical sciences

Correspondências

Av. Carlos Tarasconi, 281/202.
Bairro Sagrada Familia. CEP: 95320-000
Nova Prata – RS. Brasil.
www.sbjechem.com
southbchem@gmail.com

CONTENTS

GRAPHICAL METHOD FOR DETERMINATION OF MQ-SERIES GAS SENSOR CIRCUIT PARAMETERS FOR A STAND-ALONE GAS ALARM SYSTEM

AJIBOYE, Aye Taiwo; OPADIJI, Jaye Femi; AJAYI, Adebimpe Ruth

University of Ilorin, Faculty of Engineering and Technology, Department of Computer Engineering. Nigeria.

ABSTRACT

Background: MQ-series gas sensors belong to the metal oxide semiconductor (MOS) family of sensors that can sense the presence of many gases. These sensors find their application in gas alarm systems as key components. While necessary sensor circuit output voltage value for alarm point in a stand-alone gas alarm system is desirable, but what exact combination of the sensor circuit parameters is required? Hitherto, the determination of these circuit parameters has not been given much attention in the research community. **Aim:** the purpose of this work is to explore a structured graphical approach of determination of MQ series gas sensor circuit parameters for a stand-alone gas alarm system that yields desired sensor circuit output voltage value for the alarm point; the main objective of the study was to develop mathematical model equations that relate the: (i) sensor resistance (R_S) with the gas concentration (x) and the sensor resistance at standard calibration concentration of the sensor base gas in the clean air (R_o) and (ii) sensor circuit output voltage (V_{RL}), load resistance (R_L) and sensor resistance (R_S). It is expected from the model equations developed that graphical correlations of the sensor circuits parameters will be generated. Using these graphs for a particular case of an MQ-4 gas sensor under the influence of LPG, the parameters that yield desired sensor circuit output voltage of 2V for 1000 ppm of LPG alarm point will be determined. **Methods:** Model equations were developed for the sensor dynamics, and based on these model equations, graphs for the determination of required sensor parameters were plotted for a case of MQ-4 gas sensor response to LPG. **Results and Discussion**: The results yielded optimal values for R_O, R_S and R_L of $20k\Omega$,$30k\Omega$ and $20k\Omega$ respectively, for alarm settings of 1000 ppm and a desired sensor circuit output voltage of 2 V. Based on determined parameters, the calibration equation for determination of best concentration value for a given value of emulated LPG concentration was developed. Using the method proposed in this study makes the process of determining the MQ-series gas sensor circuit parameters less cumbersome as their value can easily be obtained from the resulting graphs. **Conclusions:** a structured graphical approach for determination of MQ-series gas sensor circuit parameters for alarm points in a stand-alone gas alarm system showed that using MQ-4 gas sensor and LPG as the target gas, and for a sensor circuit output voltage of 2 V for alarm point at 1000 ppm of LPG, the corresponding value of R_O, R_S and R_L obtained were $20k\Omega$, $30k\Omega$, and $20k\Omega$ respectively. Hence, a structured graphical approach is suitable for determining MQ series gas sensor circuit parameters for a stand-alone gas alarm system under the influence of its associated gases.

ASSESSMENT OF SERUM SCLEROSTIN LEVEL AS A BIOMARKER ASSOCIATED WITH BONE DISORDERS IN B-THALASSEMIA PATIENTS IN AL- NAJAF CITY, IRAQ

SHARBA, Intisar Razzaq, and AL-DUJAILI, Arshad Noori

University of Kufa, Faculty of Science, Department of Biology, Iraq.

ABSTRACT

Background: β-thalassemia is a blood disorder in which the body does not make hemoglobin normally. **Aim**: To assess serum sclerostin in female patients with beta-thalassemia and compare with the healthy controls and to predict its complication associated with the bone pathophysiology, for designed improvement the lifestyle goodliness for these patients. **Material and methods**: Sixty-nine female beta-thalassemia (βT) patients (54 βT major and 15 βT Intermedia), aged 8-40 years who dependent on transfused blood, and 20 healthy controls were evaluated serum sclerostin, and was examined the relationship with hematological parameters RBC, Hb, PCV, WBC, PLT, BMI, splenic status, iron, and ferritin levels. The information of beta-thalassemia patients was collected and records by the questioner. **Results**: A significantly increased serum sclerostin level (mean 26.80±0.91) pg/ml was showed in βT patients compared with the healthy controls (10.03±0.68, $p < 0.001$) pg/ml. Furthermore, a significant decrease ($p<0.05$) of the sclerostin level was observed in β-thalassemia major compared to intermedia β-thalassemia patients. Serum sclerostin level revealed a significant increase in progress age; it is highest in the age group (30-40) year as compared with age group (8-18) and (19-29) year respectively. Sclerostin showed no associations with the RBC, Hb, PCV, and significantly positively correlated ($p<0.05$) with serum iron, ferritin levels, WBC, and PLT count. Significantly higher sclerostin levels in splenectomized and underweight groups were

observed compared to unsplenectomized and normal-weight groups ($p<0.05$) of βT patients. **Conclusions:** Sclerostin plays an important role in beta-thalassemia patients and can serve as a biomarker associated with the bone pathophysiology and indicator to prevent the continuation of such serious diseases caused by iron overload in these patients.

Page – 10

COMPARISON OF TWO STAINING METHODS FOR ANODIZING IN ALLOY 6063 ALUMINUM PROFILES

PESSUTTO, Ana Carla, and JONKO, Eliena

Universidade de Caxias do Sul, Engenharia Química. Brazil

ABSTRACT

Background: Aluminum stands out for being a light, corrosion-resistant, and recyclable metal, achieving wide coverage in the market. When incorporated into alloying elements, it is possible to acquire other desirable characteristics. Alloy 6063, intended for architectural purposes, has aesthetic, structural, and strength functions. Anodized finishing is performed through an electrolytic process, ensuring a more resistant aluminum oxide film than that formed naturally. For decorative purposes, the anodic film coloration can be performed by several methodologies, in this case, for the coloration by organic adsorption, with the use of aniline, and the electrolytic coloration, composed of tin sulfate salts, both for obtaining the black color. **Aim:** Compare of two different staining methods on the surface of anodized profiles of aluminum alloy 6063. **Methods:** Profile samples were collected and tests were carried out to measure the thickness of the anodic layer, immersion tests with 3,5 percent sodium chloride, for 1000 hours, and neutral saline mist, for 600 hours. **Results and Discussion**: Both methodologies proved to be resistant to immersion tests with sodium chloride, as well as with neutral saline mist, and these tests are quite aggressive and provide corrosion of the material when not well treated. Corrosion points were only seen at the intersections performed, and in the rest of thearea, no points were detected. **Conclusions:** The result of both methodologies was positive, considering tht there was no corrosion in the tested samples, except in the intersections performed, as well as the maintenance of the color in both tested methodologies, which was not expected in the literature. For future work, it is suggested to deepen the study to perform electrochemical impedance spectroscopy tests for exaluate the strength of the anodic film and perform anodizing with the same parameters, however, with different anilines to analyze their behavior.

Page – 21

EXPERIMENTAL STUDY OF THE INFLUENCE OF TEMPERATURE ON PASTEURIZATION OF PÊRA RIO IN NATURA ORANGE JUICE

GALIASSI, Gabriela Regina Rosa, and RAMIREZ, Maribel Valverde

Universidade Federal de Mato Grosso, Faculdade de Engenharia

ABSTRACT

Background: Heat treatment is one of the most used methods to preserve food, such as orange juices, which are an excellent source of ascorbic acid. To avoid vitamin C degradation and reduce loss, fast heating is recommended. However, little is known about heat transfer during juice pasteurization. **Aim:** Therefore, this work aimed to determine the vitamin C content and the convective heat transfer coefficient in the pasteurization of orange juice. **Methods:** To perform the experiment, in the juice container, two regions were analyzed: the central region and near the wall. For the time-temperature control, thermometers were installed in the two regions mentioned. Every 120 seconds, the temperature was measured. The vitamin C content in the juice was evaluated before and after pasteurization using the iodometric method. The convective coefficient was evaluated using the method of dimensionless numbers and the experimental method. **Results and Discussion:** In pasteurization, the solution was heated to 80 °C, where heating lasted 3000 seconds and cooling for 2520 seconds. The graph showing the relationship of the convective heat transfer coefficient and temperature follows the same trend of the literature. The convective coefficient is higher in the region near the wall. As time passes and temperature decreases, the central region tends to equilibrium, and the coefficient becomes more constant. The vitamin C content remained constant before and after pasteurization. The values of the dimensionless numbers used in the calculations are in the same order of magnitude as the literature. **Conclusions:** The pasteurization did not cause ascorbic acid degradation since the heating step was fast in the heat treatment. The graphic showed that there is a dependence of

the dimensionless of temperature with the dimensionless Biot and Fourier. It was noted that studying the thermal behavior in the cooling of orange juice is extremely important to ensure its quality.

Page – 37

PREVENTION OF CANDIDIASIS IN PATIENTS USING REMOVABLE DENTURES

SEVBITOV, Andrey; DOROFEEV, Aleksey; MIRONOV, Sergey; AL-KHOURY, Samer; TIMOSHIN, Anton

I.M. Sechenov First Moscow State Medical University (Sechenov University). Russia.

ABSTRACT

Background: Despite innovations in orthopedic dentistry, the manufacture of removable dentures belongs to the most popular orthopedic care category. Removable dentures are combined stimuli that affect the mucous membrane and neuro-receptor apparatus. Acrylic plastic prostheses, widely used in prosthetic dentistry, have a negative side mechanical, chemical-toxic, sensitizing, and thermal insulating effect on oral tissue and prosthetic impression area. This is often complicated by a violation of the biocenosis of the oral cavity, the growth of pathogenic microflora that releases toxins, especially an increase in the number of yeast colonies that irritate the oral mucosa and prosthetic stomatitis. According to the WHO, one-fifth of the world's population suffers or has suffered various candidiasis forms at least once. The worldwide increase in the incidence of the disease is primarily related to the fact that this infection is opportunistic, more than half of the world's population is a carrier of fungi of this kind, i.e., in most cases, it is an endogenous infection, which makes candidiasis different from other opportunistic mycoses. **Aims:** The purpose of this study was to study the prevalence of candidiasis in patients using removable dentures and to evaluate the effectiveness and prevention of candidiasis treatment. **Methods:** 100 patients with oral candidiasis of various age groups from 45 to 65 years were observed. Of these, 60 patients with removable plate prostheses; 40 patients with partially removable prostheses. **Results and Discussion:** Chronic forms of candidiasis were diagnosed in 40 patients and with exacerbation of chronic forms of candidiasis-60 people. The number of untreated carious cavities and poor hygienic condition of the oral cavity directly affects the severity of candidiasis. Acute forms of candidiasis were observed mainly in patients with high DMF and PMA indices. The severity of candidiasis depends on the degree and duration of wearing dentures and hygienic conditions - the most severe forms of invasive candidiasis were observed in the presence of removable plate prostheses, the complete absence of teeth, and the use of a prosthesis for more than 10-15 years. A combined lesion of the oral mucosa and the red border of the lips was observed mainly in patients older than 60 years. **Conclusions:** The presence of candidiasis in the oral cavity in patients with removable plate prostheses leads to a statistically significant change in the indicators of local immunity of the oral cavity: an increase in the concentration of serum IgG and IgA and the values of the coefficient of the balance of local immunity factors.

Page – 43

TO AUTHORS

SOUTHERN BRAZILIAN JOURNAL OF CHEMISTRY

GRAPHICAL METHOD FOR DETERMINATION OF MQ-SERIES GAS SENSOR CIRCUIT PARAMETERS FOR A STAND-ALONE GAS ALARM SYSTEM

AJIBOYE, Aye Taiwo[1*]; OPADIJI, Jaye Femi[1]; AJAYI, Adebimpe Ruth[1];

[1] University of Ilorin, Faculty of Engineering and Technology, Department of Computer Engineering. Nigeria.

** Corresponding author*
e-mail: ajiboye.at@unilorin.edu.ng

Received 12 October 2021; received in revised form 19 November 2021; accepted 27 November 2021

ABSTRACT

Background: MQ-series gas sensors belong to the metal oxide semiconductor (MOS) family of sensors that can sense the presence of many gases. These sensors find their application in gas alarm systems as key components. While necessary sensor circuit output voltage value for alarm point in a stand-alone gas alarm system is desirable, but what exact combination of the sensor circuit parameters is required? Hitherto, the determination of these circuit parameters has not been given much attention in the research community. **Aim:** the purpose of this work is to explore a structured graphical approach of determination of MQ series gas sensor circuit parameters for a stand-alone gas alarm system that yields desired sensor circuit output voltage value for the alarm point; the main objective of the study was to develop mathematical model equations that relate the: (i) sensor resistance (R_S) with the gas concentration (x) and the sensor resistance at standard calibration concentration of the sensor base gas in the clean air (R_o) and (ii) sensor circuit output voltage (V_{RL}), load resistance (R_L) and sensor resistance (R_S). It is expected from the model equations developed that graphical correlations of the sensor circuits parameters will be generated. Using these graphs for a particular case of an MQ-4 gas sensor under the influence of LPG, the parameters that yield desired sensor circuit output voltage of 2V for 1000 ppm of LPG alarm point will be determined. **Methods:** Model equations were developed for the sensor dynamics, and based on these model equations, graphs for the determination of required sensor parameters were plotted for a case of MQ-4 gas sensor response to LPG. **Results and Discussion**: The results yielded optimal values for R_O, R_S and R_L of $20\ k\Omega$, $30\ k\Omega$ and $20\ k\Omega$ respectively, for alarm settings of 1000 ppm and a desired sensor circuit output voltage of 2 V. Based on determined parameters, the calibration equation for determination of best concentration value for a given value of emulated LPG concentration was developed. Using the method proposed in this study makes the process of determining the MQ-series gas sensor circuit parameters less cumbersome as their value can easily be obtained from the resulting graphs. **Conclusions:** a structured graphical approach for determination of MQ-series gas sensor circuit parameters for alarm points in a stand-alone gas alarm system showed that using MQ-4 gas sensor and LPG as the target gas, and for a sensor circuit output voltage of 2 V for alarm point at 1000 ppm of LPG, the corresponding value of R_O, R_S and R_L obtained were $20\ k\Omega$, $30\ k\Omega$, and $20\ k\Omega$ respectively. Hence, a structured graphical approach is suitable for determining MQ series gas sensor circuit parameters for a stand-alone gas alarm system under the influence of its associated gases.

Keywords: *alarm point, base gas, calibration-concentration, gas concentration, gas sensor resistance*

1. INTRODUCTION:

MQ-series gas sensors belong to the family of metal oxide semiconductor (MOS) gas sensors that can detect the presence of some volatile, oxidizable, or reducible gases in an oxygenated environment (Gómez, Pelegri-Sebastia and Lajara, 2020). This group of sensors has been found useful in food quality control (Peris and Escuder-Gilabert, 2009), hazardous gas detection (Chadry and Suryani, 2018), environmental monitoring (Capelli, Sironi and Del Rosso, 2014; Capelli and Sironi, 2017), medical treatment and diagnosis (Chen, Wang, and Choi, 2013) and electronic nose development (Górska-Horczyczak *et al.*, 2016; Cui *et al*., 2019; Kanade and Shaligram, 2014). MQ-series gas sensors are commonly used in this regard owned to their high

sensitivity, stability, and long life characteristics (Örnek and Karlik, 2012). The resistance of the active sensing layer of these sensors changes when in contact with the target gas. The relationship between the sensor resistance and gas concentration is non-linear (Liu et al., 2012) and depends on the gas type. When connected as one of the basic components in the sensor circuit, a certain voltage that depends on the type and concentration of the gas can be measured at the circuit output (Nayyar, Puri, and Le, 2016; Ponzoni *et al*., 2017).

The MQ-series gas sensors form the major component in many gas alarm systems due to their cost and sensitivity advantages. As reported by (Nnokwe, Ubochi, and Onwuzuruike, 2020) is a microcontroller-based gas leakage detection system that employs an MQ-6 gas sensor for sensing of LPG. This device monitors the concentration of leaked gas on a liquid crystal display (LCD) and sends messages to a user's mobile device as part of alarming conditions. Methane concentration measuring instrument was developed by (Harun and Sokku, 2019) using MQ-135 and Arduino UNO as sensor and processor, respectively. The measured gas concentration is displayed on an LCD screen. An LPG leakage detection system in which MQ-2 was used as the sensor, LCD as the display, and the information regarding the gas leakage sent as SMS to the registered phone number via GSM module was presented by (Hasibuan and Idris, 2019). A combination of MQ-6 gas sensor and microprocessor was used by (Katrandzhiev and Karnobatev, 2016) as the main components to realize LPG concentration measuring device, which also produces audible sound and visible light as signs of alarm when there is gas leakage.

Developed by (Ahmed *et al*., 2018) is a microcontroller-based gas alarm system that triggers a buzzer and LED indicator when the alarm set point for the MQ-9 gas sensor was 37,000 ppm of Methane gas. Designed by (Kumar and Kumari, 2019) are an Arduino-based system with MQ2, MQ4, and MQ135 gas sensors capable of monitoring the concentration of gases and also gives alarm when the concentration of the various types of gases in the atmosphere is above the threshold value and also sends a notification to designated mobile phones through SMS via GSM module. Present in (Munsadwala *et al*., 2019) is an IoT-based hazardous gas identification, and visualization device is consisting of MQ07 and MQ135 for sensing the CO and CO_2; and air quality, respectively. The sensors output was processed by Arduino microcontroller, and the output from the controller was sent to the cloud storage via IoT infrastructure. An LPG leakage concentration detection, monitoring, and control system which employed MQ-6, Arduino microcontroller, LCD display, GSM module, buzzer, and relay DC motor for sensing, processing, visualizing the gas concentration, sending situation message to the registered phone number, producing audible sound and automatically controlled the stove gas release knob respectively was presented by (Soundarya *et al*., 2014).

A toxic and hazardous gas concentration detecting, measuring, and monitoring system using MQ-2 gas sensor, Arduino, and nRF24L01P Wireless Transceiver Module as a sensor, processor, and data transfer technology, respectively, was developed by (Mahbub, 2019). An Arduino-based embedded system for detecting toxic gas in the air was developed by (Holovatyy *et al*., 2018). This system monitors the gas concentration and triggers the alarm (Buzzer and red light) when the concentration is abnormal. The alarm message is sent as SMS to the registered phone number via the GSM module and displayed on the LCD and personal computer screen. Also developed by (Ibrahim, 2018) is a microcontroller-based carbon monoxide and carbon dioxide detector using MQ-7 and MQ-135 for carbon monoxide and air quality sensing, respectively. The gas concentration was displayed in ppm on LCD, and the alarm is triggered when the threshold for the safe gas concentration is reached. The research conducted by (Jamal *et al*., 2019) focused on the development of a smart real-time monitoring instrument to detect and measure in addition to heat stress the toxic gases (CO, NO_2, and H_2S) concentration in ppm on Java developed Graphical User Interface (GUI) using the Internet of Things (IoT) technology. The designed system used MQ7, MQ136, and MQ131 gas sensors, Atmega 328-PU with its Wi-Fi shield 101 to sense, control, and Wi-Fi communication between Remote Terminal Unit and GUI.

Present by (Shahadat, Mallik, and Islam, 2019) is a system for monitoring LPG leakage and activation of alert that gives the buzzer sound, switching on specified relay(s), and sending an alert message to the administrator for the necessary actions. In this system, the gas leakage concentration is sensed by an MQ-6 gas sensor whose output is fed to the microcontroller node for processing. When the reference threshold value is crossed, the controller switches on the relay(s) and buzzer(s), alerting the administrator via the IoT server for necessary action.

It was discovered from the consulted literature that majority of the gas alarm systems that employ MQ-series gas sensors as sensing elements, microcontrollers are normally used to interface the sensor(s) with the alarm unit. This is because additional functions like gas concentration monitoring, storage, displaying, and sending of data and information to remote terminals are required to be performed by the system. But suppose all the aforementioned additional functionalities are not required. In that case, a straightforward, simple, economical, and reliable stand-alone gas alarm system can be achieved by connecting the sensor circuit to the alarm output unit via a simple switching component like a transistor. To realize this type of stand-alone gas alarm system, a unique combination of sensor circuit parameters is required to achieve the required sensor circuit output voltage to activate the switching circuit that links the sensor circuit with the alarm output unit (buzzer or light source) at the alarm point. The alarm point is the value of gas concentration at which the alarm is expected to come on or a particular action to take place, and it is normally set for a given gas and sensor. However, determining the sensor circuit parameters to achieve the required sensor circuit output voltage for a given alarm point has not been well researched. Therefore, this study presents a structured graphical method for determining the sensor circuit parameter that yielded the needed sensor circuit output voltage for the alarm point.

To achieve the aim of this study, the mathematical model equations that relate the: (i) sensor resistance (R_S) with the gas concentration (x) and the sensor resistance at standard calibration concentration of the sensor base gas in the clean air (R_O) and (ii) sensor circuit output voltage (V_{RL}), load resistance (R_L) and sensor resistance (R_S) were developed. Based on these model equations, the graphs which relate the parameters together were plotted. Using these graphs for a particular case of an MQ-4 gas sensor under the influence of LPG, the parameters that yielded the desired sensor circuit output voltage of 2V for 1000 ppm of LPG alarm point were determined.

2. MATERIALS AND METHODS:

This section is devoted to developing mathematical relationships among the gas, sensor, and sensor circuit parameters. Also, based on the developed model equations, the graphs that summarize the effects of these parameters on one another were plotted. The desired circuit parameters value were then graphically determined from the plotted graphs.

2.1 MQ-series Gas Sensor Model Equations

The MQ-series gas sensor resistance, R_S is related to other gas and sensor parameters, as shown in Equation (1) (Ajiboye *et al*., 2021).

$$R_S = 10^{\wedge(m log_{10}x + log_{10}c + log_{10}R_O)} \quad \text{(Eq.1)}$$

Where m and c are as defined in (Ajiboye *et al*., 2021.

Figure 1 shows the MQ-series gas sensor electrical equivalent circuit where R_H the sensor heater resistance is. Based on Figure 1, the sensor output voltage is as expressed in Equation (2) where V_{CC} is the supply voltage across the circuit.

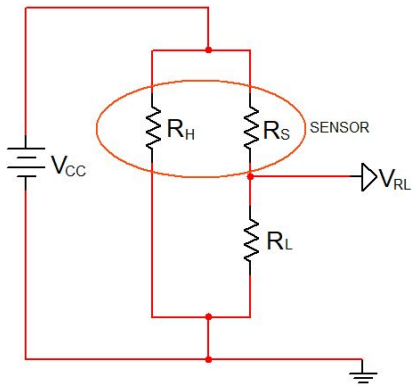

Figure 1. MQ-series gas sensor electrical equivalent circuit

$$V_{RL} = \frac{R_L V_{CC}}{(10^{(m log_{10}x + log_{10}c + log_{10}R_O)} + R_L)} \quad \text{(Eq. 2)}$$

From Equation (2), the concentration (x) can be expressed as a function of other parameters and variables, as shown in Equation (3).

$$x = 10^{\left(\frac{log_{10}\left(\frac{R_L V_{CC}}{V_{RL}} - R_L\right) - log_{10}c - log_{10}R_O}{m}\right)} \quad \text{(Eq. 3)}$$

2.2 Determination of sensor circuit parameters

The developed model equations were used to plot the graphs that relate the sensor and gas parameters together in this section. Using these graphs, the value of the parameter for the sensor circuit was determined.

2.2.1 Determination of R_O

The first parameter required for the characterization of the MQ-series gas sensor circuit is $\mathrm{R_O}$. This parameter is normally determined using the experimental method because the value varies from sensor to sensor (Rumantri, Khakim, and Iskandar, 2018; Shahid *et al*., 2018). The variation is because keeping the sensor manufacturing condition constant is not practically achievable. Therefore variation in the resistance of the sensor under the same conditions of gas and environment is inevitable (Kim *et al*., 2006; Vandana *et al*., 2016). For easy understanding of the relationship among $\mathrm{R_S}$, x and $\mathrm{R_O}$ for the MQ-4 gas sensor considered in this study under the influence of its base gas ($\mathrm{CH_4}$) the mesh plot of Figure 2 was carried out using Equation (1) for $10\ \mathrm{k\Omega} \leq \mathrm{R_O} \leq 60\ \mathrm{k\Omega}$ and $200\ \mathrm{ppm} \leq \mathrm{x} \leq 10000\ \mathrm{ppm}$. The graph of Figure 3 which relate $\mathrm{R_O}$ and $\mathrm{R_S}$ when the sensor was assumed to be under the influence of the $\mathrm{CH_4}$ was extracted from Figure 2 when the concentration was 1000 ppm of $\mathrm{CH_4}$ which is the base gas calibration concentration. Many types of Figure 3 can be gotten from Figure 2 at different concentrations, but the one considered in this study is for the analysis of the trend of $\mathrm{R_S}$ as $\mathrm{R_O}$ varies when the sensor is in the base gas at a calibration concentration of 1000 ppm.

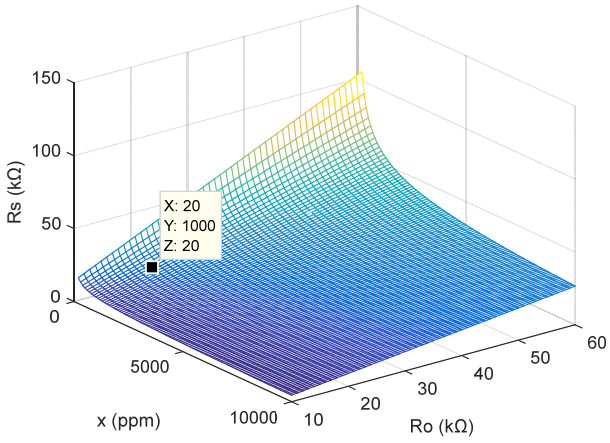

***Figure* 2.** Mesh plot of $\mathrm{R_S}$ versus x and $\mathrm{R_O}$ for MQ-4 gas sensor in the $\mathrm{CH_4}$

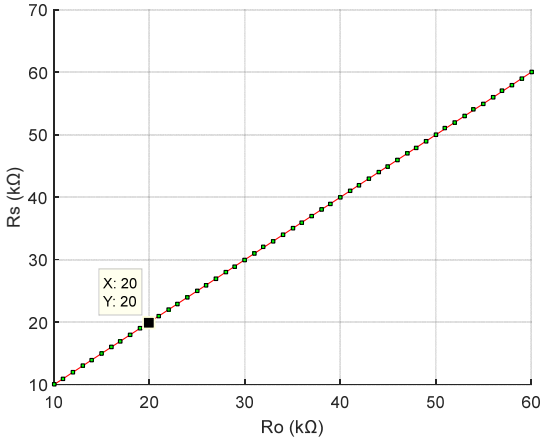

Figure 3. Plot of $\mathrm{R_S}$ versus $\mathrm{R_O}$ for MQ-4 sensor in the $\mathrm{CH_4}$ at a concentration of 1000 ppm

2.2.1 Determination of R_S in the gas under investigation

For the purpose of this study, LPG was considered because of its domestic and industrial applications. Therefore, fixing of alarm point using MQ-4 gas sensor for LPG is presented. Based on Equation 1, Figure 4 is the mesh plot of $\mathrm{R_O}$,$\boldsymbol{x}$ and $\mathrm{R_S}$ for MQ-4 gas sensor under the influence of LPG was obtained for $10\ k\Omega \leq R_O \leq 60\ k\Omega$ and $200\ ppm \leq x \leq 10000\ ppm$. $\mathrm{R_S}$ can be determined from Figure 4 for a given value of $\mathrm{R_O}$ and x. The alarm point is determined by the x value for a given gas. Since the gas under consideration in this study is LPG, a practical threshold value that human beings can withstand (1000 ppm) is used as the alarm point. Based on this concentration, the graph of Figure 5 which relate $\mathrm{R_S}$ and $\mathrm{R_O}$ was extracted from Figure 4 to show the relationship between these parameters when $\mathrm{x} = 1000\ \mathrm{ppm}$. It

should be noted that at any given value of x on the surface of Figure 4, the like of Figure 5 can be generated for a better understanding of the trend of the relationship between R_S and R_O for the concentration in question. The value of R_S for any specified value of R_O can easily be obtained from Figure 5.

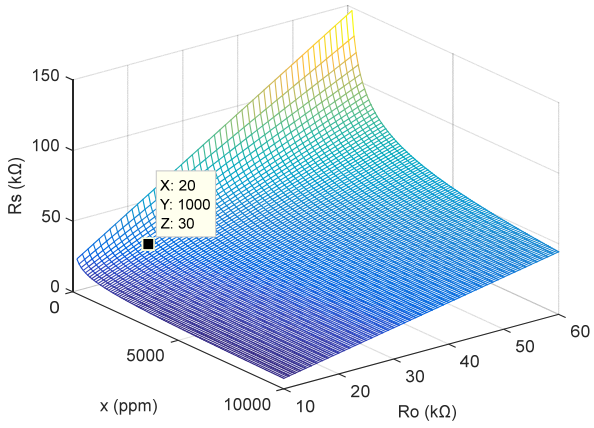

Figure 4. Mesh plot of R_S versus x and R_S for MQ-4 gas sensor in LPG

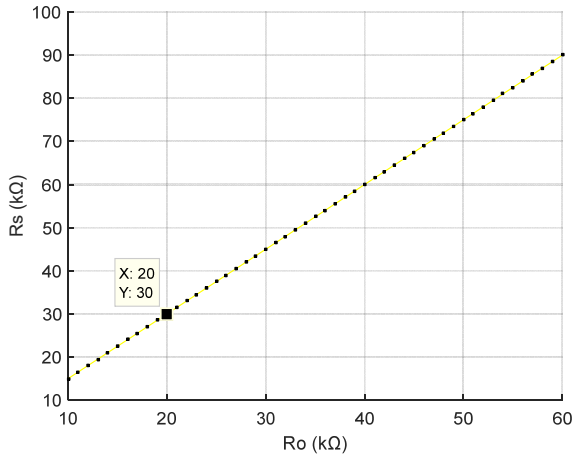

Figure 5. Plot of R_S versus R_O for MQ-4 gas sensor in LPG at concentrations of 1000 ppm

2.2.2 Determination of the sensor circuit R_L for alarm point

Applying Equation 2, the relationship among V_{RL}, R_O and R_L is demonstrated in the mesh plot of Figure 6 for $10\ k\Omega \leq R_O \leq 60\ k\Omega$ and $10\ k\Omega \leq R_L \leq 47\ k\Omega$. Figure 6 make the relationship among V_{RL}, R_S and R_L comprehendible at a glance. For any given value of R_S the relationship between V_{RL} and R_L can be established.

For the purpose of this study, it was assumed that $R_O = 20\ k\Omega$, therefore, $R_S = 30\ k\Omega$ as can easily be evaluated from Figure 5. The graph that relates V_{RL} and R_L together was extracted from Figure 6 for clarity purpose and is as shown in Figure 7. Using Figure 7, the value of R_L for any desired value of V_{RL} for the sensor circuit can be determined.

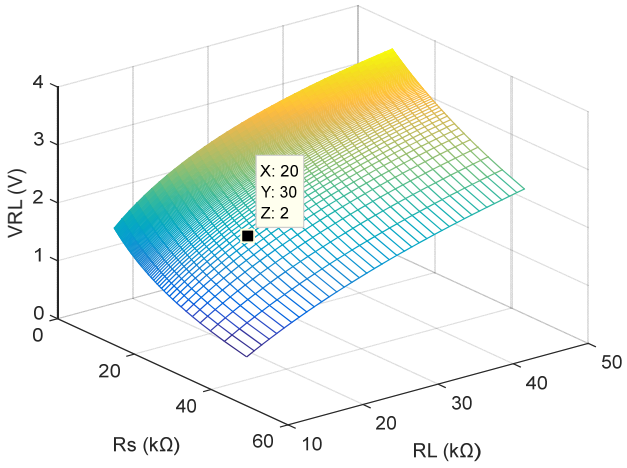

Figure 6. Mesh plot of V_{RL} versus R_S and R_L for MQ-4 gas sensor in LPG

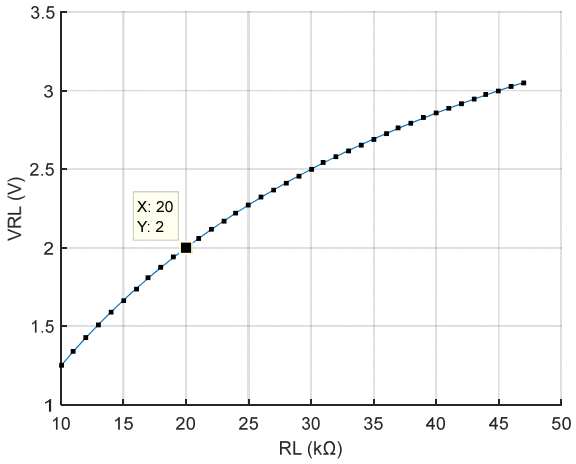

Figure 7. Plot of V_{RL} versus R_L for MQ-4 gas sensor in LPG

2.3 Experimental Setup

Using the determined sensor circuit parameters, the Arduino-based gas-alarm system shown in Figure 8 was developed and calibrated using simulation and emulation data. The simulation and emulation were carried out by

applying Equation 3 and the experimental setup shown in Figure 9, respectively.

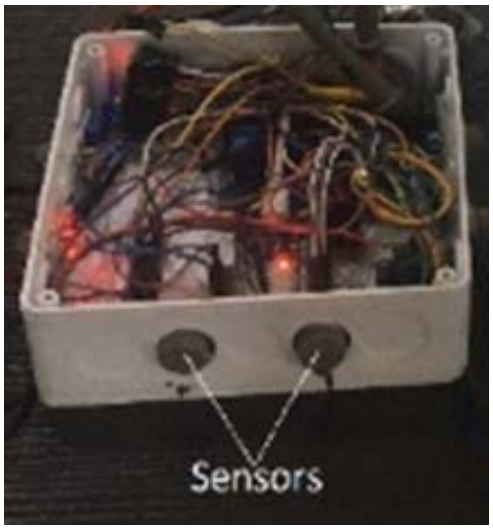

Figure 8. Developed Arduino-based gas-alarm system

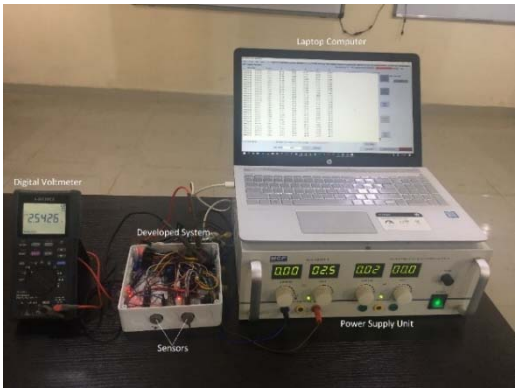

Figure 9. system emulation experimental setup

The setup consists of a digital meter for monitoring the sensor circuit emulated voltage, the developed system, a variable dc power supply unit for supplying the sensor circuit emulated voltage, and a laptop PC for monitoring and storage of system output (emulated concentration). The developed system was powered from an in-built +5V dc source, and the output of the variable power supply was connected to the input pin of the microcontroller to mimic the sensor circuit output voltage. Then the voltage from the variable power supply was varied within 1.545 V and 3.455 V, which is the sensor circuit expected output voltage range when LPG concentration was in the range of 200 to 10000 ppm. The system output, LPG concentration levels were logged into the laptop PC as the input voltage to the microcontroller was varying.

3. RESULTS AND DISCUSSION:

The mesh plot of Figure 2 makes the presentation of the relationship among $\mathrm{R_S}$, x and $\mathrm{R_O}$ for MQ-4 gas sensor in $\mathrm{CH_4}$ to be compact. Also, the extraction of Figure 3 from Figure 2 for the demonstration of the relationship between $\mathrm{R_S}$ and $\mathrm{R_O}$ when x = 1000 ppm provides room for a better understanding of the relationship and makes the range of these parameters clearer. As can be seen from Figure 3, the relationship between $\mathrm{R_S}$ and $\mathrm{R_O}$ is linear, which make it easy to determine $\mathrm{R_S}$ for any given value of $\mathrm{R_O}$ or vice versa. Since $\mathrm{R_O} = 20\ k\Omega$ when the sensor is assumed to be in $\mathrm{CH_4}$ at calibration concentration of 1000 ppm in clean air, the value of $\mathrm{R_S}$ is also $20\ k\Omega$ as can be seen from Figure 3.

To capture the relationship among $\mathrm{R_S}$, x and $\mathrm{R_O}$ with easy when MQ-4 is in the vicinity of LPG, the mesh plot of Figure 4 was constructed. It can be seen from Figure 4 that at any spot on the mesh, the value of $\mathrm{R_S}$ for any combination of x and $\mathrm{R_O}$ value can be determined. Furthermore, Figure 5 was extracted from Figure 4 to make a visualization of the relationship between $\mathrm{R_S}$ and $\mathrm{R_O}$ clearer. Figure 5 reveal that the relationship between $\mathrm{R_S}$ and $\mathrm{R_O}$ is linear. Therefore, the value of $\mathrm{R_S}$ for a given value of $\mathrm{R_O}$ can easily be determined from Figure 5, but $\mathrm{R_O} = 20\ k\Omega$ for this study; therefore, from Figure 5, the corresponding value of $\mathrm{R_S}$ is $30\ k\Omega$.

The relationship among $\mathrm{V_{RL}}$, $\mathrm{R_S}$ and $\mathrm{R_L}$ was present in Figure 6. From this Figure, the circuit response to any combination of $\mathrm{R_S}$ and $\mathrm{R_L}$ within the specified range can be captured at a glance. Since the value of $\mathrm{R_S}$ has been determined to be $30\ k\Omega$ using Figure 5, this value of $\mathrm{R_S}$ yielded Figure 7 from Figure 6. It can be seen from Figure 7 that $1.25\ V \leq \mathrm{V_{RL}} \leq 3.05\ V$ and $10\ k\Omega \leq R_L \leq 47\ k\Omega$ and $\mathrm{V_{RL}}$ bears a nonlinear relationship with R_L. Assuming the required sensor circuit voltage value of 2 V, then the corresponding value of $\mathrm{R_L}$ that can produce this voltage using Figure 7 will be $20\ k\Omega$.

The system calibration graph of Figure 10 was obtained by plotting the simulated (ideal) against emulated (assumed practical) LPG concentration data.

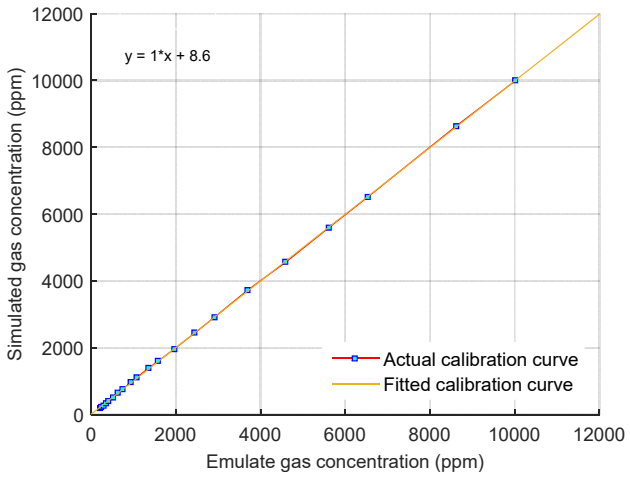

***Figure 10*.** system calibration curve

Since the plot yielded a straight-line graph, the data were fitted linearly. The resulting system calibration equation that can be used to find the best concentration for a given value of emulated LPG concentration is shown in Equation (4), where y and x are the predicted and emulated LPG concentrations in ppm respectively.

$$y = x + 8.6 \qquad \text{(Eq. 4)}$$

At this stage, it can be seen that a structured graphical method for the determination of sensor circuit parameters, namely, R_S, R_O and R_L for alarm point, which is required for the proper functioning of MQ-series-based, a stand-alone gas alarm system has been developed and demonstrated.

4. CONCLUSIONS:

A structured graphical method for determining MQ-series gas sensor circuit parameters for alarm points in a stand-alone gas alarm system was developed and demonstrated using MQ-4 gas sensor and LPG as the target gas. The developed method is concise, straightforward forward and time-saving. The method is less prone to analytical error since all that is required is the proper visual reading of the parameter value from the graph. For a particular case of expected sensor circuit output voltage of 2 V for alarm point at 1000 ppm of LPG, the corresponding value of R_O, R_S and R_L obtained were $20\ k\Omega$, $30\ k\Omega$, and $20\ k\Omega$ respectively. An Arduino-based stand-alone gas-alarm system was developed and calibrated using simulation and emulation LPG concentration data.

The method can be applied to any type of MQ-series gas sensor under the influence of its associated gases.

5. DECLARATIONS

5.1. Study Limitations

No limitations were known at the time of the study.

5.2. Acknowledgements

Not applicable.

5.3. Funding source

This research was funded by the authors.

5.4. Competing Interests

No conflict of interest exists in this publication.

7. REFERENCES:

1. Ahmed, N. B., Tahsin, K. N., Khan, S., Hoq, M. and Alam, D. (2018). Design and implementation of a microcontroller based flammable gas detector and automatic alarm system to ensure the industrial and domestic safety. *Asian Journal of Science and Technology,* 9(1), 7425-7429.

2. Ajiboye, A., Opadiji, J., Yusuf, A. and

Popoola, J. (2021). Analytical determination of load resistance value for MQ-series gas sensors: MQ-6 as case study.*Telkomnika, 19*(2), 575-582.

3. Capelli, L. and Sironi, S. (2017). Monitoring odour emisssions from an oil and gas plant: Electronic nose performance testing in the field. In *2017 ISOCS/IEEE International Symposium on Olfaction and Electronic Nose (ISOEN)*, 1-3.

4. Capelli, L., Sironi, S. and Del Rosso, R. (2014). Electronic noses for environmental monitoring applications. *Sensors, 14*(11),19979-20007.

5. Chadry, R., and Suryani, A.I. (2018). Embedded System Using Field Programmable Gate Array (FPGA) myRIO and LabVIEW Programming to Obtain Data Patern Emission of Car Engine Combustion Categories. *JOIV: International Journal on Informatics Visualization,* 2(2), 56-62.

6. Chen, S., Wang, Y. and Choi, S. (2013). Applications and technology of electronic nose for clinical diagnosis.

7. Cui, S., Inocente, E. A. A., Acosta, N., Keener, H., Zhu, H., and Ling, P.P. (2019). Development of fast e-nose system for early-stage diagnosis of aphid-stressed tomato plants. *Sensors, 19*(16), 3480.

8. Gómez, J.C., Pelegri-Sebastia, J., and Lajara, R. (2020). Circuit Topologies for MOS-Type Gas Sensor. *Electronics,* 9(3), 525.

9. Górska-Horczyczak, E., Guzek, D., Molęda, Z., Wojtasik-Kalinowska, I., Brodowska, M. and Wierzbicka, A. (2016). Applications of electronic noses in meat analysis. *Food Science and Technology, 36*, 389-395.

10. H. Electronics, "Technical Data MQ-4 Gas Sensor," ed, p. 2.

11. Hanwei (2019). Technical Data MQ-6 Gas Sensor. E. H. Sensors, ed. China: Hanwei Sensors, Ed., ed, 1-2.

12. Harun, S. F. and Sokku, S. R. (2019). Measurement of Level Content of Methane in Household Waste Based on Arduino and Gas Sensor. *Journal of Physics: Conference Series*, *1244*(1), 012042.

13. Hasibuan, M. S. and Idris, I. (2019) Intelligent LPG gas leak detection tool with SMS notification. *Journal of Physics: Conference Series*, *1424*(1), 012020.

14. Holovatyy, A., Teslyuk, V., Lobur, M., Pobereyko, S. and Sokolovsky, Y. (2018). Development of arduino-based embedded system for detection of toxic gases in air. *IEEE 13th International Scientific and Technical Conference on Computer Sciences and Information Technologies (CSIT)*, 1, 139-142.

15. Ibrahim, A. A. (2018) Carbon Dioxide and Carbon Monoxide Level Detector. *21st International Conference of Computer and Information Technology (ICCIT)*, 1-5.

16. Jamal, H., Huzaifa, M., Sodunke, M. A. and Odiete, J. O. (2019). Smart Heat Stress and Toxic Gases Monitoring Instrument with a Developed Graphical User Interface Using IoT. *International Conference on Electrical, Communication, and Computer Engineering (ICECCE)*,1-6.

17. Kanade, A. and Shaligram, A. (2014). Development of an E-Nose using metal oxide semiconductor sensors for the classification of climacteric fruits. *International Journal of Scientific and Engineering Research, 5(2).*

18. Katrandzhiev, N. T. and Karnobatev, N. N. (2016). Elaboration of a Microprocessor Unit for Gas Measurement with Sensor MQ-6. *Scientific Works of the University of Food Technologies,* 63(2), 299 – 306.

19. Kim, J. Y., Kang, S. W., Shin, T. Z., Yang, M. K. and Lee, K. S. (2006). Design of a smart gas sensor system for room air-cleaner of automobile-thick-film metal oxide semiconductor gas sensor. *International Forum on Strategic Technology*, 72-75.

20. Kumar, P. N. S. and Kumari, A. K. (2019). Design of Gas Detection and Monitoring System using IoT. *International Journal of Engineering Research and Technology (IJERT),* 8, 463 - 468.

21. Liu, X., Cheng, S., Liu, H. and Hu, S. (2012). Daqiang Zhang 2 and Huansheng Ning, a survey on gas sensing technology review. *Sensors,* 12(7), 9635-9665.

22. Mahbub, M. (2019). Toxic and hazardous gas detection, measurement, and monitoring system for safety assurance in home and industrial application of wireless sensor node. *Engineering and Technology Research,* 1, 089- 098.

23. Munsadwala, Y. , Joshi, P., Patel, P. and Rana, K. (2019). Identification and visualization of hazardous gases using IoT. *4th International Conference on Internet of Things: Smart Innovation and Usages (IoT-SIU)*, 1-6.

24. Nayyar, A., Puri, V. and Le, D.-N. (2016). A comprehensive review of semiconductor-type gas sensors for environmental monitoring. *Review of Computer Engineering Research,* 3(3), 55-64.

25. Nnokwe, C. C., Ubochi, B. C. and Onwuzuruike, K. V. (2020). Development of a Gas Leakage Detection System. *Journal of Electrical Engineering, Electronics, Control, and Computer Science,* 6(4), 23-28.

26. Örnek, Ö., and Karlik, B. (2012). An overview of metal oxide semiconducting sensors in electronic nose applications. in *Proc. of the 3rd International Symposium on Sustainable Development*, *2*, 506-515.

27. Peris M., and Escuder-Gilabert, L., (2009). A 21st century technique for food control: Electronic noses. *Analytica chimica acta, 638(1),* 1-15.

28. Ponzoni, A., Baratto, C., Cattabiani, N., Falasconi, M., Galstyan, V. and Nunez-Carmona, E. Metal oxide gas sensors, a survey of selectivity issues addressed at the SENSOR Lab, Brescia (Italy). *Sensors,17*(4), 714.

29. Rumantri, R., Khakim, M. and Iskandar, I. (2018). Design and characterization of low-cost sensors for air quality monitoring system. *Jurnal Pendidikan IPA Indonesia,* 7, 347-354.

30. Shahadat, M. M., Mallik, A. and Islam, M. (2019). Development of an automated gas-leakage monitoring system with feedback and feedforward control by utilizing IoT. *Facta universitatis-series: Electronics and Energetics,* 32(4), 615-631.

31. Shahid, A., Choi, J.-H., Rana, A. U. H. S. and Kim, H.S. (2018). Least squares neural network-based wireless E-Nose system using a SnO_2 sensor array. *Sensors,* 18(5),1446.

32. Soundarya, T., Anchitaalagammai, J., Deepa, P. and Karthick Kumar, S. (2014). C-leakage: Cylinder LPG Gas leakage Detection for home safety. *IOSR Journal of Electronics and Communication (IOSR-JECE),* 9(1), 53-58.

33. Vandana, K., Baweja, C., Simmarpreet, and Chopra, S. (2016). Influence of Temperature and Humidity on the Output Resistance Ratio of the MQ-135 Sensor. *Int. J. Adv. Res. Comput. Sci. Softw. Eng,* 6(4), 423-429.

SOUTHERN BRAZILIAN JOURNAL OF CHEMISTRY

ASSESSMENT OF SERUM SCLEROSTIN LEVEL AS A BIOMARKER ASSOCIATED WITH BONE DISORDERS IN B-THALASSEMIA PATIENTS IN AL- NAJAF CITY, IRAQ

SHARBA, Intisar Razzaq[1*]; AL-DUJAILI, Arshad Noori;

[1] University of Kufa, Faculty of Science, Department of Biology, Iraq.

** Correspondence author*
e-mail: intisar.sharba@uokufa.edu.iq

Received 26 May 2021; received in revised form 11 September 2021; accepted 27 november 2021

ABSTRACT

Background: β-thalassemia is a blood disorder in which the body does not make hemoglobin normally. **Aim**: To assess serum sclerostin in female patients with beta-thalassemia and compare with the healthy controls and to predict its complication associated with the bone pathophysiology, for designed improvement the lifestyle goodliness for these patients. **Material and methods**: Sixty-nine female beta-thalassemia (βT) patients (54 βT major and 15 βT Intermedia), aged 8-40 years who dependent on transfused blood, and 20 healthy controls were evaluated serum sclerostin, and was examined the relationship with hematological parameters RBC, Hb, PCV, WBC, PLT, BMI, splenic status, iron, and ferritin levels. The information of beta-thalassemia patients was collected and records by the questioner. **Results**: A significantly increased serum sclerostin level (mean 26.80±0.91) pg/ml was showed in βT patients compared with the healthy controls (10.03±0.68, $p < 0.001$) pg/ml. Furthermore, a significant decrease ($p<0.05$) of the sclerostin level was observed in β-thalassemia major compared to intermedia β-thalassemia patients. Serum sclerostin level revealed a significant increase in progress age; it is highest in the age group (30-40) year as compared with age group (8-18) and (19-29) year respectively. Sclerostin showed no associations with the RBC, Hb, PCV, and significantly positively correlated ($p<0.05$) with serum iron, ferritin levels, WBC, and PLT count. Significantly higher sclerostin levels in splenectomized and underweight groups were observed compared to unsplenectomized and normal-weight groups ($p<0.05$) of βT patients. **Conclusions:** Sclerostin plays an important role in beta-thalassemia patients and can serve as a biomarker associated with the bone pathophysiology and indicator to prevent the continuation of such serious diseases caused by iron overload in these patients.

Keywords: *Sclerostin, β thalassemia, BMD, iron overload, ferritin, and biochemical analysis of blood.*

1. INTRODUCTION

Beta-thalassemia (βT) is a hereditary hemopathy characterized by a defect in the production of the beta-globin chain resulting from a genetic defect on chromosome 11 (Galanello and Origa, 2010). Significant clinical symptoms of these patients are ineffective erythropoiesis, with extramedullary involvement, hemolysis, and severe anemia (Almousawi, and Sharba, 2019; Thein, 2013). Bone abnormalities play an important role in β-thalassemia patients, which arises from the hematological disorder and its complications with hypertransfusion, iron overload, treatment and iron chelation, nutritional deficits, and sedentarism (Sapunarova *et al.*, 2020). Affecting bone metabolism in βT and instability of bone mineral turnover with amplified resorptive average and inhibition of osteoblast activity leads to diminished bone mineral density (BMD) (Voskaridou *et al.,* 2012).

Sclerostin is a member of the Wnt signaling pathway inhibitor. It is a glycoprotein expressed predominantly by mature osteocytes under physiological and pathological conditions released into circulation and binding with the cell membrane receptors of osteoblasts (Drake *et al.,* 2010; Wijenayaka *et al*., 2011). Also, it was found that osteoclast precursors can secrete sclerostin in bone marrow and reductions in the development of their maturation (Delgado-Calle *et al.,* 2017). Additionally, studies have demonstrated that sclerostin can be assessed in several clinical states, such as inflammatory (Wehmeyer *et al*., 2016). Sclerostosis, fracture risk spinal injury (Morse *et al.,* 2012), multiple myeloma (Terpos *et al.*, 2012), ankylosing chronic kidney disease,

type-II diabetes, and another disease (Kim *et al*., 2013; Pelletier *et al.,* 2013). The major role of Sclerostin in β Thalassemia patients is related to the reduced bone mineral density and the development of osteoporosis (Voskaridou *et al*., 2012). However, the research about the role of sclerostin in female patients with beta-thalassemia is still rather inadequate, and it required further investigations; for this causes, the current study aimed to assess serum sclerostin in female patients with beta-thalassemia and comparison with the healthy controls, the relationship between sclerostin levels with the hematological parameters, age, BMI and splenic status, to predict of its complication that associated with bone pathophysiology such as osteoporosis, for designed improvement the lifestyle goodliness for these patients.

2. MATERIALS AND METHODS

2.1. Study design

According to the approval of the ethical committee regulations of Kufa University, faculty of science at protocol number 2014. Sixty-nine females with β-thalassemia (54 major βT and 15 intermedia βT), the aged range from (8–40) year. Patients were enrolled at The Thalassemia Center in Al–Zahraa Educational Hospital in Al–Najaf province, Iraq. They were frequently blood transfused and treated every two or three weeks to maintain a Hb level of more than 10 g/dl and regulate iron-chelating therapy. Twenty participate of healthy females with matched age served as a control group; the patient and controls. This study was carried out from July 2014 to March 2015. β-thalassemia patients were classified into many divisions according to types of β-thalassemia into two groups Major and Intermedia β-Thalassemia, three aged groups Group 1 (8 –18 year), Group 2 (19 –29 year), and Group 3 (30 – 40 year), Splenic situation divided into Splenectomized unsplenectomized patients (Sharba and Al-Dujaili, 2020). Also, according to Body Mass Index (BMI), patients were divided into two groups: normal weight and underweight the normal range (5th – 85th) % for (≤ 20) years of age, and (18.5 – 25) kg/m^2 for (>20) years of age. (WHO, 2006).

2.2. Methods

An electronic balance and height unit carried out the BMI measurement to measure weight (kg) divided on the height square (m^2), according to Equation 1. (WHO, 2006). Both patients and healthy were withdrawn 5 ml of venue blood for hematological criteria were conducted on EDTA anticoagulated blood by using a completely automated hematology analyzer Mythic 18 (RINGELSAN CO., Turkey) for estimated complete blood count (CBC), which included RBC, PCV, Hb, WBC, and PLT (Wasmuth, 2010). The serum samples for ferritin, iron, and sclerostin were prepared through cool-centrifugation and freezing at (−80 °C) after the collection and stored until the time of the analysis. Estimated serum ferritin using the enzyme-linked immunosorbent assay (ELISA) immunoenzymatic technique using the bioelisa ELx 80000 reader (biokit, USA). According to the Manufacturing Firm, the Human Accu Bind Ferritin ELISA Kit (Monobind Inc., USA, code number 2825-300). (Anderson and Kelly, 1981). The assay Human Sclerostin (SOST) ELISA Kit was conducted according to the manufacturing company (CUSABIO BIOTECH Co., Ltd., PRC, code number CSB-E13146h) that depended on the technique of the quantitative sandwich enzyme immunoassay. Serum iron concentration was measured by iron (using the chromogen ferrozine method) kit (bt 35i, Turkey). The principal transferrin-bound iron is released at acid pH and reduced from ferric Fe^{3+} to ferrous ions Fe^{2+} iron. These ions react with ferrozine to form a violet-colored complex, which is measured spectrophotometrically at 560 nm. This absorbance is proportional to serum iron concentration in the sample (Persijn *et al*., 1971).

BMI= weight (kg) / height square (m^2) (Eq. 1)

2.3. Statistical analysis

The data were statistically analyzed by the computer software of packed SPSS V. 25 (Inc., Chicago, IL, USA). Data with normal distribution were defined as mean ± standard error (SE) and compared between two groups by independent t-test. While not normally distributed data as the median and interquartile range (IQR) and Mann-Whitney U tests. Nominal data is defined as frequency and percent. Pearson or Spearman rank correlation coefficients for finding related between serum sclerostin and study parameters. A receiver operator characteristic curve (ROC) with an area under the curve (AUC) was then applied to identify the predictive value of sclerostin for patients among the healthy group. statistically

significant at $p < 0.05$.

3. RESULTS AND DISCUSSION:

3.1. The general characteristics of the studied groups

The general characteristics of the studied groups are shown in Table 1. In this table, 69 β-thalassemia patients (major βT 54 (78.2%), and intermedia βT 15 (21.8%), splenectomized 29 (42%) and unsplenectomized 40 (58%) indicated no significant difference ($p>0.05$) in the mean age of the β-thalassemia patients (16.62± 0.96) years when compared with the healthy controls (20.75±1.86) year, p=0.612. The results showed that β-thalassemia patients a significant difference ($p<0.05$), decreased levels of Hb (7.7±0.14) g/dl, RBC (3.13±0.07) 10^6/ml, and P.C.V (23±0.41) %, to compared with the healthy controls (12.01±0.19) g/dl, p=0.027, (4.36±0.07) 10^6/ml, p=0.038 and (36.34±0.52) %, p=0.036 respectively. But significantly increase in values of WBC (11.05±0.26) 10^3/ml and PLT (361.86±13.92) 10^3/ml in β-thalassemia patients, as compared to the healthy controls (7.59±0.33)10^3/ml, p=0.036, (244±14.23) 10^3/ml, p=0.034. The current results agree with Arshad *et al*. (2014), who reported that Thalassemia patients might have abnormalities associated with lower Hb levels due to the decrease of erythrocyte numbers and decreased values of RBC indexes (MCV, MCH, MCHC, HCT). Thus, these patients suffer from anemia resulting in less oxygen content in the blood. Some studies concluded that decreased Hb, PCV, and RBC count levels, observed in β-thalassemia patients, are due to their early degradation and continuous breakdown of erythrocytes because of the abnormal globin molecule leading to erythrocyte rupture before maturation (Shanthi *et al.,* 2013). Some studies referred to RBC mass, WBC, and PLT count a significant difference in β-thalassemia patients. These were attributed that might be due to continuing severe anemia accompanied by hyper-cellular (thrombocytosis and leukocytosis) resulting in stimulation of erythropoietin hormone, which acts on the bone marrow to increase proliferation of blood cells or resulting in the immune system activation by receiving blood from diverse donors (Yassin *et al*., 2013; Arshad *et al*., 2014).

BMI was showed a significant decrease ($p<0.05$) in β thalassemia patients in healthy inverse controls (17.59±0.43 vs. 22.15±0.36 kg/m^2, p=0.001). Iron and ferritin were reported high significant in β-thalassemia patients (172.2 ± 4.4) µg/ml and (5156.5±438.7) ng/ml, more than to the healthy controls (29.86±2.32) µg/ml, and (99.15±8.95) ng/ml, p=0.0001, respectively. These results correspond with Eissa and El-Gamal (2014), finding the relationship of growth differentiation factor (GDF15) (reflecting ineffective erythropoiesis), BMI, and iron overload, resulting in this who suggested that ferritin as markers of low BMI of β-thalassemia patients. Many researchers have postulated that the pathogenesis of growth failure β-thalassemia is multifactorial. The key contributing factors to stunt growth and delay in onset of puberty in β-thalassemia major patients may include chronic anemia, transfusions iron overload, hypersplenism, chelation toxicity, and developed endocrinopathies secondary to iron overload that include hypothyroidism, hypogonadism, GH deficiency/insufficiency. In addition to other contributing factors such as deficiency of essential nutritional elements, chronic liver disease, which are major contributing factors in producing underweight patients (Skordis, 2011; Salih and Al-Mosawy, 2013; Manali *et al*., 2015). In such cases, blood transfusions are frequently needed in β-thalassemia, which causes increased free iron overload, which leads to the development of abnormalities in the body. Moreover, the purpose of transfusion includes improvement of anemia, suppression of erythropoiesis, and inhibition of increased gastrointestinal iron absorption. As no excretory mechanism exists, excess iron gets deposited as hemosiderin and ferritin in the liver, spleen, and endocardium (Pasricha *et al*., 2013)**.**

3.2. Sclerostin level effects by study categories (Thalassemia types, age, BMI, and splenectomy status)

ROC curve analysis and AUC of cutoff thresholds estimating serum sclerostin levels identified between beta-thalassemia patients and healthy controls group were shown in Figure 1. The results of ROC curve analysis showed that sclerostin (pg/ml) was a highly positive cutoff ratio of > 12.83 (AUC= 0.95; 95%CI= 0.919-0.996, sensitivity = 0.91; and specificity = 0.10, p=0.0001).

A significant increase ($p<0.05$) in sclerostin level in patients (26.80±0.91) pg/ml compared with the healthy controls (10.03±0.68) pg/ml (Figure 2A). A significant increase in Sclerostin level in β-thalassemia intermedia (32.28±3.20) pg/ml more than in β-thalassemia major (25.28±0.64) pg/ml. (Figure 2B). However, these results mentioned a

significant ($p<0.05$) decrease in the sclerostin level of age group (8-18) about (23.83±0.49) pg/ml as compared with that age group (19-29) and (30-40) about (29.45±1.55) pg/ml and (46.7±1.25) pg/ml respectively. It is also noticeable that the same significant decrease in age groups (19-29) and (30-40) was compared. (Figure 2C). Additionally, Sclerostin level indicated a significant increase ($p<0.05$) in the splenectomized group (28.95±1.49) pg/ml to compare with the unsplenectomized group (25.23±1.09) pg/ml (Figure 2D). The results in (Figure 2E) show that serum sclerostin levels significantly decrease ($p<0.05$) in underweight (24.44 ±0.66) pg/ml less than in the normal weight groups (31.51±2.09) pg/ml.

In the present study, Table 2 and Figure 1 show a significant increase in the serum Sclerostin level in female patients with β-thalassemia, compared with the control group, figure 1A. These results coincided with Voskaridou *et al.* (2012), suggesting that high sclerostin is an important marker for increased osteocyte activity in thalassemia patients. Especially, Sclerostin expression by osteocytes and the major function is regulating the formation of bone. Therefore, suppression of sclerostin may suppose the increase of the osteoblastic bone formation. Moreover, it plays a role important in osteoporosis (Lewiecki, 2011). A previous study suggested that the increased serum Sclerostin level in β-thalassemia is probable of many causes. One of the driving forces of drugs, the most commonly used iron chelator, is suppression of DNA synthesis, which was enhanced formation and proliferation of elements of the bone (osteoblast, fibroblast, collagen, then differentiation of osteoblast precursor), in contrast to these agents causes osteoblast apoptosis (Haidar *et al*., 2011). In addition, the study of Chen *et al*. (2013) concluded that when the use of iron chelator of such as desferrioxamine, a hypoxia-inducible factor (HIF-1α) catalyzes, thereby causes active sclerostin expression, as a chief manager of hypoxia. (HIF-1α) acts as regularly combined angiogenesis to osteogenesis. However, these hypoxias and that HIF-1α inhibited osteoblast growth through inhibiting the Wnt pathway. Ultimately, Wnt act as antagonist Sclerostin was up-regulated in osteoblasts.

Recent studies reported that most thalassemia patients suffer from many severe complications such as osteoporosis, low (BMD), and poor bone quality, resulting in decreased bone matrix and increased threat of fractures. These findings concluded that circulating sclerostin is elevated in thalassemia patients with osteoporosis and correlated with their BMD (Lapauw *et al*., 2013; Hashemieh *et al*., 2014). Baldini *et al*. (2010) explained that the imperative of the blood cell manufacture and over activation of the hematopoietic system then stimulates osteoclasts and osteoblasts, all of these risk factors for enhancing bone turnover and osteoporosis cooperates with increase sclerostin expression. Figure 1B found that circulating Sclerostin level significantly decreased in β-thalassemia major compared with thalassemia intermedia. The reason, but it is possible that the study subjects had a wide range age of about (19) in patients with β- thalassemia major but the range of age patients with thalassemia intermedia about to (33), which leads to affect the relationship between sclerostin and age. In this study, age-related to sclerostin levels in females showed a significant increase in serum sclerostin associated with progressed age in β-thalassemia patients figure 1C. These were consistent with Mödder *et al*. (2011), who revealed that lower serum sclerostin in young women under 30 years resulted in skeletal immaturity, lower osteocytes activity, or both. In addition, Wnt-related protein expression by osteoblastic was regulated by aging. The researchers reported that it related to age and increased sclerostin levels. It seems that aging increases active osteocytes for sclerostin production; however, physiological changes that companion with age, such as disorder in some hormones, possibly will contribute to the rise of sclerostin (Ardaw *et al*., 2011).

The study showed a significant decrease in the serum sclerostin level in underweight as compared with normal weight of female patients with β-thalassemia Figure 1D. These are founding agreement with the results of Klangjareonchai *et al*. (2014), which concluded that sclerostin, an osteocyte-specific protein, is found related to adiposity and glucose metabolism. Many studies have observed sclerostin found positively related to BMI or other measures of adiposity in studies of non-diabetic subjects (Urano *et al*., 2012; Sheng *et al*., 2012; Amrein *et al*., 2012). Study each of Yeo Pei *et al*. (2014), and Hashemieh *et al*. (2014) revealed that low bone mineral density (BMD), growth failure, osteopenia, and osteoporosis in later life are significant problems in children with β-thalassemia. In addition, a confident relationship between serum sclerostin and BMD or bone mineral content is also found in healthy adults (Mödder *et al*., 2011; Garnero *et al*., 2013). One interpretation is that bones with higher mass contain more osteocytes, which secrete more sclerostin than the fewer osteocytes in a skeleton

of the lower mass (Richards *et al*., 2012).

All these problems are an effect of decreasing BMI in patients with β-thalassemia, and the present study hypothesis that serum sclerostin level decrease in underweight groups of these patients, consequently increased BMI followed by elevating of BMD, which attendant to increase of sclerostin level. Figure 1E observed a significant increase in serum Sclerostin level in the splenectomized group compared with the non-splenectomized group of female patients with β-thalassemia.

The reasons for this are unclear, but a probable increase in sclerostin levels might reflect the increased average age of splenectomized, which showed in the results of the current study (19.83±1.49) are higher than in non-splenectomized patients (14.3±1.14) and increased sclerostin level with progress age-previous discussed. On the other hand, the non-splenectomized group in the present study revealed low BMI (15.69±0.57) kg/m2 in comparison of those in the splenectomized group (17.82 ± 0.61) kg/m^2, these compatible with Salih and Al-Mosawy (2013), which explained decreasing underweight frequency in splenectomized patients. Since the sclerostin level decrease in the underweight group that was previously discussed in the present study led to increasing the sclerostin level of the splenectomized group, the results may discuss as the fluctuations in serum sclerostin related to other biological changeability such as nutritional, physical activity, and other existence factors for individuals.

3.3. Relationship of Sclerostin level with the hematological Parameters in beta-thalassemia patients

The correlation coefficient of sclerostin with other variables in beta-thalassemia patients showed in Table 2. Serum level of Sclerostin no correlated with RBC (r=0.094), PCV (r=0.031), and, Hb (R =0.054), respectively. While it is correlated positively significantly ($p<0.05$) with WBC (r=0.770) and PLT and (r=0.260), respectively. A positive significance ($p<0.05$) correlated between Sclerostin level with Serum Iron (r =0.513) and Ferritin levels (r =0.522). The current study results have found serum concentration of Sclerostin nonexistence of a relationship with RBC, PCV, and HB. These results presented a significantly positive correlation to WBC and PLT, iron, and ferritin level. Elevated sclerostin level in thalassemia patients is related to osteoporosis, which refers to an imbalance between bone cells, active osteoblasts, osteoclasts, and osteocytes (Voskaridou *et al.,* 2012). Inflammation influence of bone cells activity, the result of the activation of leukocytes is in patients with β-thalassemia stimulation of proinflammatory cytokines, thereby inducing osteocytes to release sclerostin (McLean, 2009). A recent study showed the development of osteoporosis and bone marrow density in β-thalassemia major directly correlated with iron overload, ferritin level, and liver iron concentration (Rossi *et al*., 2014). As the sclerostin is an important elemental in the progress of osteoporosis in these patients (Voskaridou *et al.,* 2012), the present study is educated that elevated serum sclerostin level is associated with a high level of iron. A previous study demonstrated that oxidative stress result from iron overload might be a necessary mechanism of the negative effects of aging on bone mass and strength (Manolagas, 2010). An increase in sclerostin level is possible due to ROS rise, which greatly impacts the generation and survival of bone cells, including osteoclasts, osteoblasts, and osteocytes, by high effects of oxidative stress on apoptosis osteoblast. Iron level indirectly affected the sclerostin level. Endocrinopathies are frequent in thalassemia patients due to the oxidative stress that causes the damage of these endocrine organs (Ardawi *et al.,* 2012; Garnero *et al*., 2013). Likely, iron overload reduced the synthesis and release of their hormones such as parathyroid and estrogen hormones by iron overload. These hormones act as sclerostin production antagonists, increasing sclerostin expression.

4. CONCLUSIONS:

Sclerostin plays an important role in beta-thalassemia patients and can serve as a biomarker associated with the bone pathophysiology and indicator to prevent the continuation of such serious diseases caused by iron overload in these patients.

5. DECLARATIONS

5.1. Study Limitations

No limitations were known at the time of the study.

5.2. Acknowledgements

The authors would like to express their gratitude to all participants of thalassemic patients

in the Thalassemia Center of Al–Zahraa Educational Hospital in Al–Najaf province, and the Department of Biology of the University Kufa for their assistance.

5.3. Funding source

The authors funded this research.

5.4. Competing Interests

The authors have declared that no competing interests exist.

5.5. Open Access

6. HUMAN AND ANIMAL-RELATED STUDIES

The work involves the use of the database of the thalassemia patients.

6.1. Ethical Approval

The Ethics Committee approved this study protocol of Faculty of Science, Kufa University at approval number 2014, and conducted in accordance with the Declaration of Helsinki.

6.2. Informed Consent

Informed consent was verbally obtained from the participants as well as from the parents of the minor participants.

7. REFERENCES:

1. **Galanello,** R., and Origa, R. (2010). Beta-thalassemia. Orphanet journal of rare diseases, 5(1), 1-15.
2. **Almousawi**, A. S., and Sharba, I. R. (2019). Erythroferrone Hormone, a Novel Biomarker, is associated with Anemia and Iron Overload in Beta-Thalassemia Patients. Journal of Physics: Conference Series, 1294, 062045.
3. **Delgado-Calle**, J., Sato, A. Y., and Bellido, T. (2017). Role and mechanism of action of sclerostin in bone. Bone, 96, 29-37.
4. **Sapunarova,** K., Goranova-Marinova, V., Georgiev, P., Deneva, T., Tsvetkova, S., & Grudeva-Popova, Z. (2020). Associations of serum sclerostin with bone mineral density, markers of bone metabolism, and thalassemia characteristics in adult patients with transfusion-dependent beta-thalassemia. Annals of medicine, 52(3-4), 94–108.
5. **Wehmeyer**, C., Frank, S., Beckmann, D., Böttcher, M., Cromme, C., König, U., Fennen, M; Held, A; Paruze, P; Hartmann, C; Stratis, A; and Dankbar, B. (2016). Sclerostin inhibition promotes TNF-dependent inflammatory joint destruction. Science translational medicine, 8(330), 330ra35-330ra35.
6. **Amrein** K, Amrein S, Drexler C, Dimai HP, Dobnig H, Pfeifer K, Tomaschitz A, Pieber TR, and Fahrleitner-Pammer A. (2012).Sclerostin and its association with physical activity, age, gender, body composition, and bone mineral content in healthy adults. J Clin Endocrinol Metab. 97(1):148–154.
7. **Ardawi** M. S., Rouzi A. A., Al-Sibiani S. A., Al-Senani N. S., Qari M. H., and Mousa SA. (2012). High serum sclerostin predicts the occurrence of osteoporotic fractures in postmenopausal women: The Center of Excellence for Osteoporosis Research Study. J Bone Miner Res. 27(12):2592–2602.
8. **Arshad** B, Iqbal T, Jami A and Hasan IJ. (2014). Hematological and Biochemical Changes in Male Patients with Thalassemia Major. Pak. j. life soc. Sci. 12(1): 31-35.
9. **Baldini M,** Forti S, Marcon A, Ulivieri FM, Orsatti A, Tampieri B, Airaghi L, Zanaboni L, and Cappellini MD**.** (2010). Endocrine and bone disease in appropriately treated adult patients with beta-thalassemia major. Annals of Hematology.89(12):1207-1213.
10. **Bellido** T, Saini V, and Pajevic PD. (2013). Effects of PTH on osteocyte

function. Bone 54 (2): 250–7.

11. **Center** for Disease Control (CDC). (2014). Body Mass Index: BMI for Children and Teens.

12. **Chen** D, Li Y, Zhou Z, Wu C, Xing Y, Zou Y, and Tian W. (2013). HIF-1α Inhibits Wnt Signaling Pathway by Activating Sost Expression in Osteoblasts. PLoS ONE. 8(6): e65940.

13. **Drake** MT, Srinivasan B, Modder UI, Peterson JM, McCready LK, Riggs BL, Dwyer D, Stolina M, Kostenuik P, and Khosla S. (2010). Effects of parathyroid hormone treatment on circulating sclerostin levels in postmenopausal women. J Clin Endocrinol Metab. 95(11):5056-5062.

14. **Easa** ZO. (2009). Complications of High Serum Ferritin Level after Splenectomy in â Thalassemic Patients. Kufa Med. Journal. 12(1):243-250.

15. **Eissa** DS and El-Gamal RA. (2014). Iron overload in transfusion-dependent β-thalassemia patients: defining parameters of comorbidities. Egypt J Haematol. 39(3):164-70.

16. **Garnero** P, Sornay-Rendu E, Munoz F, Borel O, and Chapurlat RD. (2013). Association of serum sclerostin with bone mineral density, bone turnover, steroid, and parathyroid hormones, and fracture risk in postmenopausal women: the OFELY study. Osteoporos Int. 24(2):489–494

17. **Ginzburg** Y. and Rivella S. (2012). β-thalassemia: a model for elucidating the dynamic regulation of ineffective erythropoiesis and iron metabolism. Blood. 118 (16): 4321-4330.

18. **Haidar** RK, Musallam M, and Taher AT. (2011). Bone disease and skeletal complications in patients with β- thalassemia major. Bone. 48(3): 425–432.

19. **Hashemieh** M, Azarkeivan A, Radfar M, Saneifard H, Hosseini-Zijoud SM, Noghabaei G, and Yaseri M. (2014). Prevalence of Osteoporosis among Thalassemia Patients from Zafar Adult Thalassemia Clinic, Iran. IRANIAN JOURNAL OF BLOOD AND CANCER (IJBC). 6(3): 143-148

20. **Ibrahim** HA, Fouda MI, Yahya RS, Abousamra NK, Abd Elazim RA (2013b). Erythrocyte Phosphatidylserine Exposure in β-Thalassemia. J Blood Lymph 4: 115.

21. **Klangjareonchai** T, Nimitphong H, Saetung S, Bhirommuang N, Samittarucksa R, Chanprasertyothin S, Sudatip R, and Ongphiphadhanakul B. (2014). Circulating sclerostin and irisin are related and interact with gender to influence adiposity in adults with prediabetes. Int J Endocrinol. 2014:261545.

22. **Kim** MK, Lee JW, Baek KH, Song KH, Kown HS, Oh KW, Jang EH, Kang M, and Lee KW. (2013). Endocrinopathies in transfusion-associated iron overload. Clinical Endocrinology. 78(2):271–277.

23. **Lapauw B,** Vandewalle S, Taes Y, Goemaere S, Zmierczak H, Collette J, and Kaufman JM. (2013). Serum Sclerostin Levels in Men with Idiopathic Osteoporosis. Eur Jn Endocrinol. 168(4):615-620.

24. **Lewiecki** EM. (2011). Sclerostin: a novel target for intervention in the treatment of osteoporosis. Discov Med. 12(65):263–273.

25. Manali Arora, Nayeemuddin SM, Ghatak S, Singh B. (2015). Growth Impairment and Dental Caries in Thalassemia Major Patients. Indian Journal of Clinical Anatomy and Physiology (IJCAP). 1(1): 15-21.

26. **Manolagas** SC. (2010). From estrogen-centric to aging and oxidative stress: a revised perspective of the pathogenesis of osteoporosis. Endocr. Rev. 31(3): 266–300.

27. **McLean** RR. (2009). Proinflammatory cytokines and osteoporosis. Curr Osteoporos. Rep. 7(4):134-139.

28. **Mödder** UI , Hoey KA , Amin S , McCready L K , Achenbach SJ , Riggs BL , Melton LJ , an d Khosla S. (2011). Relation of age, gender, and bone mass to circulating sclerostin levels in women and men. J Bone Miner Res 26(11):373–379.

29. **Moester** MJ, Papapoulos SE, Löwik CW, and van Bezooijen RL. (2010). Sclerostin: Current knowledge and future perspectives. Calcif Tissue Int 87(2): 99-107.

30. **Morse** LR, Sudhakar S, Danilack V, Tun C, Lazzari A, Gagnon DR, Garshick E, and

Battaglino RA. (2012). Association between sclerostin and bone density in chronic spinal cord injury. J Bone Miner Res. 27(2):352–359.

31. **Pasricha** SR, Frazer DM, Bowden DK, and Anderson GJ. (2013). Transfusion suppresses erythropoiesis and increases hepcidin in adult patients with β-thalassemia major: a longitudinal study. Blood. 122(1):124-133.

32. **Pelletier** S, Dubourg L, Carlier MC, Hadj-Aissa A, and Fouque D. (2013).The relation between renal function and serum sclerostin in adult patients with CKD. Clin J Am Soc Nephrol. 8(5):819–823.

33. **Persijn**, J.P., Clin. ACTA 35:91, (1971).phenotype of beta-thalassemia. Proc Natl Acad Sci USA105:1620–1625.

34. **Richards** WG, Ke HZ, Li X, and Ominsky MS. (2012). Sclerostin and Dickkopf-1 as therapeutic targets in bone diseases. Endocr Rev. 33(5):747–783.

35. **Rossi** F, Perrotta S, Bellini G, Luongo L, Tortora C, Siniscalco D, Francese M, Torella M, Nobili B, Di Marzo, and Maione S. (2014). Iron overload causes osteoporosis in thalassemia major patients through interaction with transient receptor potential vanilloid type1 TRPV1channels. Haematologica. 99(12):1876-84.

36. **Salih** KM and Al-Mosawy WF. (2013). Evaluation Some Consequences of Thalassemia Major in Splenectomized and Non-Splenectomized Iraqi Patients. Int J Pharm Pharm Sci, 5(4): 385-388.

37. **Shanthi** G, Balasubramanyam D, and Srinivasan R. (2013). Studies on the Haematological Aspects of Beta β–Thalassemia in Tamilnadu. RJPBCS. 4(3): 784-790.

38. **Sheng** Z, Tong D, Ou Y, Zhang H, Zhang Z, Li S, Zhou J, Zhang J, and Liao E. (2012). Serum sclerostin levels were positively correlated with fat mass and bone mineral density in Central South Chinese postmenopausal women. Clinical Endocrinology (Oxf). 76(6):797–801.

39. **Skordis** N. (2011). Endocrine investigation and follow-up in Thalassemia Time for specific guidelines. Thalassemia Reports. 1(s2):e22, 70-82.

40. **Taher** AT, Musallam KM, Cappellini MD, Weatherall DJ. (2011). Optimal management of beta-thalassemia intermedia. Br J Haematol. 152(5):512-23.

41. Taher AT, Porter JB, Viprakasit V, Kattamis A, Chuncharunee S, Sutcharitchan P, Siritanaratkul N, Galanello R, Karakas Z, Lawniczek T, Habr D, Ros J, Zhu Z, and Cappellini MD. (2012). Deferasirox continues to reduce iron overload in non-transfusion-dependent thalassemia: a one-year, open-label extension to a one-year, randomized, double-blind, placebo-controlled study. Blood. 120(5):970-977.

42. **Terpos** E, Christoulas D, Katodritou E, Bratengeier C, Gkotzamanidou M, Michalis E, Delimpasi S, Pouli1 A, Meletis J, Kastritis E, Zervas K and Dimopoulos M. (2012). Elevated circulating sclerostin correlates with advanced disease features and abnormal bone remodeling in symptomatic myeloma: reduction post-bortezomib monotherapy. Int J Cancer.131:1466–1471.

43. **Thein** SL. (2013). Molecular basis of β-thalassemia. Cold Spring Harb Perspect Med. 3(5):a011700.

44. **Urano** T, Shiraki M, Ouchi Y, and Inoue S. (2012). Association of circulating sclerostin levels with fat mass and metabolic disease-related markers in Japanese postmenopausal women. Journal of Clinical Endocrinology and Metabolism. 97(8): E1473–E1477.

45. **Voskaridou** E, Christoulas D, Plata E, Bratengeier C, Anastasilakis AD, Komninaka V, Kaliontzi D, Gkotzamanidou M, Polyzos SA, Dimopoulou M, and Terpos E. (2012). High circulating levels of sclerostin correlate with bone mineral density in patients with thalassemia and osteoporosis: the role of the Wnt signaling in the pathogenesis of bone loss in thalassemia. Horm Metab Res. 44(12):909-13.

46. **Wasmuth** AK. (2010). Evaluation of the Mythic 18, hematology analyzer for its use in dogs, cats, and horses. Inaugural-Dissertation. Faculty of Veterinary Medicine, University of Zurich.

47. **Wijenayaka** AR, Kogawa M, Lim HP, Bonewald LF, Findlay DM, and Atkins GJ. (2011). Sclerostin Stimulates Osteocyte Support of Osteoclast Activity by a RANKL-

Dependent Pathway. PLoS One 6:e25900.

48. **World** Health Organization (WHO). (2006). BMI Classification". Global Database on Body Mass Index.

49. **Yassin** M, Sirdah M, Al Haddad R, Lubbad AM, Al-Yazji M. (2013). Genotype-phenotype characteristics of β thalassemia children in the Gaza Strip, Palestine. J Genet Disor Genet. 2:2.

50. **Yeo** PS, Noor AM, Suzana S, and Roslee R. (2014). Bone Health Status among Thalassemia Children. International Journal of Public Health Research. 4(1):399-404.

Table 1. *Demographic of the clinical characteristics between female patients with β-thalassemia and the healthy controls*

Clinical characteristics	Patients n= 69	Healthy Controls n= 20	P- Value
Age (year)	16.62 ± 0.96	20.75 ± 1.86	
Group (8 – 18) n (%)	51(74%)		0.612
Group (19 – 29) n (%)	12(17.4%)		
Group (30 – 40) n (%)	6(8.7%)		
Major βT n (%)	54(78.2%)	0	NA
Intermedia n (%)	15(21.8%)	0	
Hb (mg/dl)	7.7 ± 0.14 *	12.01 ± 0.19	0.027
RBC (10^6/ml)	3.13 ± 0.07 *	4.36 ± 0.07	0.038
WBC (10^3/ml)	11.05 ± 0.26 *	7.59 ± 0.33	0.036
PCV %	23 ± 0.41 *	36.34± 0.52	0.036
PLT (10^3/ml)	361.86 ± 13.92 *	244 ± 14.23	0.034
BMI (kg/m^2)	17.59 ± 0.43 *	22.15 ± 0.36/	
Underweight, n (%)	13.09±0.52, 40(58%)	0	0.001
Normal weight, n (%)	23.7±2.04, 29(42%)	20(100%)	
Iron (µg/ml)	172.2 ± 4.4 *	29.86 ± 2.32	0.0001
Ferritin (ng /ml)	5156.5 ± 438.7 *	99.15 ± 8.95	0.0001
Splenectomized n (%)	29 (42%)	0	NA
Unsplenectomized n (%)	40(58%)	0	NA

* statistically significant at p< 0.05; NA: not application; RBC: red blood corpuscles; Hb: hemoglobin; PCV: pact corpuscular volume; WBC: White Blood Cells. BMI: body max index; PLT: platelets. Data represented as mean± standard division.

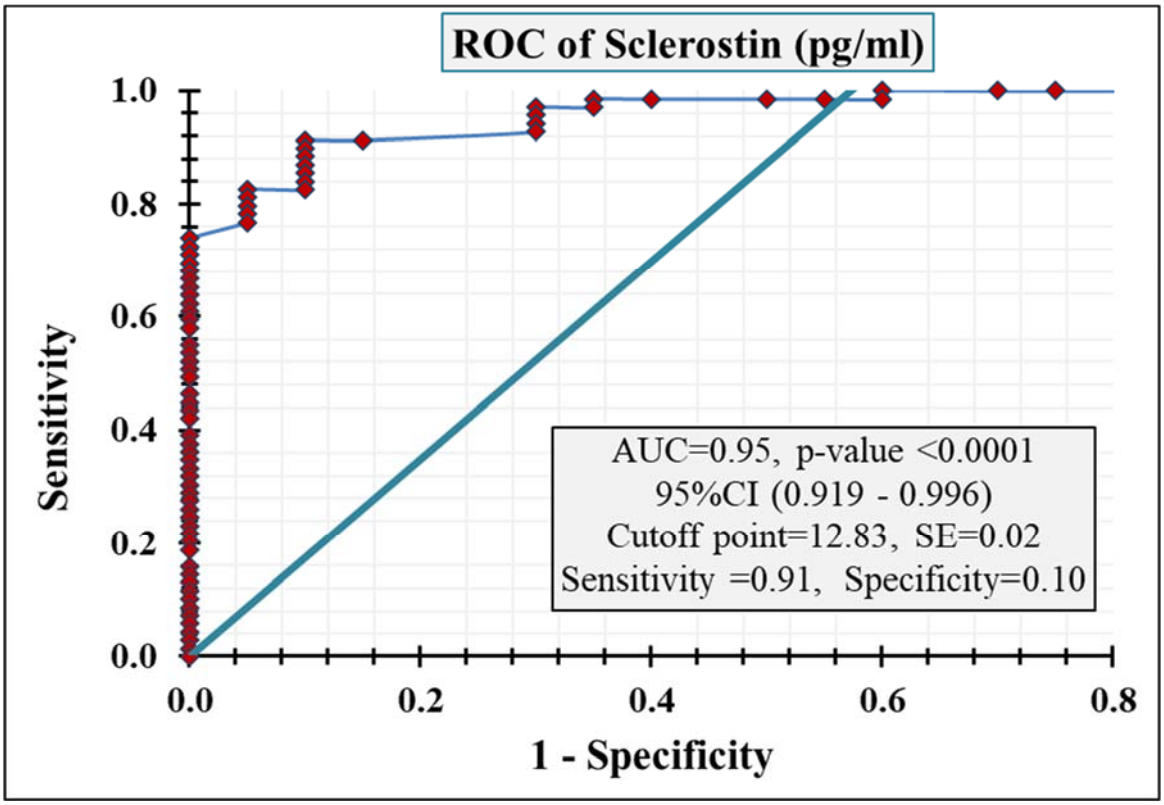

Figure 1. *ROC curves of sclerostin for beta-thalassemia patients. ROC: receiver operating characteristic; AUC: area under the curve*

Table 2: Correlation coefficient of sclerostin with other variables in beta-thalassemia patients

.

Variables	Sclerostin (pg/ml)	
	P-value	R
RBC (10^6/ml)	0.440	0.094
PCV %	0.751	0.031
PLT (10^3/ml)	0.030	0.260 *
Hb (mg/dl)	0.661	0.054
WBC (10^3/ml)	0.001	0.770 **
Iron (µg/ml)	0.0006	0.513 **
Ferritin (µg/ml)	0.0005	0.522 **

Significant difference * p-value <0.05. ** p-value <0.01

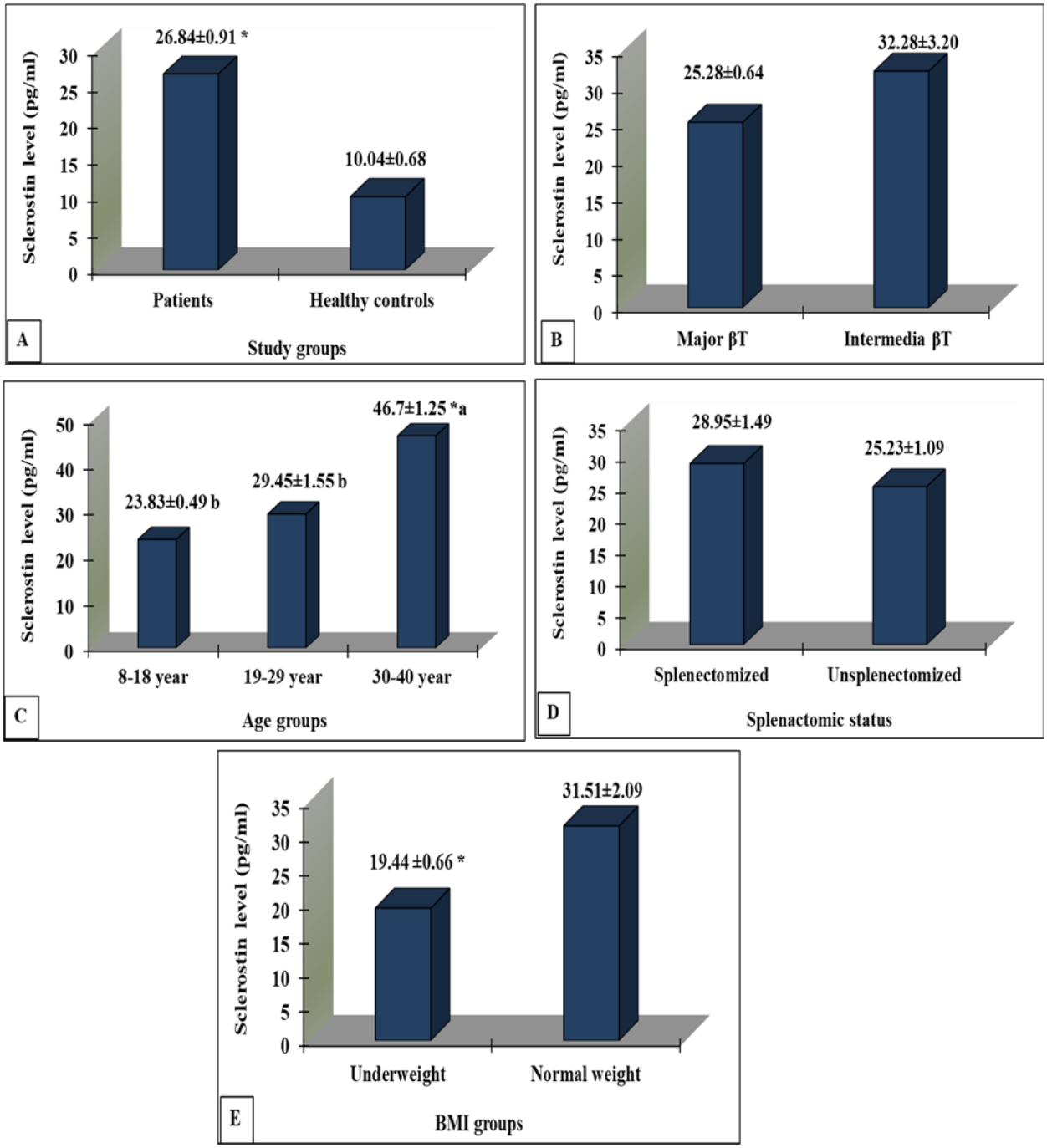

Figure 2. A: Comparison of Sclerostin levels in studied groups βT patients and healthy control groups. B: Effects of thalassemia types on Sclerostin levels in patients with βT major and βT intermedia. C: Effects of Age on Sclerostin levels among age groups. D: Effects of splenectomy status on Sclerostin levels in splenectomized and un splenectomized groups. E: Effects of BMI on Sclerostin levels in underweight and normal-weight groups. * and deferent litters significant $p<0.05$. data represented as mean ±SD

SOUTHERN BRAZILIAN JOURNAL OF CHEMISTRY

COMPARISON OF TWO STAINING METHODS FOR ANODIZING IN ALLOY 6063 ALUMINUM PROFILES

PESSUTTO, Ana Carla[1*]; JONKO, Eliena[2];

[1]Universidade de Caxias do Sul, Engenharia Química.

[2] Universidade de Caxias do Sul, Laboratório de Corrosão e Proteção Superficial.

** Corresponding author*
e-mail: acpessutto1@gmail.com

Received 15 October 2021; received in revised form 30 November 2021; accepted 02 December 2021

ABSTRACT

Background: Aluminum stands out for being a light, corrosion-resistant, and recyclable metal, achieving wide coverage in the market. When incorporated into alloying elements, it is possible to acquire other desirable characteristics. Alloy 6063, intended for architectural purposes, has aesthetic, structural, and strength functions. Anodized finishing is performed through an electrolytic process, ensuring a more resistant aluminum oxide film than that formed naturally. For decorative purposes, the anodic film coloration can be performed by several methodologies, in this case, for the coloration by organic adsorption, with the use of aniline, and the electrolytic coloration, composed of tin sulfate salts, both for obtaining the black color. **Aim:** Compare of two different staining methods on the surface of anodized profiles of aluminum alloy 6063. **Methods:** Profile samples were collected and tests were carried out to measure the thickness of the anodic layer, immersion tests with 3,5 percent sodium chloride, for 1000 hours, and neutral saline mist, for 600 hours. **Results and Discussion**: Both methodologies proved to be resistant to immersion tests with sodium chloride, as well as with neutral saline mist, and these tests are quite aggressive and provide corrosion of the material when not well treated. Corrosion points were only seen at the intersections performed, and in the rest of thearea, no points were detected. **Conclusions:** The result of both methodologies was positive, considering tht there was no corrosion in the tested samples, except in the intersections performed, as well as the maintenance of the color in both tested methodologies, which was not expected in the literature. For future work, it is suggested to deepen the study to perform electrochemical impedance spectroscopy tests for exaluate the strength of the anodic film and perform anodizing with the same parameters, however, with different anilines to analyze their behavior.

Keywords: *Aluminium alloys. Anodizing. Corrosion resistance. Coloring.*

1. INTRODUÇÃO

O mercado do alumínio (Al) em escala industrial no Brasil, de acordo com informações da Revista Alumínio (2019), registrou aumento no consumo de produtos fabricados de Al em cerca de 10 % do ano de 2017 para o ano de 2018, sendo este oriundo de matéria-prima virgem e de reciclagem, com tonelagem de 1 milhão e 383 mil.

Levando-se em consideração as questões ambientais, em alta no atual cenário mundial, é de suma importância avaliar os impactos causados durante a produção e a utilização dos metais. Dentre estes, o Al tem destaque por ser um metal leve e versátil, além de resistente à corrosão e reciclável, obtendo ampla aplicação no mercado.

Em busca de materiais com durabilidade, resistência à corrosão e de embelezamento da superfície, podem ser realizados, embasado na engenharia de superfície, tratamentos que envolvem as mudanças das propriedades visando obter estas características.

A anodização é um dos tipos tratamentos de superfície mais aplicados sobre peças de Al. O processo é realizado com o intuito de formar uma fina camada de óxido de alumínio (Al_2O_3) que possibilita o aumento da vida útil do material, principalmente pelo fato de formar um filme cristalino, com poros de maior espessura, resistente à abrasão e à corrosão, proporcionando maior durabilidade aos meios que ficará exposto.

Devido à camada de óxido ser bastante porosa, a mesma pode vir a ser base para a aplicação de cores, quando o material for utilizado para fins decorativos. Há diferentes metodologias que podem propiciar cor ao material, sendo as

mais frequentes a pôr imersão, através da adsorção de substâncias orgânicas com o uso de anilinas ou outros componentes; e a pôr coloração eletrolítica, com o auxílio de eletrólitos e de sais metálicos, havendo entre estes processos diferenciações na aparência e na durabilidade.

Com isso, verifica-se a necessidade de comparar estes dois métodos para colorir a camada anódica sobre perfis da liga de alumínio 6063, avaliando-se o desempenho da resistência que o material possui contra a corrosão em meios neutros e em meios agressivos, além da resistência às intempéries enquadrados em cada processo.

2. MATERIAIS E MÉTODOS

2.1. Materiais

Os corpos de prova utilizados foram perfis extrudados de liga de alumínio AA 6063, conforme Tabela 1, com tratamento térmico de solubilização, têmpera e envelhecimento (T6), amplamente utilizado para perfis destinados à construção civil. Os corpos de prova possuiam dimensões de base, em milímetros (mm), de acordo com a Figura 1.

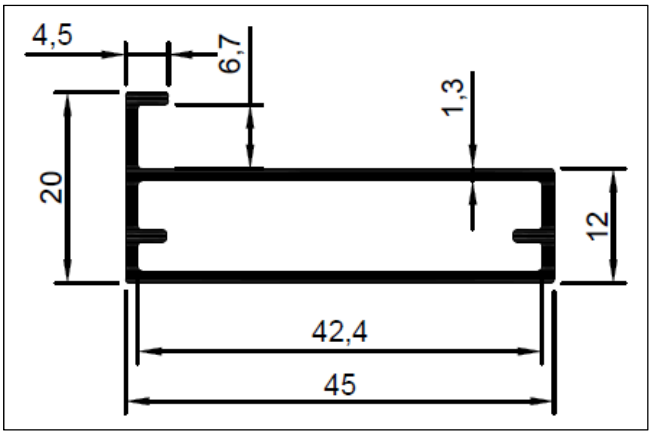

Fonte: As Autoras (2020).

Figura 1. *Base dos corpos de prova utilizados nos ensaios. Fonte: As Autoras (2020).*

O processamento dos corpos de prova foi realizado nas dependências da empresa Alumiconte Componentes de Alumínio Eireli, localizada no município de Vila Flores, no estado do Rio Grande do Sul. Ressalta-se que dados como o volume dos tanques, programas e marcas dos retificadores, bem como aditivos e marca de produtos químicos utilizados durante o processo não foram explanados por se tratar de dados de referências submetidas por acordo de sigilo industrial. As etapas foram executadas de acordo com a Figura 2.

A primeira etapa do processo foi a coleta de perfis extrudados com 6 metros de comprimento, com a liga e o tratamento térmico já especificados. Em seguida, foi realizado o jateamento mecânico, com o auxílio de um equipamento que jateia sobre os perfis milhares de pequenas esferas de aço inox a uma velocidade média de 95 mm/s.

O jateamento por granalhas é um tratamento mecânico que gera tensões residuais compressivas, endurecendo as camadas próximas à superfície, melhorando o desempenho à fadiga nesta região. Entretanto, o jateamento também proporciona um aumento na rugosidade superficial, podendo acarretar no surgimento de trincas (BORGES, 2017). O objetivo do jateamento, neste caso, remete à homogeneização da superfície, eliminando possíveis manchas e riscos, beneficiando o uso e a uniformidade do material.

Em seguida, foi realizado o corte dos corpos de prova com 20 centímetros de comprimento, por meio de uma máquina de corte da marca Emmegi, monocabeça descendente com lâmina de 400 milimetros, realizando-se o detalhamento das arestas com o auxílio de uma lima.

Os corpos de prova foram furados nas extremidades com uma fresa universal, por meio uma broca, e em seguida, enganchados com pequenos ganchos de alumínio, uns nos outros, em bases de Al de liga 6063, para que o material pudesse receber a passagem de corrente elétrica durante o processo de anodização, conforme demonstrado na Figura 3.

Fonte: As Autoras (2020).

Figura 3. *Corpos de prova enganchados com ganchos de alumínio, sendo as bases de apoio deste mesmo material, favorecendo a passagem de corrente elétrica durante o processo de anodização.*

Logo, deu-se início ao processo de anodização. Os corpos de prova foram imersos em uma solução de H_2SO_4, com concentração de 147 g/L, em temperatura ambiente de 20 ºC, durante o tempo de 10 minutos (min), caracterizado por banho de desengraxe. Neste mesmo banho havia a presença de um aditivo, que tem por função auxiliar na remoção de graxas, gorduras e outras impurezas presentes na superfície. Em seguida, passou-se por um banho de lavagem composto por água desmineralizada e elementos químicos presentes do arraste do banho anterior, também mantido a temperatura ambiente.

O banho seguinte, caracterizado por fosqueamento, possuía a composição de uma solução de hidróxido de sódio (NaOH) a uma concentração de 65,33 g/L, Al dissolvido a uma concentração de 101,7 g/L, além de um aditivo responsável por evitar a formação de lodo ou incrustações e manter o efeito acetinado uniforme. O banho possuía uma temperatura de 53 ºC e permaneceu em imersão durante o tempo de 5 min. Em seguida, os corpos de prova foram imersos em três (03) banhos de lavagem compostos por água desmineralizada e o arraste dos produtos químicos do banho anterior, que devido à viscosidade deste, necessitam de maior quantidade de lavagens, trabalhados em temperatura ambiente.

O estágio seguinte foi o banho de neutralização, composto por uma solução de H_2SO_4 a uma concentração de 147 g/L, com temperatura de 30 ºC e tempo de imersão de 5 min. O banho também continha um aditivo que tem por função auxiliar na remoção de impurezas presentes na superfície do material. Sequentemente, os corpos de prova foram submetidos ao banho de lavagem, a temperatura ambiente, composto por água desmineralizada e o arraste do banho anterior.

Na etapa seguinte, foi realizada a anodização. Nesta, o tanque havia contatos de cobre (Cu) na base superior, responsável por reter a estrutura da gancheira onde os corpos de prova estavam enganchados, o que possibilitava a condução da corrente elétrica ao material. Também era composto por eletrodos da liga de Al 6063 nas laterais e centro do tanque, posicionados verticalmente. Foi utilizado um retificador de 8.000 amperes (A) para a passagem de corrente elétrica. O banho era composto por uma solução de H_2SO_4, com concentração de 197,96 g/L e 11,16 g/L de Al dissolvido. Também foi acrescido um aditivo, que tem por função auxiliar na formação de camadas mais duras e evitar a queima do filme de óxido de alumínio.

A temperatura do banho de anodização estava em 21 ºC, com aceitação de variação de ± 2 ºC, durante a imersão por 30 min, com uma densidade de corrente em 1,5 A/dm², para uma espessura de aproximadamente 20 micrometros (µm).

Para que se pudesse manter a temperatura dentro desta faixa, tendo em vista que a reação da formação do óxido de alumínio gera calor, utilizou-se um chiller da marca York e um trocador de calor de placas, da marca APV, modelo SR-26 B. Posteriormente, os corpos de prova passaram por dois (02) banhos de lavagem compostos por água desmineralizada e elementos químicos presentes devido ao arraste do banho anterior, em temperatura ambiente.

Após, a camada anódica formada sobre a superfície dos corpos de prova foi colorida. Os estágios foram realizados de maneiras diferentes para os dois métodos de coloração aplicados.

Para a coloração eletrolítica, os corpos de prova foram direcionados ao banho de coloração eletrolítica composto por sais de $SnSO_4$, com concentração de 10,81 g/L na solução, em temperatura de 24 ºC, e aceitação de variação de ± 1 ºC. Também constituído por H_2SO_4 a 20 g/L e

por um aditivo, responsável pela estabilidade e uniformidade de cor dos corpos de prova, evitando que ocorra a redução do estanho, além de auxiliar na condutividade elétrica do banho. Neste estágio, assim como no banho de anodização, contava-se com a presença de contatos de cobre (Cu) para a condutividade de corrente, além de eletrodos posicionados nas laterais e no centro do banho, compostos de aço inox 316. O equipamento de coloração utilizado nesta etapa foi de 4.000 A e manteve-se 0,8 A/dm². Para obter-se a coloração preta, o retificador possuia um programa com diferentes correntes, tempos e amplitudes de onda, que desta forma, depositaram o Sn na base do poro. Para o preto, o tempo de imersão sob ação da corrente foi de 12 min. Posteriormente, os corpos de prova foram imersos em um banho de lavagem composto por água desmineralizada e os elementos químicos presentes no banho anterior, devido arraste, à temperatura ambiente.

Em seguida, os corpos de prova foram direcionados para a selagem, descrita como "selagem A" na Figura 2. Este banho possuía Níquel (Ni) a 1467,75 ppm e Fluor (F) a 700 ppm, além do pH mantido em 6,80. A temperatura do banho era de 30 ºC e o tempo de imersão deve ser relativo à camada formada, mantendo-se 1 min/µm. Neste caso, os corpos de prova foram mantidos imersos por 20 min. Posteriormente, os corpos de prova foram imersos em uma lavagem composta por água desmineralizada, Ni e F, além de outros possíveis contaminantes.

Após, os corpos de prova foram mantidos por 30 min em uma estufa com temperatura próxima a 75 ºC, com queima por GLP (gás liquefeito de petróleo) para a secagem completa do material.

Para a realização da coloração por adsorção orgânica, os corpos de prova passaram pelos mesmos processos de jateamento até a etapa de anodização e formação do filme anódico, com mesmas condições de processo já citadas.

Posteriormente, foram encaminhados para o laboratório onde foi preparado um banho em laboratório, onde os corpos de prova foram imersos em uma solução contendo anilina na cor preta, Sanodal Preto Escuro H-BL, da marca Clariant, com concentração de 10 g/L, à temperatura de 57 ºC, e faixa de aceitação ± 2 ºC, durante o tempo de imersão de 30 min. A solução foi tamponada com acetato de sódio, em concentração de 8 g/L e com ácido acético a 0,4 mL/L, a fim de manter-se o pH em 5,6.

A anilina utilizada se destaca pela resistência à luz e ao calor, possuindo características para a exposição em áreas externas, direcionadas à fins arquitetônicos. Após, os corpos de prova foram imersos em duas etapas de lavagem, trabalhados à temperatura ambiente, compostas por água desmineralizada.

Em seguida, os corpos de prova foram direcionados a uma "selagem B", conforme descrito na Figura 2, composta por Ni a 1800 ppm e por F a 300 ppm. A selagem para as anilinas deve possuir menor concentração de F, que de acordo com o fornecedor, é necessária para evitar a perda de cor. A temperatura foi mantida em 18 ºC e o pH em 7,12, mantendo-se o tempo de imersão de 1 min/µm, que neste caso, foi de 20 min. Em seguida, os corpos de prova foram submetidos a um banho de lavagem, seguido de aquecimento na estufa durante 30 min, a 75 ºC, com queima por GLP para a secagem completa do material.

As etapas do processo realizado, de forma resumida, estão apresentadas na Tabela 2.

Por fim, todos os corpos de prova, tanto da coloração por adsorção orgânica, quanto pela coloração eletrolítica, foram direcionados aos ensaios de caracterização.

2.2. Métodos

Os métodos de análise foram realizados a fim de obter-se um padrão comparativo entre as metodologias de coloração do filme anódico por adsorção orgânica e por coloração eletrolítica.

2.2.1. Microscopia eletrônica de varredura por emissão de campo (MEV/FEG)

Para a visualização da superfície a nível microscópico foi realizado um ensaio através de um microscópio eletrônico de varredura por emissão de campo (MEV/FEG), da marca Tescan, modelo Mira 3, que consegue fazer a ampliação de determinada amostra em até um milhão de vezes. No EDS energia foi utilizado um detector do tipo SSD (*silicon drift detector*), foi possível obter análises qualitativas, além da distribuição elementar para obtenção dos elementos químicos presentes no material (UCS, 2020). Este ensaio foi realizado no Laboratório Central de Microscopia (LCMIC), da Universidade de Caxias do Sul (UCS).

Foi realizada a verificação da morfologia do filme anódico transversalmente e a medição da espessura da camada anódica. Os corpos de prova foram cortados com lado de 20 mm através

do auxílio de uma fresa universal de metal duro. Após, realizou-se o embutimento em moldes a fim de facilitar o manuseio, se fazendo necessário o lixamento e polimento no sentido da camada anódica para o metal (ABNT NBR 12611:2006). As amostras já embutidas, lixadas e polidas são apresentadas pela Figura 4.

Fonte: As Autoras (2020).

Figura 4. *Corpos de prova embutidos para a leitura da espessura da camada anódica no MEV/FEG.*

Como o embutimento foi realizado com material isolante, eles tendem a acumular a carga elétrica do feixe primário e geram artefatos na imagem. Deste modo, tornou-se necessário o recobrimento das amostras com ouro (processo de metalização ou "*sputtering*"), onde o depósito do metal é realizado em vaporização a vácuo (PVD), sendo este bastante eficiente, mesmo em objetos muito irregulares, pois os átomos atingem sua superfície oriundos de todas as direções, melhorando o sinal e a qualidade das imagens. A marca da metalizadora é Benton Deck V e este procedimento foi realizado no Laboratório Central de Microscopia (LCMIC), da Universidade de Caxias do Sul (UCS).

A espessura da camada de ouro (Au) deve ser suficientemente fina para não influir na resolução da imagem, mas suficientemente espessa, para garantir uma boa produção de elétrons secundários, que serão usados para formar a imagem. Devido este elemento químico não fazer referência ao processo aplicado aos corpos de prova, não será realizada a avaliação do mesmo.

2.2.2. Névoa Salina Neutra

Para a exposição dos corpos de prova em névoa salina neutra, tem-se por base as normas ASTM B117 (2018). O método consiste em manter os corpos de prova em uma câmara fechada que simula a atmosfera marinha, sob um ambiente corrosivo controlado, por meio de uma solução de cloreto de sódio (NaCl P.A.) a 5 % ± 1 %, com pH mantido em uma faixa de 6,5 a 7,2 e temperatura de 35 ºC ± 2 ºC (PERTILE; BEUX; BIRRIEL, 2018).

O ensaio foi realizado no Laboratório de Corrosão e Proteção Superficial (LCOR), da UCS, que realiza ensaios de corrosão para verificação de desempenho e caracterização de materiais com um equipamento da marca Bass, modelo USX-6000/2009 - Cíclico.

Todos os corpos de prova foram limpos, previamente, com água deionizada e a proteção de bordas foi procedida com cera de abelha.

2.2.3. Ensaio de Imersão

O ensaio de imersão foi baseado na norma ASTM G31-12a para a determinação dos fatores que influenciam na corrosão do alumínio com tratamento de conversão por anodização. Este consiste em imergir os corpos de provas em béqueres, com temperatura ambiente, por um período pré-determinado. Os principais efeitos que podem ser analisados e considerados a olho nu são a descoloração, mudança de brilho e pontos de corrosão. Também foi realizado um corte em forma de X em cada corpo de prova.

Foram utilizadas as soluções de NaOH 0,1 M, H_2SO_4 0,1 M e NaCl a 3,5 % em béqueres de vidro de 2 L. Os corpos de prova ficaram imersos, nas duas primeiras soluções durante o período de 240 horas, a temperatura ambiente, sendo o primeiro em duplicata e o segundo em triplicada para cada metodologia de coloração. Já na última solução, os corpos de prova ficaram mantidos em imersão pelo período de 1.000 horas, em triplicata. Estes ensaios foram realizados nas dependências da empresa Alumiconte Componentes de Alumínio Eireli.

3. RESULTADOS E DISCUÇÃO:

Neste Capítulo, são apresentados os resultados obtidos nos ensaios de determinação

da espessura da camada anódica. Também foram realizados os ensaios de névoa salina neutra e ensaios de imersão. Estes resultados serão comparados às especificações teóricas obtidas na literatura, com o intuito de validar o método mais apropriado e resistente quanto à aplicação da anodização, com coloração por meio dos métodos de adsorção orgânica e de coloração eletrolítica.

3.1. Análises de microscopia eletrônica de varredura (MEV/FEG)

Foram realizadas as análises morfológicas da secção transversal de corpos de prova anodizados e coloridos por adsorção orgânica e por coloração eletrolítica, além de medir a espessura da camada anódica formada.

3.1.1. Análise morfológica da secção transversal

Foi realizada a análise morfológica de corpos de prova com metodologia de coloração por adsorção orgânica por MEV/FEG, conforme demonstra a Figura 5, em sua secção transversal.

Na Figura 5 (1), pode-se observar dois corpos de prova em paralelo com magnificação de 2.000 vezes. Na descrição de (a) observa-se o substrato de alumínio, em (b) tem-se a camada anódica formada e em (c) tem-se a resina utilizada para o embutimento dos corpos de prova. Na Figura 5 (2), com magnificação de 10.000 vezes, observa-se em (a) o substrato de alumínio, em (b) o filme de óxido de alumínio e em (d) tem-se a camada barreira formada, que separa o substrato metálico do filme anódico.

A análise morfológica de corpos de prova com coloração eletrolítica por MEV/FEG é demonstrada pela Figura 6, em sua secção transversal.

Na Figura 6 (1), tem-se dois corpos de prova em paralelo com magnificação de 2.000 vezes. Na descrição de (a) apresenta-se o substrato de alumínio, em (b) tem-se a camada anódica formada e, em (c), a resina utilizada para o embutimento dos corpos de prova. Na Figura 6 (2), com magnificação de 10.000 vezes, visualiza-se em (a) o substrato de alumínio, em (b) o filme de óxido de alumínio e em (d) a camada barreira que separa o substrato metálico do filme de óxido de alumínio.

Os filmes de óxido de alumínio (Al_2O_3) apresentam-se uniformes, tanto nas imagens da secção transversal dos corpos de prova com coloração por adsorção orgânica, quanto às com coloração eletrolítica. Esta uniformidade se deve a diversos fatores do processo, dentre eles, a escolha do eletrólito, a temperatura e o tempo de imersão na solução eletrolítica.

Neste estudo foi utilizado o ácido sulfúrico como eletrólito, que de acordo com a literatura, proporciona um crescimento do filme anódico mais poroso, com caráter constante do crescimento dos poros. Com relação ao tempo de imersão nesta solução, tem-se uma relação direta com a espessura, onde quanto maior for o tempo de anodização, maior será a espessura do filme de Al_2O_3, dentro da espessura máxima que pode ser atigida nestas condições (BENSALAH *et al.*, 2009; GRUBBS, 1999 *apud* PACHECO, 2016).

3.1.2. Valores das medidas de espessuras do filme anódico

Na Figura 7 são apresentados os valores das medidas de espessura de dois corpos de prova por MEV/FEG para a metodologia de coloração por adsorção orgânica.

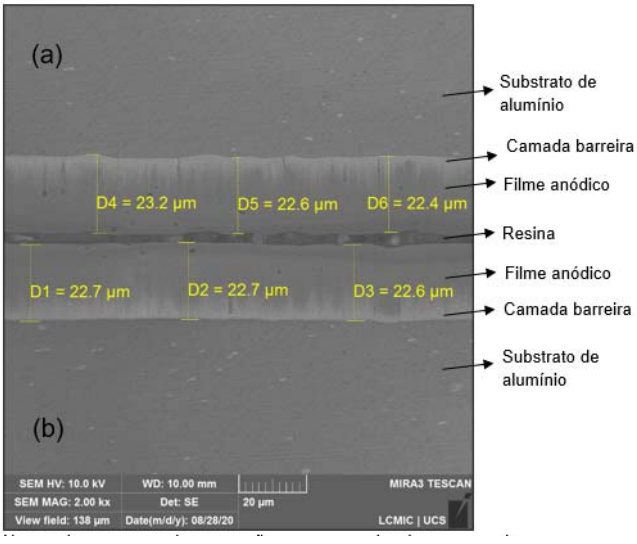

Fonte: As Autoras (2020).

Figura 7. *Valores das medidas das espessuras da camada anódica de corpos de prova com coloração por adsorção orgânica.*

No corpo de prova da Figura 7 (a), a média obtida da espessura do filme anódico é de 22,7 µm e no corpo de prova da Figura 7 (b) é de 22,7 µm. Observa-se, agora numericamente, que a camada anódica possui espessura uniforme em ambos os corpos de prova, obtendo valores próximos, e está se dá por motivos já apontados no item 4.2.1. Ressalta-se que há a presença de alguns picos e vales, que são formados devido à presença destes na própria camada do substrato do metal, tendo em vista que o filme de óxido de alumínio se forma sobre esta superfície (COURROL; PRETO, 2011).

Também foram medidas as espessuras dos corpos de prova eletrocoloridos por meio do MEV/FEG, conforme demonstra a Figura 8.

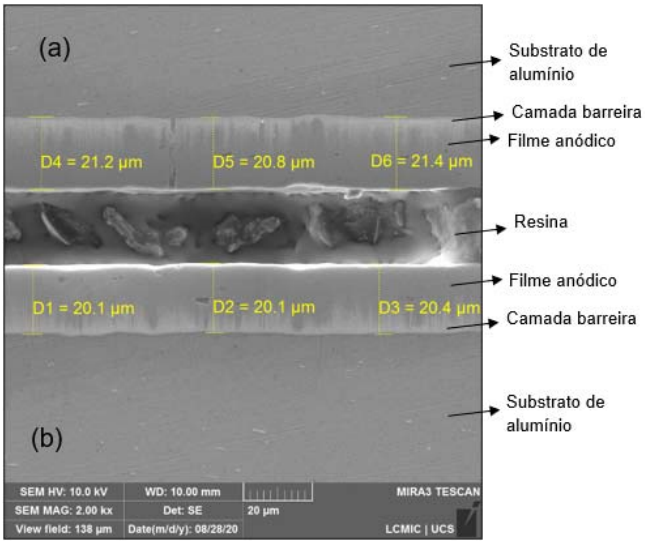

Fonte: As Autoras (2020).

Figura 8. *Valores das medidas das espessuras da camada anódica de corpos de prova com coloração eletrolítica.*

No corpo de prova da Figura 8 (a), a média obtida da espessura do filme anódico é de 21,1 µm e no corpo de prova da Figura 8 (b) é de 20,2 µm. Também é possível observar que as camadas anódicas são uniformes e regulares, com alguns picos e vales característicos do substrato do metal, assim como no método da coloração por adsorção orgânica.

É importante ressaltar que há um determinado tempo crítico, a partir do qual já não ocorre aumento da espessura do filme, uma vez que ocorre não só o crescimento do filme anódico, como a dissolução parcial do mesmo por parte do eletrólito (GRUBBS, 1999 *apud* PACHECO, 2016). Por este motivo, a metodologia de anodização para fins arquitetônicos tem limitação da espessura da camada anódica obtida.

As espessuras obtidas em ambas metodologias se enquadram na faixa de materiais aptos para exposição de alta ou excessiva agressividade, que abrangem ambientes marinhos e industriais, conforme normativa apresentada pela ABAL (ABAL, 2008), e também, pela QUALANOD (2020), que caracteriza a necessidade de uma espessura igual ou superior a 20 µm para que estes filmes anódicos possam manter a adsorção do corante e da solidez à luz.

3.2. Resultados da Névoa Salina Neutra

Foram realizados os ensaios de névoa salina neutra nos corpos de prova da metodologia de coloração por adsorção orgânica e de coloração eletrolítica.

Para a metodologia de coloração por adsorção orgânica, a olho nu, foram visualizadas previamente ao ensaio algumas manchas esbranquiçadas na superfície dos corpos de prova, de acordo com a Figura 9, onde os corpos de prova foram caracterizados por 0423/2020 pelo LCOR.

Fonte: LCOR | UCS (2020).

Figura 9. *Corpos de prova com coloração por adsorção orgânica previamente ao ensaio de névoa salina neutra.*

Após 192 horas (h) de exposição na névoa salina neutra, observou-se o surgimento de pequenas manchas em várias regiões da superfície dos três corpos de provas. Em 336 h de exposição, nenhuma alteração visual foi visualizada, se comparada às 192 h de exposição.

Posteriormente, a 504 horas, manchas maiores foram observadas sobre quase a totalidade da superfície de todos os corpos de prova, conforme apresenta a Figura 10 a e 10 b, respectivamente.

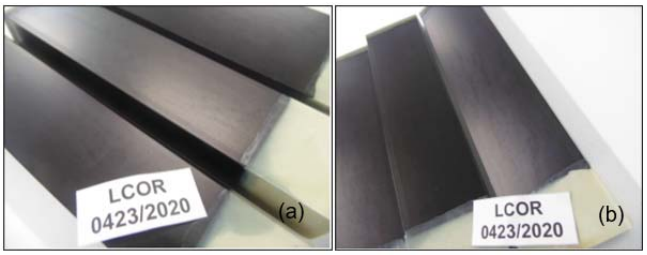

Nota: (a) referente a 192 h de exposição; (b) referente a 504 h de exposição.

Fonte: LCOR | UCS (2020).

Figura 10. *Corpos de prova com coloração por adsorção orgânica posterior exposição à névoa salina neutra após 192 h e 504 h de ensaio.*

O ensaio foi finalizado após 600 h de exposição, onde não houveram alterações quando comparadas às variações visualizadas em 504 h.

De acordo com a QUALANOD (2020), para ensaios de névoa salina neutra mantem-se os corpos de prova pelo tempo máximo de 336 h e como resultado, não deve apresentar quaisquer pontos de corrosão sobre a superfície, exceto se estes se fizerem presentes a menos de 1,5 mm das marcas de contato ou dos cantos das peças. Sendo assim, os corpos de prova anodizados e com coloração por adsorção orgânica apresentaram resultado positivo, pois apenas foram visualizadas pequenas manchas sobre a superfície, demonstrando que os óxidos formados na anodização foram protetivos contra a corrosão. Após este período, manchas maiores foram visualizadas apenas no período de 504 h, demonstrando que o filme anódico manteve-se resistente por um longo período posterior ao pré-estabelecido pela normativa. Ainda assim, não foram visualizados pontos específicos de corrosão, além das manchas.

Para a metodologia de coloração eletrolítica, a olho nu, nenhuma observação se fez necessária sobre a visualização prévia dos corpos de prova, conforme apresenta a Figura 11, caracterizados pelo LCOR como 0422/2020.

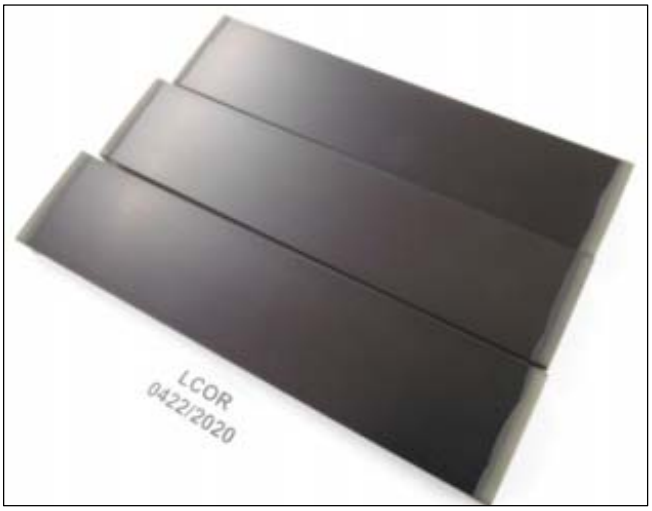

Fonte: LCOR | UCS (2020).

Figura 11. *Corpos de prova com coloração eletrolítica previamente ao ensaio de névoa salina neutra.*

Em 192 horas foram visualizadas pequenas manchas sobre a superfície dos três corpos de prova, conforme apresenta a Figura 12.

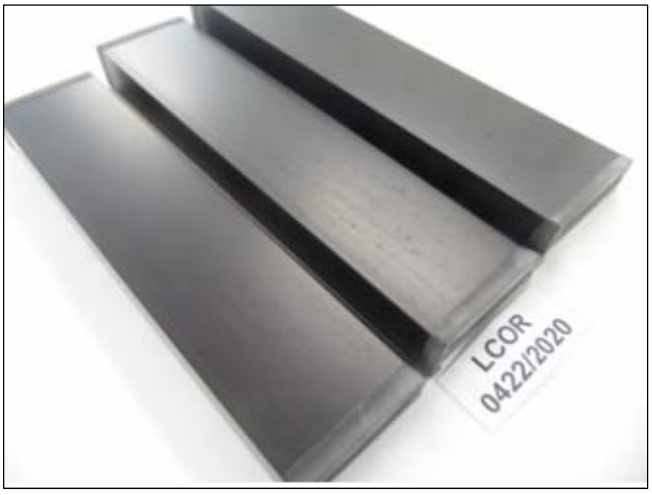

Fonte: LCOR | UCS (2020).

Figura 12. *Corpos de prova com coloração eletrolítica posteriormente à exposição de 192 h.*

O ensaio foi finalizado após 600 h de exposição, e nenhuma outra alteração foi visualizada sobre a superfície dos corpos de prova, quando comparadas as manchas surgidas posterior 192 h de exposição.

Como já mencionado, a QUALANOD (2020) ressalta o período de 336 h para ensaios de névoa salina neutra em corpos de prova anodizados. Sendo assim, os corpos de prova anodizados e com coloração eletrolítica demonstraram-se resistentes à exposição, pois apenas foram visualizadas pequenas manchas sobre a superfície no período de 192 h. Até a finalização do ensaio, em 600 h, nenhuma outra alteração foi revelada visualmente. Desta forma, demonstra-se que os filmes anódicos e a metodologia de coloração são satisfatórios, tendo em vista a resistência às exposições em tempos maiores que os estipulados pela normativa, além de não apresentarem pontos de corrosão sobre a superfície.

Os resultados obtidos da exposição à névoa salina neutra para a metodologia de coloração por adsorção orgânica apresentaram o surgimento de manchas maiores se comparada a metodologia de coloração eletrolítica, conforme já se esperava de acordo com o que apresenta a literatura. Portanto, devido ao fato dos corpos de prova terem se mantido por longo período de exposição, demonstra-se que a anilina utilizada em comparação à coloração eletrolítica foi eficaz, tendo em vista que a mesma possui alguma modificação em sua composição que a torna mais resistente que as demais comercialmente fornecidas. Estes resultados satisfatórios, para as duas metodologias, também podem estar relacionados à análise de MEV/FEG que detectaram um filme regular e homogêneo.

3.3. Resultados dos ensaios de imersão

Os corpos de prova anodizados e coloridos por meio da coloração por adsorção orgânica foram submetidos ao ensaio de imersão em uma solução de NaCl 3,5 %. Na Figura 13, tem-se a aparência destes posteriormente ao período de 48 h, 240 h, 408 h, 552 h e 1.000 h de imersão.

Durante o período de 48 h e 240 h de imersão, representado respectivamente pelas Figuras 13 (a) e 13 (b), nenhuma alteração foi possível ser visualizada a olho nu sobre a superfície. No tempo de imersão de 408 h, Figura 13 (c), visualizou-se alguns pontos de corrosão na interseção realizada nos corpos de prova.

Em 552 h, representado pela Figura 13 (d), estes pontos de corrosão aumentaram de tamanho, sendo visíveis apenas na interseção, estando a área superficial com aparência igual ao corpo de prova padrão. Também não houve descoloração e nem mudança de brilho na superfície a olho nu.

Em 1.000 h, de acordo com a Figura 13 (e), o corpo de prova apresentou pontos de corrosão ainda mais sobressalentes sobre a interseção realizada. No restante da área superficial, nenhum outro ponto de corrosão foi visualizado a olho nu. Também não foram notadas alterações de cor e nem perda de brilho, conforme demonstra a Figura 14.

Fonte: As Autoras (2020).

Figura 14. *Aparência dos corpos de prova com metodologia de coloração por adsorção orgânica posteriormente 1.000 h de imersão em NaCl 3,5 %.*

O alumínio, quando em contato com uma faixa de pH de 4,0 a 9,0, entra em uma zona de passivação. Neste caso, e sta zona de passivação é o próprio filme de óxido de alumínio formado na anodização, que é mais resistente que o formado naturalmente. Entretanto, o alumínio e suas ligas têm sua passividade destruída quando em contato com íons cloretos (Cl^-), sendo a corrosão mais frequente por pites, que ocorre em pontos ou áreas localizadas (GENTIL, 2017).

Também é possível constatar que a área onde não houve interseção, não ocorreram pontos de corrosão, demonstrando a resistência do filme de óxido de alumínio formado durante a anodização.

Os corpos de prova anodizados e com a metodologia da coloração eletrolítica foram submetidos ao ensaio de imersão em uma solução de NaCl 3,5 %. Na Figura 15, tem-se a aparência destes corpos de prova posteriormente ao período de 48 h, 240 h, 408 h, 552 h e 1.000 h de imersão.

Durante o período de 48 h, representado

pela Figura 15 (a), nenhuma alteração visual foi observada. Após as 240 h de exposição à imersão, representado pela Figura 15 (b), nenhuma alteração visual sobre a superfície foi observada, mantendo-se os corpos de prova semelhantes ao padrão. No tempo de imersão de 408 h, conforme Figura 15 (c), visualizaram-se alguns pontos de corrosão na interseção realizada nos corpos de prova.

Ainda na interseção, após 552 h de imersão, representado pela Figura 15 (d), estes pontos de corrosão aumentaram de tamanho. Ressalta-se que o restante da área superficial se manteve com aparência igual ao corpo de prova padrão, a olho nu, não sendo notada nenhuma alteração de cor e nem de brilho.

Em 1.000 h, conforme Figura 15 (e), os corpos de prova apresentaram pontos de corrosão ainda mais sobressalentes, entretanto, estes se mantiveram apenas sobre a interseção. Nas demais áreas não são visualizados pontos de corrosão a olho nu. Também não houve alteração de cor e nem perda de brilho, conforme demonstra a Figura 16.

Fonte: As Autoras (2020).

Figura 116. *Aparência dos corpos de prova com metodologia de coloração de adsorção orgânica durante a imersão dos mesmos em uma solução de NaCl 3,5 % após 1.000 horas.*

Assim como na metodologia de coloração por adsorção orgânica, ocorreu a presença de pites, em pontos localizados, devido ao contato com os íons Cl^-. Também é possível constatar que a área onde não houve interseção não sofreu nenhum tipo de corrosão, demonstrando a resistência do filme de óxido de alumínio formado durante a anodização, quando caracterizado a olho nu.

Ressalta-se que nenhuma das metodologias de coloração aplicadas interferiram para a proteção ou causa mais rápida da corrosão, sendo que ambas apresentaram os mesmos resultados visualmente.

4. CONCLUSÕES:

O presente estudo teve por objetivo comparar o desempenho à corrosão e à estabilidade da cor em relação a dois métodos de coloração em um filme anódico, por meio da coloração por adsorção orgânica e da coloração eletrolítica, sobre corpos de prova de alumínio da liga 6063. Logo, a partir dos resultados obtidos, conclui-se que:

- Pode-se observar que os corpos de prova anodizados e coloridos por adsorção orgânica e por coloração eletrolítica apresentaram filmes anódicos uniformes e homogêneos entre os pontos medidos em cada metodologia, com espessuras médias de 22,70 µm e 20,67 µm, respectivamente;
- Para o ensaio de névoa salina neutra, ambas as metodologias apresentaram resultados satisfatórios, o que não era esperado pela literatura;
- Nos ensaios de imersão com NaCl não houve perda de coloração e a corrosão foi visível posteriormente a 408 h de exposição em ambas as metodologias.

A partir dos resultados obtidos neste estudo, verifica-se que a metodologia de coloração eletrolítica possui resistência à corrosão, se mantendo com coloração uniforme e boa aparência após ensaios realizados. A coloração por adsorção orgânica também apresentou as mesmas características, se atribuindo estes resultados à anilina testada, que possui modificação estrutural, fazendo com que a mesma resista aos ensaios, sem perder as propriedades. Desta forma, pode-se concluir que é possível equivaler as metodologias utilizadas para coloração do filme anódico de acordo com os parâmetros testados.

5. DECLARAÇÕES:

5.1. Limitações do estudo

Nenhuma limitação era conhecida no momento do estudo.

5.2. Fonte de financiamento

Essa pesquisa foi financiada pelos autores.

7. REFERÊNCIAS:

1. ABAL – Associação Brasileira do Alumínio. **Coletânea de normas técnicas de alumínio e suas ligas**. São Paulo: ABAL, 2008. 758 p.

2. AMERICAN SOCIETY FOR TESTING AND MATERIALS. **ASTM B117-18**: Standard pratice for operating salt spray (fog) apparatus. West Conshohocken, 2018.

3. ASSOCIAÇÃO BRASILEIRA DE NORMAS TÉCNICAS. **NBR 12611**: Alumínio e suas ligas - tratamento de superfície – determinação da espessura da camada anódica – método de microscopia óptica. Rio de Janeiro, 2006.

4. BENSALAH, W. *et al*. Mechanical failure of anodized film of aluminium in bending. **Materials and Design**, [*S.l.*], v. 30, n. 8, p. 3141-3149, Sept. 2009.

5. BORGES, A. A. C. **Efeito do jateamento com granalhas de aço na tensão residual e no comportamento mecânico da liga de alumínio 6083**. 2017. 158f. Tese (Doutorado em Tecnologia Nuclear – Materiais) – Instituto de Pesquisas Energética e Nuclear (IPEN). São Paulo, 2017.

6. CLARIANT International Ltd. **Variação nas cores** – o tingimento de alumínio anodizado. Clariant International Ltd. Suiça: 2015. 47 p.
7. CLARIANT Ltda. **Sanodye Blue 2LW**. Disponível em: chemiepraktika.pbworks.com. Acesso em: 30 abr. 2020.

8. COURROL, L. C.; PRETO, A. O. **Óptica geométrica** [online]. 1. ed. São Paulo: Editora Unifesp, 2011. 168 p.

9. GENTIL, V. **Corrosão**. 6. ed. Rio de Janeiro: LTC, 2017. 360 p.

10. PACHECO, D. M. C. **Otimização e rastreabilidade do processo de oxidação anódica, com coloração orgânica de componentes em ligas de alumínio**. 2016. 83f. Dissertação (Mestrado em Engenharia Metalúrgica e de Materiais) - Faculdade de Engenharia da Universidade do Porto. Porto, 2016.

11. PERTILE, T. S.; BEUX, T. D.; BIRRIEL, E. J. Denominações dos defeitos encontrados em superfícies pintadas e galvanizadas submetidas a ensaios acelerados de corrosão. *In*: INTERCORR. 38., São Paulo, 2018. **Anais** [...]. São Paulo: ABRACO. 2018. 9 p.

12. QUALANOD. **Diretivas para a Marca de Qualidade QUALANOD para Anodização do Alumínio Baseada em Ácido Sulfúrico**. Zurique, 2020.

13. REVISTA ALUMÍNIO. **Consumo de alumínio no Brasil cresce em 10% em 2018**. 25 abr. 2019. Disponível em: https://revistaaluminio.com.br/consumo-de-aluminio-no-brasil-cresce-10-em-2018/. Acesso em: 30 mar. 2020.

14. UCS. **Laboratório central de microscopia**. Disponível em:

https://www.ucs.br/site/tecnoucs/servicos-tecnologicos/tecnologia-e-pesquisa/laboratorio-central-de-microscopia/. Acesso em: 15 abr. 2020.

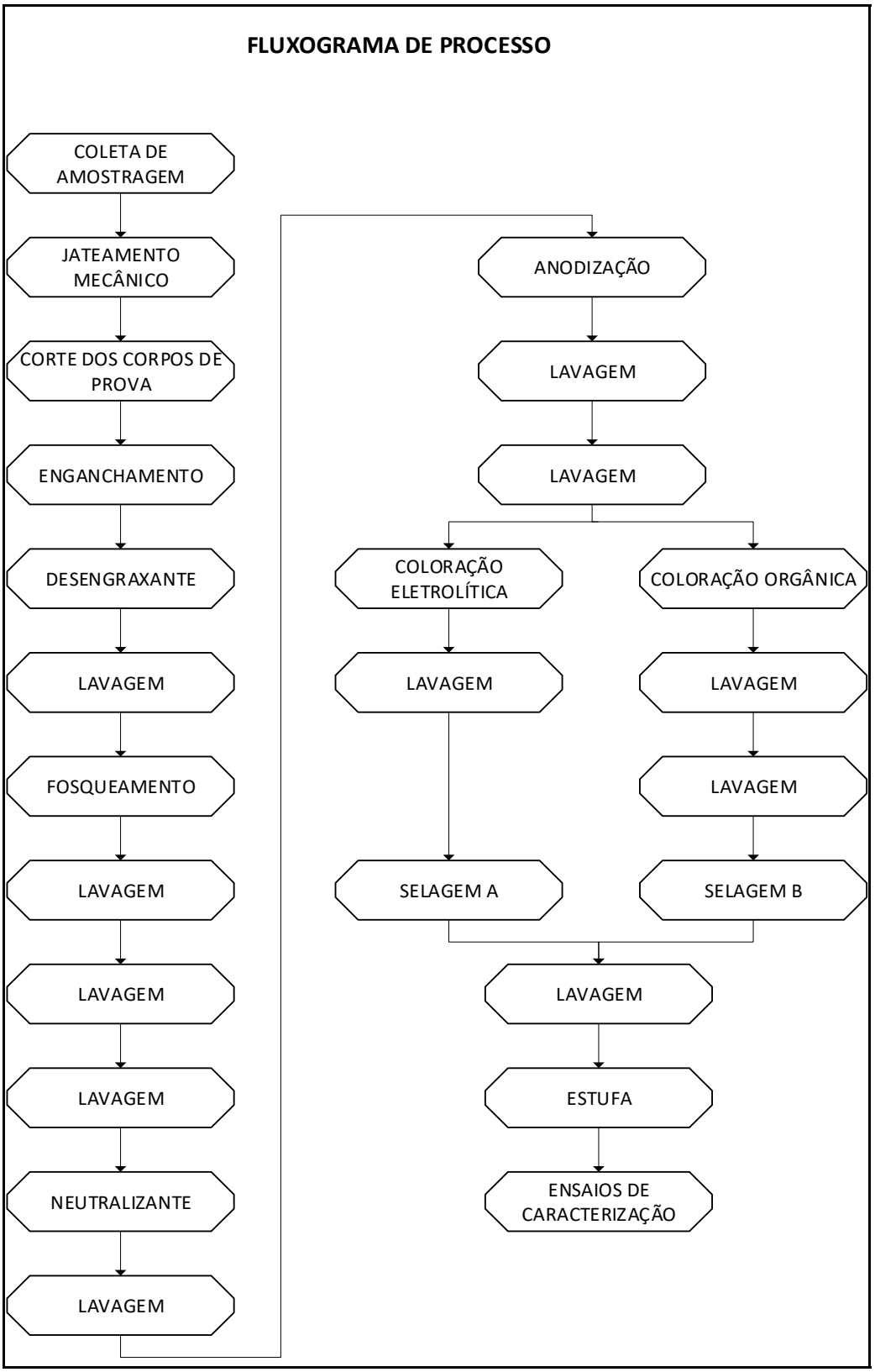

Figura 2. *Etapas realizadas com os corpos de prova para realização do tratamento de conversão de anodização e coloração do filme anódico. Fonte: As Autores (2020).*

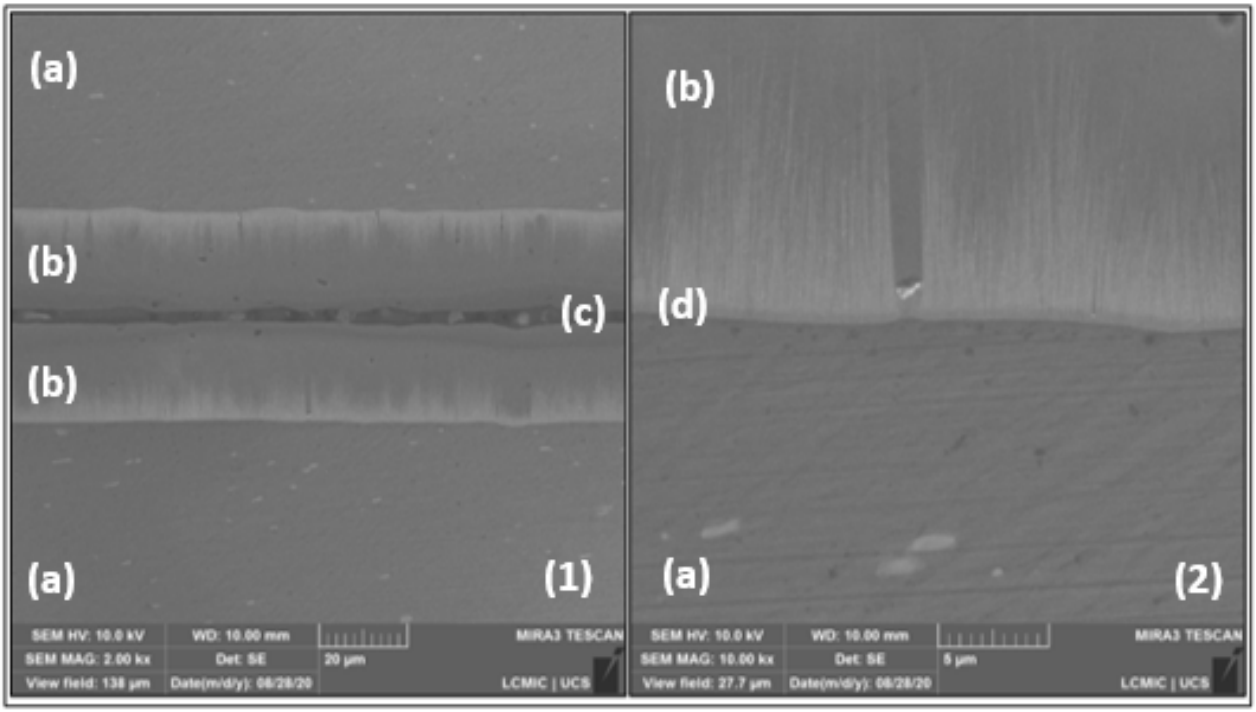

Nota: (a) substrato do alumínio; (b) filme de óxido de alumínio; (c) resina; (d) camada barreira. Magnificação de 2.000x na Figura 20 (1); magnificação de 10.000x na Figura (2).

Figura 5. *Aparência da espessura das camadas anódicas com coloração por meio da adsorção orgânica avaliado no MEV/FEG. Fonte: A Autora (2020).*

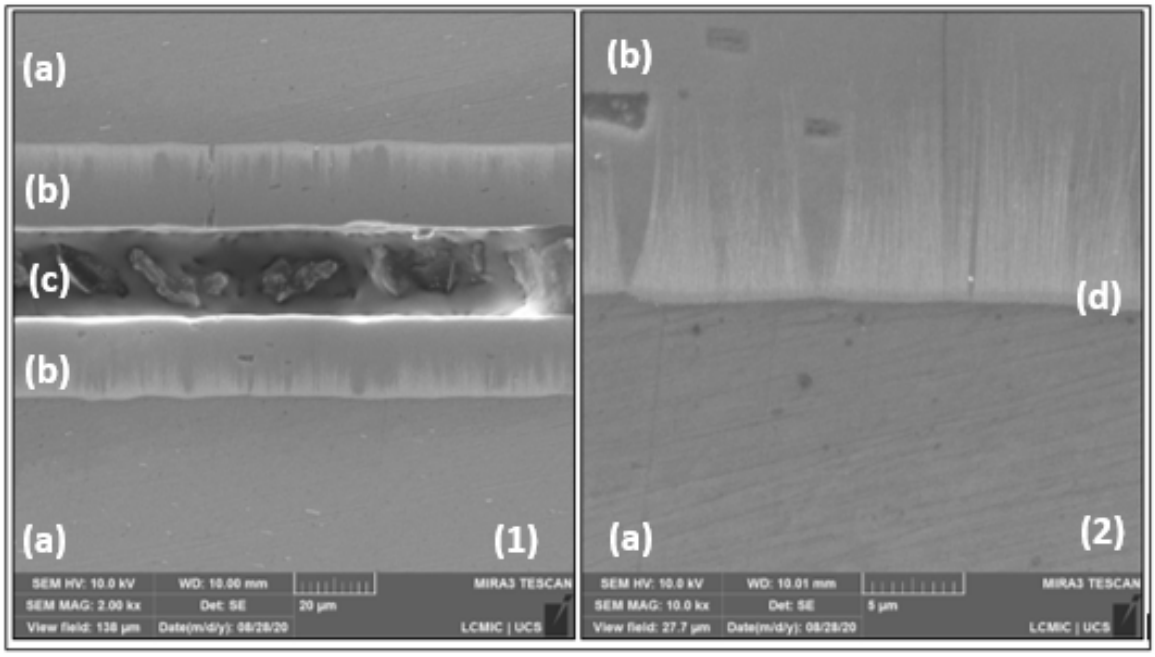

Nota: (a) substrato do alumínio; (b) filme de óxido de alumínio; (c) resina; (d) camada barreira. Magnificação de 2.000x na Figura 21 (1); magnificação de 10.000x na Figura 21 (2).

Figura 6. *Aparência da espessura da camada anódica com coloração eletrolítica através da análise do MEV/FEG. Fonte: A Autora (2020).*

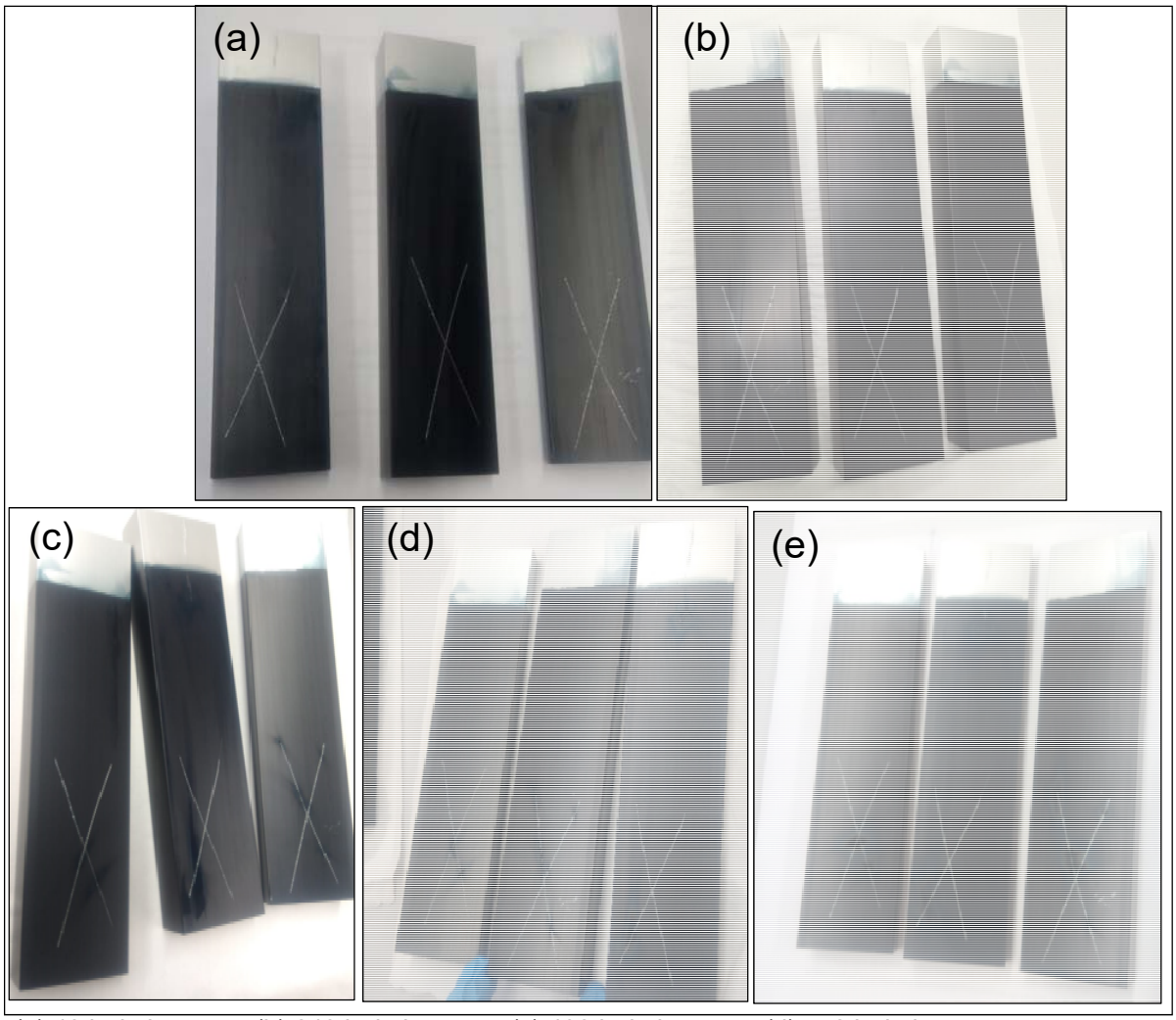

Nota: (a) 48 h de imersão; (b) 240 h de imersão; (c) 408 h de imersão; (d) 552 h de imersão; (e) 1.000 h de imersão.

Figura 13. *Aparência dos corpos de prova com metodologia de coloração por adsorção orgânica durante a imersão dos mesmos em uma solução de NaCl 3,5 % após 1.000 horas. Fonte: A Autora (2020).*

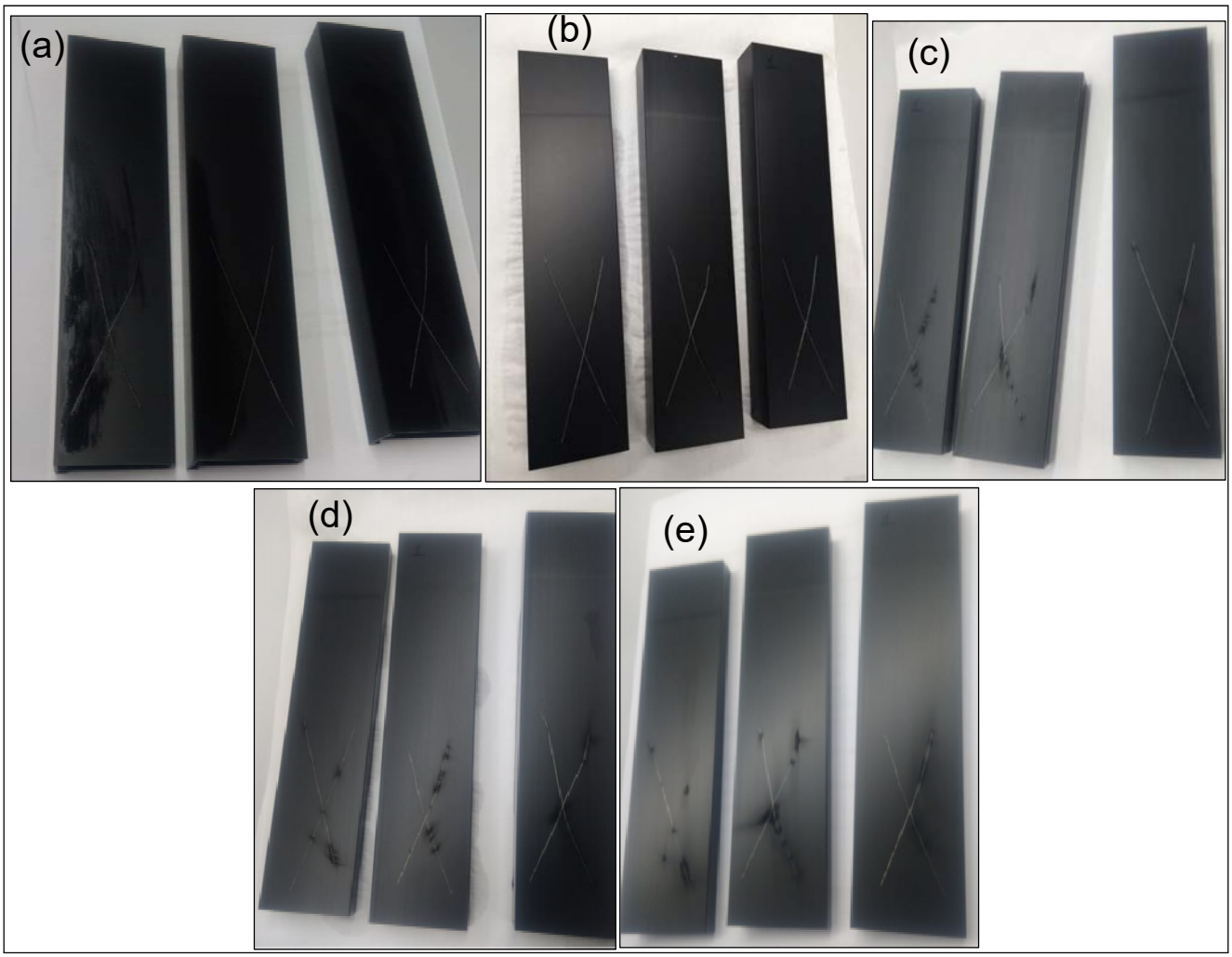

Nota: (a) 48 h de imersão; (b) 240 h de imersão; (c) 408 h de imersão; (d) 552 h de imersão; (e) 1.000 h de imersão.

***Figura 15*.** Aparência dos corpos de prova com metodologia de coloração de adsorção orgânica durante a imersão dos mesmos em uma solução de NaCl 3,5 % após 1.000 horas. Fonte: A Autora (2020).

Tabela 1. *Composição química da liga de alumínio 6063 (Elementos químicos em % mássica)*

Liga	Si (%)	Fe (%)	Cu (%)	Mn (%)	Mg (%)	Cr (%)	Zn (%)	Ti (%)	Outros (%)	Al (%)
6063	0,20 a 0,60	0,35	0,10	0,10	0,45 a 0,90	0,10	0,10	0,10	0,15	Restante

Fonte: ABAL (2008, p. 14).

Tabela 2. *Informações das etapas do processo*

Processo	Coloração por adsorção orgânica			Coloração eletrolítica		
	t (min)	T (ºC)	Concentração	t (min)	T (ºC)	Concentração
Desengraxe	10	20	147 g/L H_2SO_4	10	20	147 g/L H_2SO_4
Fosqueamento	5	53	65,33 g/L NaOH 101,70 g/L Al^{3+}	5	53	65,33 g/L NaOH 101,70 g/L Al^{3+}
Neutralizante	5	30	147 g/L H_2SO_4	5	30	147 g/L H_2SO_4
Anodização	30	21	197,96 g/L H_2SO_4 11,16 g/L Al^{3+}	30	21	197,96 g/L H_2SO_4 11,16 g/L Al^{3+}
Coloração	12	24	10,81 g/L Sn^{2+} 20 g/L H_2SO_4	30	57	10 g/L anilina
Selagem	20	30	1467,75 Ni 700 F	20	18	1800 ppm Ni 300 ppm F
Estufa	30	75	GLP	30	75	GLP

Fonte: As Autoras (2020).

SOUTHERN BRAZILIAN JOURNAL OF CHEMISTRY

EXPERIMENTAL STUDY OF THE INFLUENCE OF TEMPERATURE ON PASTEURIZATION OF *PÊRA RIO IN NATURA* ORANGE JUICE

GALIASSI, Gabriela Regina Rosa [1*]; RAMIREZ; Maribel Valverde [1]

[1] Universidade Federal de Mato Grosso, Faculdade de Engenharia

**Correspondence author*
e-mail: gabigaliassi@gmail.com

Received 15 October 2021; received in revised form 30 November 2021; accepted 03 December 2021

ABSTRACT

Background: Heat treatment is one of the most used methods to preserve food, such as orange juices, which are an excellent source of ascorbic acid. To avoid vitamin C degradation and reduce loss, fast heating is recommended. However, little is known about heat transfer during juice pasteurization. **Aim:** Therefore, this work aimed to determine the vitamin C content and the convective heat transfer coefficient in the pasteurization of orange juice. **Methods:** To perform the experiment, in the juice container, two regions were analyzed: the central region and near the wall. For the time-temperature control, thermometers were installed in the two regions mentioned. Every 120 seconds, the temperature was measured. The vitamin C content in the juice was evaluated before and after pasteurization using the iodometric method. The convective coefficient was evaluated using the method of dimensionless numbers and the experimental method. **Results and Discussion:** In pasteurization, the solution was heated to 80 °C, where heating lasted 3000 seconds and cooling for 2520 seconds. The graph showing the relationship of the convective heat transfer coefficient and temperature follows the same trend of the literature. The convective coefficient is higher in the region near the wall. As time passes and temperature decreases, the central region tends to equilibrium, and the coefficient becomes more constant. The vitamin C content remained constant before and after pasteurization. The values of the dimensionless numbers used in the calculations are in the same order of magnitude as the literature. **Conclusions:** The pasteurization did not cause ascorbic acid degradation since the heating step was fast in the heat treatment. The graphic showed that there is a dependence of the dimensionless of temperature with the dimensionless Biot and Fourier. It was noted that studying the thermal behavior in the cooling of orange juice is extremely important to ensure its quality.

Keywords: *Heat Transfer. Pasteurization. Orange Juice. Convective Coefficient.*

1. INTRODUCTION:

The citrus industry is an extremely important sector for the Brazilian economy, as the country is responsible for 34% of the fruits and 56% of the juice produced in the world. Furthermore, the orange is the most consumed fruit by the Brazilian population, and among the different cultivars is the Pêra Rio orange (Citrus sinensis L. Osbeck) (Leonello *et al.,* 2019).

Heat treatment is one of the most used methods to preserve food, such as orange juice, increasing its shelf life. However, little is known about the temperature and speed profiles during heat treatment of liquid food in commercial packaging (Ghani *et al.*, 2001).

Pasteurization is a process used in foods when the aim is to destroy pathogenic microorganisms and denature low heat resistance enzymes present in foods. In addition, another goal is to increase the shelf life of the food. The process consists of heating the food to a certain temperature and time and subsequently cooling it to a temperature lower than the previous one (Potter; Hotchikiss, 1995). The literature presents three types of pasteurization, and for orange juice, HTST (High Temperature and Short Time) is used (Jing *et al.*, 2013).

Orange juice is an excellent source of ascorbic acid, commonly known as Vitamin C, and belongs to the water-soluble vitamins. The quality of the juice can be influenced when it is exposed to oxygen and light, which can reduce the Vitamin C content and sensorially modify the product. To avoid vitamin C degradation and reduce loss, fast heating and low exposure to air are recommended when preparing the juice. Proper storage of the juice, which should be at low temperatures, helps preserve vitamin C and does not darken the juice.

If the juice is kept between 15 ºC and 25 ºC, there will be a significant loss of Ascorbic Acid (Cozzolino, 2012; Teixeira; Monteiro, 2006).

It is possible to find in the literature studies about heat transfer during pasteurization and about food cooling. Teruel *et al.* (2003), experimentally studied the cooling of *valência* oranges with forced air and water. In the chilled water system, cooling occurred uniformly and lasted about 3420 seconds. Jing *et al.* (2013) carried out a theoretical study of temperature distribution through pasteurization for orange juice in a cylindrical container based on 3D CFD simulation. Pasteurization for orange juice was simulated at three different temperatures, and the temperature field in each was obtained. Data were compared, and an optimal computational model was obtained for this case.

Also, Maharramov (2021) studied the thermal conductivity of orange and tangerine juices in a non-steady state. The author states that all known experimental installations measure the thermal conductivity of liquids in a steady-state, even if in the production and processing of liquid food products, as a rule, the main substance is in a mobile state.

This work aims to determine the vitamin C content using the iodometric method and the convective heat transfer coefficient using the method of dimensionless numbers and the experimental method in the pasteurization of orange juice.

2. MATERIALS AND METHODS:

The juice was prepared and placed in a 200 mL cylindrical glass container, sealed. To control the temperature during the experiment, thermometers (Brax Tecnologia, model -10 + 110 ºC) and a stopwatch were used. The vitamin C content was analyzed before and after the pasteurization using the iodometric method.

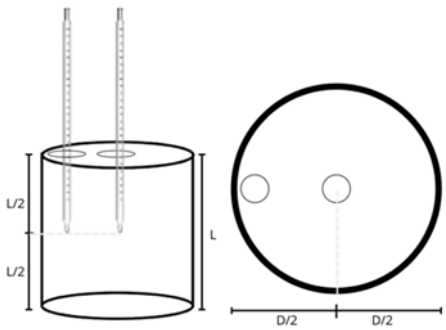

Figure 1. *Representation of the system used to control temperature and analysis regions*

The juice was heated in a water bath, and the temperature was recorded every 120 seconds.

The water bath was already heated to 80 ºC when the juice was placed in the bath. Therefore, when the central region of the container with orange juice reached 74 ºC, heating was stopped.

Then, cooling was performed, where the sample was placed inside a stainless steel pan with ice. The variation in juice temperature was monitored using thermometers, which were already installed in the cylindrical container, and this was measured every 120 seconds. When the center of the juice container reached 6 °C, cooling was stopped. Next, the bath was cooled to 0 °C.

3. RESULTS AND DISCUSSION:

3.1. Temperature Profile in pasteurization

In this study, pasteurization lasted 5520 seconds, where heating lasted 3000 seconds and cooling 2520 seconds.

It is possible to observe in Figure 2 that the two regions presented practically the same temperature variation. In the literature of Bhuvaneswari (2014) and Priest; Stewart (2006), the profile of the curve follows the same trend.

3.2. Vitamin C Content

Regarding the vitamin C content, it remained constant before and after pasteurization.

3.3. Relationship between the dimensionless temperature and Biot*Fourier

According to Incropera; De Witt (2003), when the Biot number is less than 0.1, it is reasonable to assume a uniform temperature distribution in a solid at any time during a transient process. If conduction were the dominant heat transfer in the container, a non-uniform temperature distribution and Biot number greater than 0.1 would be expected. As Biot was less than 0.1, it is suggested that there is strong natural convection occurring in the container.

The graphical behavior presents a straight line, with $R^2 = 1$, whose equation is:

$$y = 0.0667x \qquad (1)$$

This behavior shows that there is a dependence of the dimensionless of temperature with the dimensionless Biot and Fourier. The

graph for Equation 1 can be seen in Figure 3.

3.4. Convective Heat Transfer coefficient in pasteurization

In this research, heat transfer was analyzed in the cooling stage. Under these conditions, the concentrated capacity method is applied. In the wall region, heat transfer via conduction in a transient regime was used, where the concentrated capacity method was applied, given that the number of Biot was less than 0.1. In the central region of the container, Newton's theory of cooling was used. In both regions, the convective heat transfer coefficients were determined.

To determine the convective coefficient in the wall region, the thermophysical properties used in the calculations were those of glass. To determine the convective coefficient in the central region, the thermophysical properties of the fluid were used, in this case, the orange juice.

It is possible to observe in Figure 4 that the convective heat transfer coefficient is higher in the region near the wall, and there is a sharp drop in the convective coefficient curve in the wall region. This is because the temperature is very high at this moment, as it is the period when cooling starts, so the value is lower. As time passes and temperature decreases, the central region tends to equilibrium, and the coefficient becomes more constant. The standard deviation for the convective coefficient in the central region and in the wall region were 3.99 and 16.74, respectively.

3.5. Dimensionless numbers used in the calculation of the heat transfer convective coefficient in the central region

It is observed, in Table 1, in the order of magnitude of the dimensionless numbers, the occurrence of laminar regions, which remain stable over time. In their study, Fujii *et al.* (1970) obtained values in the same order of magnitude.

4. CONCLUSIONS:

It was possible to observe that both the region of the center of the container and the region of the wall have similar temperature variations, which agree with the profiles found in the literature. The convective heat transfer coefficient is higher in the wall region and tends to equilibrium over time.

It was seen that the dimensionless number of temperature has a dependence relation with the dimensionless numbers of Biot and Fourier. Still, the order of magnitude of the dimensionless numbers used to calculate the convective heat transfer coefficient indicates the occurrence of laminar regions, which remain stable over time, which was expected.

It was observed that the pasteurization did not cause ascorbic acid degradation since the heating step was fast in the heat treatment. In order to avoid this degradation and reduce its loss, it is necessary that in thermal treatments, fast heating is carried out and that the juice has low exposure to air and heat at the time of its preparation. Therefore, studying the thermal behavior in the cooling of orange juice is extremely important to guarantee its quality.

5. DECLARATIONS

5.1. Study Limitations

No limitations were known at the time of the study.

5.2. Acknowledgements

The authors thank the laboratory technicians, Silvio and Keyla, for their attention and support in carrying out the experiments, and the Federal University of Mato Grosso, for making the equipment, drugs, or supplies available for the preparation of this work.

5.3. Funding source

The authors funded this research.

5.4. Competing Interests

The authors declare the following financial interests/personal relationships, which may be considered potential competing interests: equipment, drugs, or supplies provided by the Federal University of Mato Grosso.

7. REFERENCES:

1. Bhuvaneswari, E.; Anandharamakrishnan, C.; *Innov Food Sci Emerg Technol.*, **2014**, *23*, 162.
2. Cozzolino, S. M. F.; *Biodisponibilidade de nutrientes*, 4th ed; Manole: São Paulo, Brazil, 2012.
3. Ghani, A. G. A.; Farid, M. M.; Chen, X. D.; Richards, P.; *Journal of Food Engineering*, **2001**, *48*, 147-156.
4. Jing, X.; Yong-yan, L.; Jin-feng, W.; Yi, T.; Chen, M.; *Advanced Materials Research*, **2013**, *740*, 245.
5. Leonello, E. C.; Esperancini, M. S. T.; Guerra, S. P. S.; *Citrus Res. Technol*., **2019**, *40*, e1043.
6. Maharramov, M. A.; *E3S Web of Conferences*, **2021**, *254*.
7. Potter, N. N.; Hotchikiss, J. H.; *Food Science*, 5th ed; Chapman and Hall: New York, USA, 1995.
8. Priest, F. G.; Stewart, G. G.; *Handbook of Brewing*, 2nd ed; CRC Taylor and Francis Group: Boca Raton, USA, 2006.
9. Teixeira, M.; Monteiro M.; *Alimentos e Nutrição*; Araraquara, Brazil, 2006, ch.14.
10. Teruel, B.; Cortez, L.; Neves Filho, L.; *Ciênc. Tecnol. Aliment*., **2003**, *23(2)*, 174-178.
11. Incropera, F. P.; Dewitt, D. P. *Fundamentals of Heat and Mass Transfer*. Rio de Janeiro, Brazil, 2003.
12. Fujii, T.; Takeuchi, M.; Fujii, M.; Suzaki, K.; Uehara, H.; *Int. J. Heat Mass Transfer*., **1970**, *13*, 753-787.

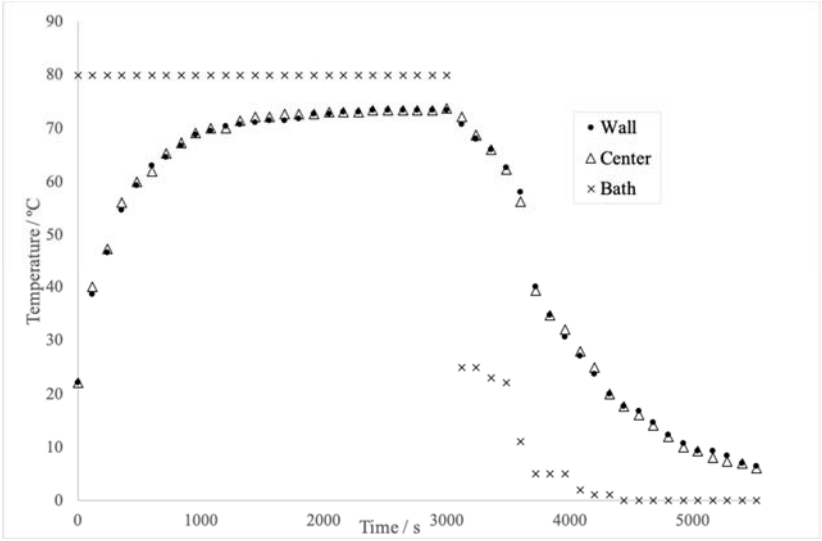

Figure 2. *Time-temperature behavior during pasteurization*

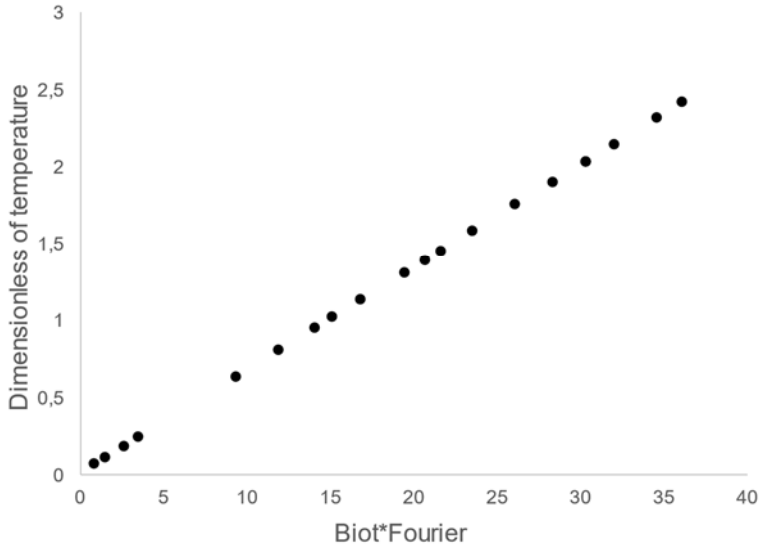

Figure 3. *Relationship between the Dimensionless of Temperature and Biot*Fourier*

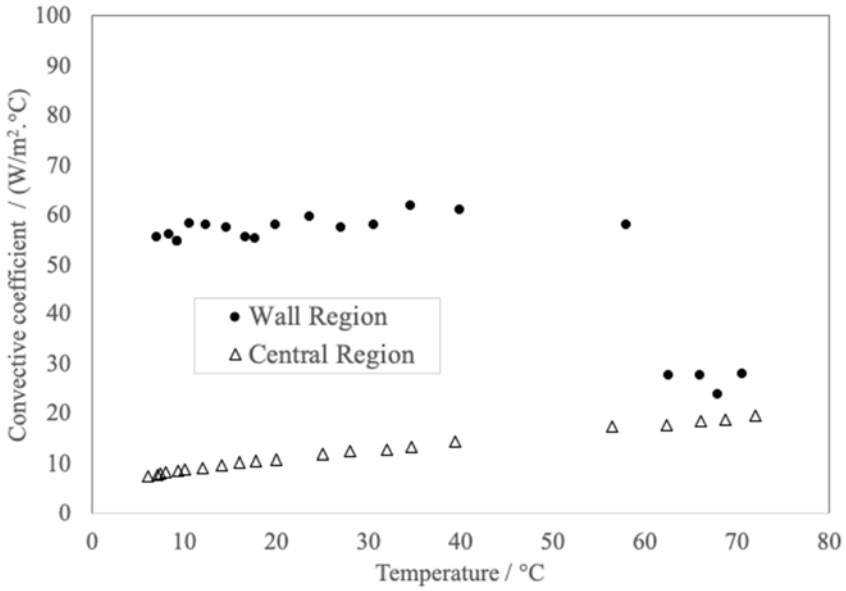

Figure 4. *Convective heat transfer coefficient in the cooling stage*

Table 1. *Dimensionless numbers used in the calculation of the heat transfer convective coefficient in the central region*

Time (s)	Temperature (ºC)	Pr	Gr	Ra	Nu
120	72.00	4.31	$8{,}90.10^{8}$	$3{,}84.10^{9}$	146.85
240	68.67	4.47	$7{,}76.10^{8}$	$3{,}47.10^{9}$	143.22
360	66.00	4.64	$7{,}17.10^{8}$	$3{,}33.10^{9}$	141.74
480	62.33	4.94	$6{,}02.10^{8}$	$2{,}97.10^{9}$	137.79
600	56.33	5.57	$5{,}52.10^{8}$	$3{,}07.10^{9}$	138.92
720	39.33	8.28	$2{,}01.10^{8}$	$1{,}66.10^{9}$	119.17
840	34.67	9.26	$1{,}41.10^{8}$	$1{,}30.10^{9}$	112.13
960	32.00	9.87	$1{,}14.10^{8}$	$1{,}12.10^{9}$	108.02
1080	28.00	10.84	$9{,}25.10^{7}$	$1{,}00.10^{9}$	104.99
1200	25.00	11.62	$7{,}52.10^{7}$	$8{,}74.10^{8}$	101.43
1320	20.00	13.00	$4{,}83.10^{7}$	$6{,}28E.10^{8}$	93.39
1440	17.67	13.69	$4{,}09.10^{7}$	$5{,}59.10^{8}$	90.74
1560	16.00	14.20	$3{,}46.10^{7}$	$4{,}91.10^{8}$	87.83
1680	14.00	14.83	$2{,}79.10^{7}$	$4{,}14.10^{8}$	84.17
1800	12.00	15.47	$2{,}21.10^{7}$	$3{,}42.10^{8}$	80.26
1920	10.00	16.14	$1{,}71.10^{7}$	$2{,}75.10^{8}$	76.00
2040	9.33	16.37	$1{,}55.10^{7}$	$2{,}54.10^{8}$	74.48
2160	8.00	16.83	$1{,}26.10^{7}$	$2{,}13.10^{8}$	71.25
2280	7.33	17.06	$1{,}13.10^{7}$	$1{,}93.10^{8}$	69.51
2400	7.00	17.18	$1{,}06.10^{7}$	$1{,}83.10^{8}$	68.61
2520	6.00	17.53	$8{,}79.10^{6}$	$1{,}54.10^{8}$	65.73

SOUTHERN BRAZILIAN JOURNAL OF CHEMISTRY

PREVENTION OF CANDIDIASIS IN PATIENTS USING REMOVABLE DENTURES

SEVBITOV, Andrey[1]; DOROFEEV, Aleksey[1]; MIRONOV, Sergey[1]; AL-KHOURY, Samer[2]; TIMOSHIN, Anton[1]

[1] I.M. Sechenov First Moscow State Medical University (Sechenov University). Russia.

[2]Dental clinic "Good Crocodile". Russia.

** Correspondence author*
e-mail: avsevbitov@mail.ru

Received 11 September 2021; received in revised form 30 November 2021; accepted 11 December 2021

ABSTRACT

Background: Despite innovations in orthopedic dentistry, the manufacture of removable dentures belongs to the most popular orthopedic care category. Removable dentures are combined stimuli that affect the mucous membrane and neuro-receptor apparatus. Acrylic plastic prostheses, widely used in prosthetic dentistry, have a negative side mechanical, chemical-toxic, sensitizing, and thermal insulating effect on oral tissue and prosthetic impression area. This is often complicated by a violation of the biocenosis of the oral cavity, the growth of pathogenic microflora that releases toxins, especially an increase in the number of yeast colonies that irritate the oral mucosa and prosthetic stomatitis. According to the WHO, one-fifth of the world's population suffers or has suffered various candidiasis forms at least once. The worldwide increase in the incidence of the disease is primarily related to the fact that this infection is opportunistic, more than half of the world's population is a carrier of fungi of this kind, i.e., in most cases, it is an endogenous infection, which makes candidiasis different from other opportunistic mycoses. **Aims:** The purpose of this study was to study the prevalence of candidiasis in patients using removable dentures and to evaluate the effectiveness and prevention of candidiasis treatment. **Methods:** 100 patients with oral candidiasis of various age groups from 45 to 65 years were observed. Of these, 60 patients with removable plate prostheses; 40 patients with partially removable prostheses. **Results and Discussion:** Chronic forms of candidiasis were diagnosed in 40 patients and with exacerbation of chronic forms of candidiasis-60 people. The number of untreated carious cavities and poor hygienic condition of the oral cavity directly affects the severity of candidiasis. Acute forms of candidiasis were observed mainly in patients with high DMF and PMA indices. The severity of candidiasis depends on the degree and duration of wearing dentures and hygienic conditions - the most severe forms of invasive candidiasis were observed in the presence of removable plate prostheses, the complete absence of teeth, and the use of a prosthesis for more than 10-15 years. A combined lesion of the oral mucosa and the red border of the lips was observed mainly in patients older than 60 years. **Conclusions:** The presence of candidiasis in the oral cavity in patients with removable plate prostheses leads to a statistically significant change in the indicators of local immunity of the oral cavity: an increase in the concentration of serum IgG and IgA and the values of the coefficient of the balance of local immunity factors.

Keywords: *Candidiasis, prosthesis, inflammation, prosthetic dentistry, biochemistry.*

1. INTRODUCTION

Despite innovations in orthopedic dentistry, the manufacture of removable dentures belongs to the category of the most popular types of orthopedic care. The nature of the prosthetic impression area tissue reactions, the development of which is determined by the quality of the prosthesis, the property of the material, the method of fixation, peculiarities of the transmission of chewing pressure, occlusal relationships, the size of the prosthetic base acquires particular importance in the formation of patients adaptation to removable, as in Figure 1 (Sevbitov *et al*., 2018; 2019, 2020).

Removable dentures are combined stimuli that affect the mucous membrane and neuro-receptor apparatus. It is known that in 52% of cases, dentures are not fixed when chewing. Furthermore, in 65% of patients using dentures,

various diseases of the prosthetic impression area mucous membrane and pathological processes in supporting tissues develop, according to Figure 2 (Sevbitov *et al*., 2019; 2020).

Acrylic plastic prostheses, widely used in the practice of prosthetic dentistry, have a negative side mechanical, chemical-toxic, sensitizing, and thermal insulating effect on oral tissue and prosthetic impression area, as seen in Figures 3 and 4 (Sevbitov *et al*., 2018; 2019; 2020).

This is often complicated by a violation of the biocenosis of the oral cavity, the growth of pathogenic microflora that releases toxins, especially an increase in the number of yeast colonies that irritate the oral mucosa and prosthetic stomatitis. It was also proved that when using adhesive preparations to improve the fixation of removable dentures, the number of yeast colonies increases statistically significantly when sown quantitatively compared with the control group of patients (Sevbitov *et al*., 2005; Ergesheva *et al*., 2018).

According to the WHO (2020), one-fifth of the world's population suffers or has at least once suffered various forms of candidiasis (Sevbitov, Ershov, *et al*., 2020). The worldwide increase in the incidence of the disease is primarily related to the fact that this infection is opportunistic, more than half of the world's population is a carrier of fungi of this kind, i.e., in most cases, it is an endogenous infection, which makes candidiasis different from other opportunistic mycoses (Enina *et al*., 2019; Turgaeva *et al*., 2020).

Candidiasis of the oral mucosa is caused by representatives of the conditionally pathogenic microflora of the oral cavity, fungi of the genus Candida, which are detected in healthy people in 50% of cases (Utyuzh *et al*., 2019; Mironov *et al*., 2020).

Factors predisposing to the development of pathology are:

Local:

1. The oral mucous membrane's integrity is violated due to acute or chronic mechanical, chemical, and iatrogenic trauma.
2. Availability of removable dentures.
3. The use of antimicrobial agents. (Mamedov *et al*., 2019; Yumashev *et al*., 2019).

Common:

1. Concomitant pathology: chronic infectious processes (HIV infection), oncological diseases, blood pathology, diseases of the gastrointestinal tract, cardiovascular and endocrine system (diabetes mellitus).
2. Taking medications: antibiotics, corticosteroids, cytostatics, hormonal contraceptives.
3. Hypovitaminosis.
4. Secondary immunodeficiency.
5. Intestinal dysbacteriosis. (Kuznetsova *et al*., 2018; Platonova *et al*., 2018).

N. D. Sheklakov in 1976 Proposed a clinical classification of candidiasis:

- poverhnostnye candidiasis of the mucous membranes, skin, nails;
- chronic generalized (granulomatous) candidiasis;
- visceral (systemic) candidiasis of various organs. (Sevbitov *et al*., 1999; 2004).

The course of the disease distinguishes acute and chronic candidiasis:

- acute pseudomembranous candidiasis (thrush);
- acute atrophic candidiasis;
- chronic hyperplastic candidiasis;
- chronic atrophic candidiasis (Evstratenko *et al*., 2018; Mazzeo *et al*., 2013).

By localization, select:

- Candida cheilitis;
- which restores candidal cheilitis;
- Candida glossitis;
- thrush (Voloshina *et al*., 2018; Silva *et al*., 2019).

Clinical picture.

Acute pseudomembranous candidiasis. Patients complain of dryness, burning, increasing with food, swelling of the tongue, the presence of plaque. The mucosa is edematous and hyperemic, covered with a white (“curd”) coating; a smooth hyperemic surface is exposed when removed. Body temperature does not increase, lymph nodes are not palpated, see Figure 5.

Acute atrophic candidiasis. Patients complain of burning, dryness, increasing with food, and mucosa swelling. The mucous membrane is bright red, dry, no plaque, visible in

Figure 6.

Chronic hyperplastic candidiasis. Patients complain of dryness, burning, increasing with food, changes in the relief of the mucosa. The mucous membrane is edematous hyperemic, covered with whitish-gray films removed with difficulty, exposing an erosive bleeding surface, as in Figure 7.

Chronic atrophic candidiasis. The mucosa in the area of the prosthetic bed (the mucous membrane of the palate and alveolar processes) is affected. Complaints of dryness and burning increase when eating. There is a bright hyperemic, dry mucosa surface in the prosthetic bed area, erosion and ulcers are possible, as in Figure 8.

Candida angular cheilitis. It is observed with a decrease in the lower third of the face (adentia, poorly made prostheses). Patients complain of burning, dryness, itching of the skin in the corners of the mouth. The swollen and hyperemic skin may form erosion with a slight discharge or dryness. A white, easily removable plaque is detected in Figure 9 (Girardin *et al*., 2019; Timoshin *et al*., 2018, 2019).

1.1 Case description.

Patient N, 62 years old, came to the dentist with dry mouth complaints, tingling in the tongue area, bleeding gums, and bad breath.

Examination: the gums are hyper-milled, swollen, the tongue is covered with a grayish-white bloom, the teeth are imprinted on the lateral surfaces of the tongue, the palate is edematous, the oral cavity is not sanitized (Figure 10).

Medical history: suffered a sore throat, pneumonia, sinusitis, and sepsis.

The patient repeatedly took antibiotics without nystatin or levorin.

The suspicion of candidosis has been confirmed by a smear taken before treatment. In a smear in large quantities, found elements of the fungus.

Prescribed treatment:

- sanitation of the oral cavity

- rational prosthetics

- rinsing soda solution of the oral cavity to release it from mucus;

Apply TYCVEOLUM with thymol for 15-20 minutes, two times a day.

On the third day, the patient subjectively noted improvement. The clinical picture also changed for the better, and on the eighth day - the puffiness disappeared, hyperimemia, the mucous became pale pink, the tongue cleared, dry mouth disappeared.

The patient noted an improvement in overall health, increased efficiency, and portability of physical activity. In addition, a smear taken after treatment showed the absence of fungal cells.

This study aimed to study the prevalence of candidiasis in patients using removable dentures and to evaluate the effectiveness and prevention of candidiasis treatment.

2. MATERIALS AND METHODS

2.1 Materials

It was observed 100 patients that came from a private clinic for 90 days, with oral candidiasis of various age groups from 45 to 65 years. Of these, 60 patients with removable plate prostheses; 40 patients with partially removable prostheses. Chronic forms of candidiasis were diagnosed in 40 patients and exacerbated chronic forms of candidiasis-60 people.

2.2 Methods

At the stage of clinical examination, all patients had their life history and diseases analyzed by examining the oral cavity of the patients. To identify carious cavities, general (examination, probing) and additional (X-ray, radiology) methods were used, and the localization of carious cavities, fillings, and extracted teeth was recorded. We paid attention to the nature of the existing injuries during a visual examination of the oral mucosa. To indicate changes in the mucous membrane color, moisture content, the severity of the vascular pattern, the presence of pathological elements, including primary and secondary, signs of keratinization and inflammation. The intensity of dental caries damage was determined by calculating the DMF indices. The hygienic condition of the oral cavity was assessed by the Green-Vermillion index (1964). The prevalence of gum inflammation was determined using the PMA index in the Parma modification (1976), which is indicated in % and bleeding according to the Muleman method (1971).

The diagnosis of oral mucosal candidiasis is detected and confirmed based on clinical and laboratory signs.

The criterion for the diagnosis of oral candidiasis was the detection of 10–15 or more

yeast cells insight.

2.2.1 Laboratory research

All patients with oral candidiasis underwent the following laboratory tests:

Microscopy of the direst smear from the mucous membrane of the oral cavity to confirm the diagnosis of oral candidiasis. Yeast cells of a round or oval shape with characteristic daughter budding cells, as well as the accumulation of long filaments of the pseudomycelium, allow making a preliminary diagnosis (Araviyski R.A., Gorshkova G.A., 1995).

Cultural diagnostics of scraping from the affected areas of the oral mucosa to identify the pathogen and determine the sensitivity to antifungal preparations were carried out on the micro panel "Fungi test", USA. The serial microdilution method investigated yeast sensitivity to amphotericin B, ketoconazole, itraconazole, and fluconazole, nystatin clotrimazole in two concentrations (maximum and minimum), which allowed us to differentiate the fungi according to their sensitivity.

Assessment of parameters of local immunity of the oral cavity - secretory immunoglobulins (A, G).

2.2.2. Candida Antibodies Blood Test, IgA, IgG

The Candida antibody test is used to detect systemic candidiasis by looking for the antibodies that form the immunity to Candida, in this research, it was monitored IgG and IgA. The test recognizes when levels of these antibodies are particularly high, signaling an overgrowth of Candida.

To perform the test, 10 ml of blood samples were collected by venipuncture from the patients (Fang-Qiu Li *et al. I, 2013;* Yanming Meng *et al. I*, 2020).

The IgA test was performed in 50 patients following the instructions of the manufacture (DRG, 2021).

The IgG test was performed on 50 patients following the instructions of the manufacture (Day, 2021).

The control group was composed of 30 patients, and it provided the baseline of comparison to the infected patients. The statistical analysis was done using Student's T-test (Fang-qiu Li *et al., 2013;* Yanming Meng *et al. I*, 2020).

3 RESULTS AND DISCUSSIONS

3.1 Results

The diagnosis of chronic atrophic candidiasis was made in 26 patients (26 %). Exacerbation of chronic atrophic candidiasis was diagnosed in 43 patients (43 %). The diagnosis of chronic hyperplastic candidiasis of the oral cavity was made to 13 (13 %) patients; 17 (13.3 %) patients who applied were diagnosed with exacerbation of chronic hyperplastic candidiasis. Pseudomembranous candidiasis of the oral cavity was diagnosed in 1 (1 %) patients.

The severity of candidiasis depends on the degree and duration of wearing dentures and hygienic conditions - the most severe forms of invasive candidiasis were observed in the presence of removable plate prostheses, the complete absence of teeth, and the use of a prosthesis for more than 10-15 years.

It should be noted that the combined lesion of the oral mucosa and the red border of the lips was observed mainly in patients older than 60 years.

The number of untreated carious cavities and poor hygienic condition of the oral cavity directly affects the severity of candidiasis. Acute forms of candidiasis were observed mainly in patients with high DMF and PMA indices.

As a result of the conducted enzyme immunoassay of the blood of patients with chronic forms of candidiasis, 80.5 % of patients have an increased content of immunoglobulins A, G in the blood serum, 9.4 % - a reduced content of immunoglobulins A and G, 7.7 % - a negative value of immunoglobulins A and G, 11.2 % - the content of immunoglobulins corresponded to normal values. In the examined patients with exacerbations of chronic forms of candidiasis, the results were obtained: 13.8 % - a reduced content of immunoglobulins A, G in the blood serum, 84.2 % - an increased content of immunoglobulins A and G, 8.6 % - the content of immunoglobulins corresponded to normal values. Most of the treated patients diagnosed with chronic oral candidiasis have an increased content of immunoglobulin G (Table 2).

3.2 Discussions

All patients with various forms of candidiasis of the oral mucosa are recommended to carry out the following treatment and follow the recommendations.

It was necessary to correct the pathological

processes of the mucous membrane of the prosthetic impression area in the shortest possible time, detected at various stages of orthopedic treatment by applying physiotherapeutic methods (laser therapy, ozone therapy), and presented in Table 1.

To accelerate the regeneration of the prosthetic impression area tissues, the use of antioxidant and epithelial agents (TYCVEOLUM, thymol mixture with milk thistle oil, wikasol) was recommended; with long-term non-healing lesions, the use of plasma therapy (plasma lifting), immune correction (galavit, gepon) ware recommended.

To stimulate the adaptation processes of prosthetic impression area tissues, it was necessary to consider the general self-health of the patient and the emotional attitude in complex dental treatment so that visits to the dentist are not perceived by stress, "hellish pain," or aversion.

Oral hygiene using soda rinses and toothpaste containing bicarbonate (blend-a-honey bicarbonate) or active oxygen (oxidizing).

The hygienic condition of removable laminar dentures is achieved by daily cleaning the denture with a gel paste and using tablets for cleaning. Professional cleaning of removable dentures should use a special device in the clinic of the type "Microcline" (if necessary, every two weeks).

Modify the diet of the patients to a limited intake of flour products from white flour, starchy foods, sweets, and fizzy drinks.

4. CONCLUSIONS

1. Removable plate prostheses have a negative effect on the oral mucosa, cause a decrease in its protective properties, which contributes to an increase in the intensity of candidiasis: 60% of patients with removable plate prostheses in the oral cavity had the maximum intensity of candidiasis.
2. The presence of candidiasis in the oral cavity in patients with removable plate prostheses leads to a statistically significant change in the indicators of local immunity of the oral cavity: an increase in the concentration of serum IgG and IgA and the values of the coefficient of balance of local immunity factors.
3. The quality of orthopedic treatment of patients with partial and complete edentulous and quality of removable dentures depends on many factors, as follows: tissue conditions of the prosthetic impression area; level of health (psycho-emotional disorders, pathology of internal organs and systems); design features of a removable denture;- materials used; side effects of the prosthesis on the tissue of the prosthetic impression area; oral hygiene of the patient and dentures; aesthetic effect.

5. DECLARATIONS

5.1. Study Limitations

No limitations were known at the time of the study.

5.2. Acknowledgements

This work was completed at Sechenov University and supported by the “Russian Strategic Academic Leadership Program”.

5.3. Funding source

The authors funded this research.

5.4. Competing Interests

There is no conflict of interest in this study.

6. HUMAN AND ANIMAL-RELATED STUDIES

6.1. Ethical Approval

The study conforms to strobe guidelines. All procedures performed in studies involving human participants were in accordance with the ethical standards of the Sechenov University ethics committee (protocol № 10-16) and with the 1964 Helsinki declaration and its later amendments.

6.2. Informed Consent

All human subjects' rights have been protected by the Sechenov University ethics committee and written informed consent was obtained from all subjects who participated in the study.

6. REFERENCES

1. Evstratenko, V., Sevbitov, A., Platonova, V., Selifanova, E., Dorofeev, A. The characteristics of crystallization of mixed saliva in patients using heroin and methadone. *Klin. Lab. Diagn*, **2018**, *63(4)*, 223.
2. Mazzeo, M., Linares, J., López, M. Analysis of saliva samples from oncological patients treated with 5-fluorouracil and leucovorin calcium by scanning electron microscopy with energy dispersive system. *J. Oral Pathol. Med*, **2013**, *42(10)*, 788.
3. Silva, P., Santos, B., Soares, G. Anti-Candida albicans activity of the association of citronelal with anfotericin B or with cetoconazole. *Periodico Tche Química*, **2019**, *16(31)*, 223.
4. Dukić, W., Dobrijević, T., Katunarić, M. Caries prevalence in chronic alcoholics and the relationship to salivary flow rate and pH. *Cent. Eur. J. Public Health*, **2013**, *21(1)*, 43.
5. Vehkalahti, M., Nikula-Sarakorpi, E., Paunio, I. Evaluation of salivary tests and dental status in the prediction of caries increment in caries-susceptible teenagers. *Caries Res*, **1996**, *30(1)*, 22.
6. Girardin, F., Hearmon, N., Negro, F. Increasing hepatitis C virus screening in people who inject drugs in Switzerland using rapid antibody saliva and dried blood spot testing: A cost-effectiveness analysis. *J. Viral Hepat*, **2019**, *26(2)*, 236.
7. Kolodkina, V., Arutyunov, A., Sirak, S., Andriutsa, N., Tsymbalov, O. Cytological characteristics of oral cavity tissues of experimental animals when using photo polymeric material. *Med. News North Cauc,* **2018**, *13(4)*, 637.
8. Gozha, L., Talalai, T., Arunov, T. Functional disorders of saliva in toxic-chemical stomatitis caused by metal prostheses. Dentistry for all, **2010**, 3, 53.
9. Zholudev, S., Zhmakin, I. Treatment and prevention of prosthetic stomatitis in persons older than 55 years, that use removable plate prostheses. *Dentist*, **2004**, *9*, 21.
10. Zholudev, S. Ways to improve the adaptation in people with problems of tolerability of removable denture materials. *Maes. Dent*, **2005**, *19*, 5.
11. Kasatkina, E. Iodine deficiency diseases in children and adolescents. *Eligible Doctor*, **2010**, *10*, 14.
12. Kalyvradzhiyan, E., Podoprigora, A., Komarova, Yu. Clinical and experimental substantiation of the use of modified adhesive composition based on polysaccharides to improve the period of adaptation to removable denture plate prosthesis. *Modern Orthop. Dentistry*, **2010**, *13*, 31.
13. Lepilin, A., Rubin, V., Proshin, N. The effect of removable plate prostheses made of acrylic plastics on the structural and functional properties of the cellular membranes of the oral mucosa. Stomatology, **2003**, *1*, 51.
14. Nartikova, V., Oglobina, O. Modern methods in biochemistry, M. **1977**.
15. Paschina, T., Egorova, G. Modern methods in biochemistry, M. **1968**.
16. Kuznetsova, M., Nevdakh, A., Platonova, V., Sevbitov, A., Dorofeev, A. Evaluation of effectiveness of a preparation on the basis of phytoecdysteroids for treatment of traumatic injuries of oral mucosa in orthodontic patients. *Int. J. Green Pharm*, **2018**, *12(S1)*, 297.
17. Mamedov, A., Morozova, N., Yumashev, A., Dybov, A., Nikolenko, D. Criteria for provisional restorations used in preparation for comprehensive orthodontic and orthopedic rehabilitation. *Periodico Tche Quimica*, **2019**, *16(32)*, 647.
18. Yumashev, A., Semenycheva, I., Rakhadilov, B. Development of biocompatible coatings for dental implants based on transition metal nitrides. *J. Global Pharma Technol*, **2019**, *11(5)*, 22.
19. Yumashev, A., Koneva, E., Borodina, M.

Electronic apps in assessing risk and monitoring of patients with arterial hypertension. *Prensa Medica Argentina*, **2019**, *105(4)*, 235.
20. Saxena, N., Habelitz, S., Marshall, G. Remineralization of demineralized dentin using a dual analog system. *Orthodon. Craniofac. Res*, **2019**, *22(S1)*, 76.
21. Rech-Ortega, C., Fernández-Estevan, L., Solá-Ruíz, M. Comparative in vitro study of the accuracy of impression techniques for dental implants: Direct technique with an elastomeric impression material versus intraoral scanner. *Med. Oral Patol. Oral Cir. Bucal*, **2019**, *24(1)*, 89.
22. Utyuzh, A., Nikolenko, D., Yumashev, A., Volchkova, I., Samusenkov, V. Adhesion of periodontal pathogens to materials used for long-term temporary crowns. *Periodico Tche Quimica*, **2019**, *16(33)*, 60.
23. Sevbitov, A., Kuznetsova, M., Dorofeev, A., Borisov, V., Mironov, S., Iusupova, I. Dental anomalies in people living in radionuclide-contaminated regions. *J. Environ. Radioact*, **2020**, *216*, 106190.
24. Sevbitov, A., Dorofeev, A., Kuznetsova, M., Timoshin, A., Ershov, K. Comparative characteristics of the crystallogram of the oral fluid in patients who use heroin and methadone. *Periodico Tche Quimica*, **2019**, *16(33)*, 94.
25. Sevbitov, A., Timoshin, A., Dorofeev, A., Davidyants, A., Ershov, K., Kuznetsova, M. Comparative characteristics of the state of hard dental tissues in drug-dependent patients who use heroin, and methadone as replacement therapy. *Periodico Tche Quimica*, **2020**, *17(34)*, 135.
26. Turgaeva, A., Kashirskaya, L., Zurnadzhyants, Yu., Latysheva, O., Pustokhina, I., Sevbitov, A. Assessment of the financial security of insurance companies in the organization of internal control. *Ent. Sust Issues*, **2020**, *7(3)*, 2243.
27. Sevbitov, A. Dental characteristics of clinical manifestations of delayed effects of radiation exposure. Abstract of the dissertation for the degree of doctor of medicine. *Central research Institute of dentistry of the Ministry of health of the Russian Federation*. Moscow, **2005**.
28. Fang-qiu Li, Chun-fang Ma, Li-ning Shi, Jing-fen Lu, Ying Wang, Mei Huang, Qian-qian Kong. Diagnostic value of immunoglobulin G antibodies against Candida enolase and fructose-bisphosphate aldolase for candidemia. *BMC Infect Dis*, **2013**, 13, 253.
29. Yanming Meng, Mei Kang, Dongdong Li, Tingting Wang, Ziwei Kuang, Ying Ma. Performance of a new Candida anti-mannan IgM and IgG assays in the diagnosis of candidemia. *Rev Inst Med Trop São Paulo*, **2020**, 62, e25.
30. *DRG - Candida Albicans IgA (EIA-3457)*. (n.d.). Retrieved November 29, 2021, from https://www.sceti.co.jp/images/psearch/pdf/DRG_EIA3415_p.pdf.
31. Day, Michael. Candida albicans IgG ELISA Kit. Quantitative assay for Candida albicans IgG. (n.d.). Retrieved November 29, 2021, from https://www.omegadx.com/Portals/0/CNS022%20Candida%20IgG%20IFU.pdf

Figure 1. *Patient with removable dentures*

Figure 2. *Lesion of the hard palate mucosa during adaptation to removable prostheses*

Figure 3. *Removable upper jaw plate prosthesis*

Figure 4. *Poor hygienic condition of the prosthesis*

Figure 5. *Acute pseudomembranous candidiasis*

Figure 6. *Acute atrophic candidiasis*

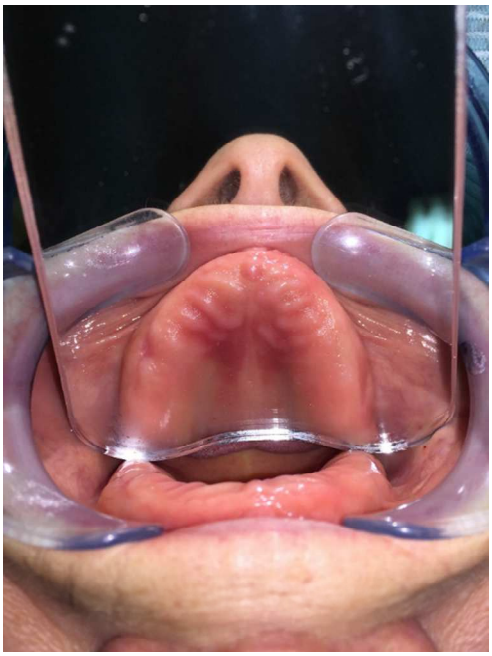

Figure 7. *Chronic hyperplastic candidiasis*

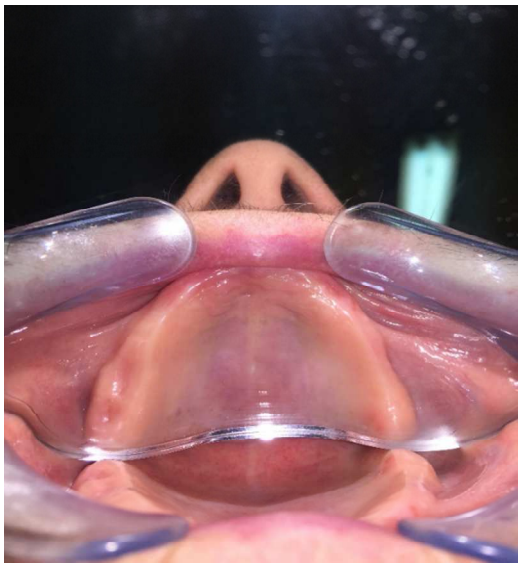

Figure 8. *Chronic atrophic candidiasis*

Figure 9. *Candida angular cheilitis*

Figure 10. *Patient N, 62 years old, Candidomycosis of the oral mucosa*

Table 1. *Characteristics of anti-Candida drugs*

Medicines	Form and dosage	Comments
Clotrimazole	Tablets.10mg 5 p / day. Up to 14 days *	Dissolve slowly and completely.
Nystatin	Suspension. 5ML (500 000U) 4 times / day for up to 14 days * OR Pills. 200,000 Units 5p / day. Up to 14 days *	Put in mouth and hold in mouth for as long as possible, then swallow. OR Dissolve in the mouth slowly and completely.
Amphotericin B	Suspension. 1ML (100mg) 4 times / day. Up to 14 days *	Place directly on the tongue. Distribute by mouth and swallow.
Fluconazole	Tablets.100 MG / day up to 14 days *	C.glrabrola and C.Krusei are usually resistant.
Ketoconazole	Pills. 200MG / day Up to 14 days *	It is necessary to take an acidic medium with orange juice on an empty stomach for absorption.

* Patients with immunosuppressive conditions may require longer therapy.

Treatment should be continued for another 48 hours after resolving clinical symptoms.

Table 2. *Results of the IgG and IgA Candida Antibodies Blood Test*

Diagnosis	% of patients have an increased content of IgA and G	% of patients have a reduced content of IgA and G	% of patients have a negative value of IgA and G	% of patients have the content of IgA and G corresponded to normal values
Chronic forms of candidiasis	80.5	9.4	7.7	11.2
Exacerbations of chronic forms of candidiasis	84.2	13.8	-	8.6

PREPARATION OF MANUSCRIPTS

Please, observe the following points in preparing manuscripts. Papers not conforming strictly to these instructions may be returned to their authors for appropriate revision or delayed in the review process.

Readability: Manuscripts should be written in clear, concise, and grammatically correct English (American English throughout). The editors cannot undertake wholesale revisions of poorly written papers. Every paper must be free of unnecessary jargon and clearly readable by any related field specialist. The abstract should be written in an explanatory style that will be comprehensible also to readers who are not experts in the subject matter.

General format: The complete paper must be written preferably in an MS-Word (Ms-Word 2003 or MSWord 2007) or in a Libre.Office (.odt) compatible file. Page size: as in the template, line spacing: single, font type: Arial. Please leave headers and footers unchanged since the editors should fill it. Please check guidelines for accurate information based on all different categories (review articles, technical notes) available. A single file of the whole manuscript should then be submitted through SBJChem's e-mail. The Journal no longer accepts submissions in any other form.

The order of the material should be as follows: Title, Author(s), Abstract, Keywords, Main text (Introduction, Review of Literature, Definitions (if any), Materials and Methods, Results, Discussion), Acknowledgements (if any), References, Appendix (if any). This structure of the main text is not obligatory, but the paper must be logically presented. Footnotes should be avoided. The main text must be written with font size 11, justify. Within each main section, three levels of subheadings are available, and the titles must be bold, bold and italic, italic respectively.

The manuscript should contain the whole text, figures, tables, and explanations according to the following (we suggest using the template file):

The first page of the material should be as follows:

Title: Should be brief and informative. The title should reflect the most important aspects of the article in a preferably concise form of not more than 100 characters and spaces. Font size 12, capital letters, center alignment.

By-line: Names (size 12, small capital) of the authors. No inclusion of scientific titles is necessary. In case of two or more authors, place their names in the same row, separate them with a semicolon (;) and please indicate the corresponding author with * in superscript. The corresponding author should be the one submitting the article online and an e-mail given (only one e-mail) below the addresses of all authors. Authors from different institutions must be labeled with numbers in superscript after the names. Addresses of the authors, phone and fax numbers should also be given (size 10). Authors should be grouped by address.

Abstract: The Journal uses a structured abstract format, composed of the sections: background, aim, materials and methods, results and discussions, and conclusions. Required for all manuscripts in which the problem, the principal results, and conclusions are summarized. The abstract must be self-explanatory, preferably typed in one paragraph, and limited to max. 300 words. It should not contain formulas, references, or abbreviations. The word ABSTRACT should be written in capital letters, Arial, size 12, bold, left alignment. The abstract should be written font Arial, size 10, justify.

Keywords: Keywords should not exceed five, not including items appearing in the title. The keywords should be supplied, indicating the scope of the paper. Size 10, italic, justify, only the word Keywords must be bold, left alignment.

Authors should include Abbreviations and Nomenclature listings when necessary.

The main text part of the material should be as follows:

The words Introduction, Materials and Methods, Results and Discussion, Conclusion, Disclosures, and References must be written in capital letters, Arial, font size 12, left alignment, bold.

Introduction: The introduction must clearly state the problem, the reason for doing the work, the hypotheses or theoretical predictions under consideration, and the essential background. It should not contain equations or mathematical notation. A brief survey of the relevant literature so that a non-specialist reader could understand the significance of the presented results.

Materials and Methods: Provide sufficient details to permit the repetition of the experimental work. The

technical description of methods should be given when such methods are new.

Results and Discussion: Results should be presented concisely. Also, point out the significance of the results and place the results in the context of other work and theoretical background.

Conclusion: Summarize the data discussed in the Results and Discussion showing the relevance of the work and how different it is from other researches. Also, point out the benefits and improvements that can be observed to develop new science standards that can change something in the related field.

Acknowledgments: (if any) These should be placed in a separate paragraph at the end of the text, immediately before the list of references. It may include funding information too.

References: In the text, references should be cited in the Harvard style (Author, year). Alternatively, the author's surname may be integrated into the text, followed by the year of publication in parentheses. Cite only essential resources, avoid citing unpublished material. References to papers "in the press" must mean that the article has been accepted for publication at the end of the paper list references alphabetically by the last name of the first author. Please, list only those references cited in the text and prepare this list as an automatically numbered list. The word References with size 12, bold, capital letters, left alignment. Guidelines for References

Journals

Journal abbreviations should be used, as defined by the Chemical Abstracts Service Source Index (see http://www.cas.org/sent.html). If the official short form can not be determined and it is not apparent how to abbreviate the title, the full journal title should be given.

1. Varma, R. S.; Singh, A. P.; J. Indian Chem. Soc., 1990, 67, 518.

If the Journal cannot be easily accessed, its Chemical Abstracts number should be given, as follows:

2. Provstyanoi, M. V.; Logachev, E. V.; Kochergin, P. M.; Beilis, Y. I.; Izv. Vyssh. Uchebn. Zadev.; Khim. Khim.Tekhnol. 1976, 19, 708. (CA 85:78051s).

If the article has a DOI number, but its complete reference is not given, the DOI number should be cited as follows:

3. Vidotti, M.; Silva, M. R.; Salvador, R. P.; de Torresi, S. I. C.; Dall'Antonia, L. H.; Electrochimica Acta (2007),doi:10.1016/j.electacta.2007.11.029.

It is recommended to give composite references instead of a list of separate references. The style of composite references is as follows:

4. Varela, H.; Torresi, R. M.; J. Electrochem. Soc. 2000, 147, 665; Lemos, T. L. G.; Andrade, C. H. S.; Guimarães,A. M.; Wolter-Filho, W.; Braz-Filho, R.; J. Braz. Chem. Soc., 1996, 7, 123; Ângelo, A. C. D.; de Souza, A.; Morgon,

N. H.; Sambrano, J. R.; Quim. Nova 2001, 24, 473.

Patents

Patents should be identified as follows (if possible, the Chemical Abstracts number should be given in parentheses):

5. Hashiba, I.; Ando, Y.; Kawakami, I.; Sakota, R.; Nagano, K.; Mori, T.; Jpn. Kokai Tokkyo Koho 79 73,771 1979.

(CA 91:P193174v)

6. Kadin, S.B.; US Pat. 4,730,004 1988. (CA 110:P23729y)

7. Eberlin, M. N.; Mendes, M. A.; Sparrapan, R.; Kotiaho, T. Br PI 9.604.468-3, 1999.

Books

With editors

8. Regitz, M. Multiple Bonds and Low Coordination in Phosphorus Chemistry; Regitz, M.; Scherer, O. J., eds.;Georg Thieme Verlag: Stuttgart, 1990, cap. 2.

Without editors

9. Cotton, F. A.: Wilkinson, G.; Advanced Inorganic Chemistry, 5th ed., Wiley: New York, 1988.

Computer programs (software)

10. Sheldrick, G. M.; SHELXL-93; Program for Crystal Structure Refinement; University of Gottingen, Germany,1993.

Theses

11. Velandia, J. R.; Ph.D. thesis, Federal Rural University of Rio de Janeiro, Brazil, 1997.

Presentations at meetings

12. Ferreira, A. B; Brito, S. L.; Abstracts, 20th Annual Meeting of the Brazilian Chemical Society, Poços de Caldas, Brazil, 1998.

Internet pages

13. http://www.sbq.org.br/jbcs, accessed June 2001. (minimal of information requested)

Authors should follow IUPAC recommendations (for all papers using chemical nomenclature) and use the International System of Units whenever possible.

Figures: The number of figures (including graphs, diagrams) should not exceed 10 and should be submitted either in JPG or PNG formats. All photographs, graphs, and diagrams should be numbered consecutively (e.g., Figure 1) in the order in which they are referred to in the text. The caption must appear below the figure (size 11, bold, italic) and should be sufficiently detailed to enable to understand apart from the text. The lettering and symbols should also be explained in the caption and only exceptionally in the figures. Figures should be of good quality and preferably in black and white. (Color figures will appear in the downloadable files, but all papers will be printed in black and white.) Scanned figures should be at an 800 dpi/bitmap resolution for line graphs. Diagrams containing chemical structures should be of high graphical quality and always be of the same size to be uniformly reduced. Figures should have a maximum width of one Journal column (8.5 cm) to be inserted on the body of the text to be applied to the standards of the Journal. If the figures exceed 8.5 cm, they will be placed at the end of the article. In addition, authors may be requested to submit each figure also as an image file in one of the following formats: jpg or png. For figures, graphs, diagrams, tables identical to material already published in the literature, authors should seek permission for publication from the companies or scientific societies holding the copyrights and send it to the editors of SBJChem along with the final form of the manuscript.

Tables: Tables should be self-explanatory. They should be mentioned in the text, numbered consecutively (e.g., Table 1), and accompanied by a title at the top (size 11, bold, italic). Please insert all the tables in the text, do not enclose huge tables which cannot be fit within the page margins.

Mathematical expressions: In general, minimize unusual typographical requirements, use solidus, built-up fractions. Avoid lengthy equations that will take several lines (possibly by defining terms of the equation in separate displays). Please use the Equation Editor of Word for drawing equations, if possible. Make subscripts and superscripts clear. Display only those mathematical expressions that must be numbered for later reference

Alternatively, that needs to be emphasized. The number displayed equations consecutively throughout the paper. The numbers should be placed in parentheses to the right of the equation, e.g. (Eq. 1).

Supplementary material: Any Supplementary material (extra figures, tables, diagrams) should be placed at the end of the manuscript and indicated as such. A single .pdf-document, including the supplementary material, should be submitted.

Editors may ask authors to split off part of the manuscript at any time of the editing process, presenting it as supplementary material.

References must follow the APA (American Psychological Association) format. So if you use computer software to generate the references, this may be useful to you. The relevant part to us is to ensure that the reader will be able to locate your references if it is necessary.

GUIDELINES FOR PUBLICATION

All guidelines below are focused on Chemistry. However, if the manuscript that will be submitted is focused on another field, the same guidelines should be considered and applied to the subject of interest.

General - Articles suitable for publication in the Southern Brazilian Journal of Chemistry cover the traditional fields of Chemistry, and **interdisciplinary** relations of chemistry with Physics, Mathematics, Biology, Pharmacy, Medicine, Engineering, and Agriculture. Articles on chemical the history of chemistry, science policy, besides articles on related fields, are also accepted as long as they have substantial content that has not been published previously in any other Journal. Articles should conform to one of the categories below:

Original Articles: for communicating original research. Articles should follow the usual form of presentation, including introduction, results, experimental section, as appropriate for the submitted work. They should have a maximum of 20 pages, including figures, tables, diagrams. All pages should be numbered following the template.

Review Articles: for communicating progress in a specific field of chemistry, to provide a critical account of state of the art from the point of view of the highly qualified and experienced specialist. They should have a maximum of 40 pages, including figures, tables, diagrams. All pages should be numbered following the template.

Authors need to have publications in the field reviewed, attesting to their experience and qualification. Before submitting the manuscript, authors should send an e-mail to the editors with an abstract of the review and a letter explaining the relevance of the publication. The material will be examined by the editors and, once approved, and authors will be requested to submit the full manuscript, according to the SBJCHEM guidelines. This manuscript will then be submitted to referees.

Technical Notes: for communicating methods, validation of methods, techniques, equipment, and accessories developed in the author's laboratory or according to the professional experience of the authors in checking some situations at the site. They should have a maximum of 25 pages, including figures, tables, diagrams. All pages should be numbered following the template.

General Subjects: subjects of general interest for chemists, such as science policy, undergraduate and post-graduate programs, history of chemistry. They should have a maximum of 40 pages, including figures, tables, and diagrams. All pages should be numbered following the template.

Interviews: for communicating interviews linked to one of the Southern Brazilian Journal of Chemistry subjects of interest. The interview should have a maximum of 20 questions or 15 pages. The person who will be interviewed does not necessarily need to be a researcher. It may be another person since the subject to be discussed shows relevance in science. All pages should be numbered following the template.

HOW TO SUBMIT A MANUSCRIPT?

This is the only email of the Journal, **southbchem@gmail.com**. Please be advised that the Journal has no representatives, and the authors should only submit manuscripts through this email account. After ensuring you have followed all applicable guidelines to your manuscript, you should send the manuscript file (Microsoft word format - .DOC) along with the cover letter file (editable PDF) to southbchem@gmail.com. The manuscript submission message to the Journal should be as follow:

Dear Editor-in-chief

Southern Brazilian Journal of Chemistry

281/202, Carlos Tarasconi Av.

District: Sagrada Familia.

Postal Code: 95320-000.

Nova Prata - RS. Brazil.

I am sharing a manuscript entitled "TITLE OF THE MANUSCRIPT," which I am submitting for consideration for publication in the Southern Brazilian Journal of Chemistry.

I, [Insert the name of the corresponding author here] (Corresponding author) certify that:

* The manuscript is the original work of all authors.

* All authors made a significant contribution to this study.

* This manuscript has not been submitted for publication and has not been published in any other journal.

* All authors have read and approved the final version of the manuscript.

Thank you for your consideration of my work. Please address all correspondence concerning this manuscript and feel free to correspond with me by email (Corresponding author's email address).

Sincerely,

CORRESPONDING AUTHOR DETAILS

[Add here the name, contact address, contact phone number, email of the corresponding author. The corresponding author must be one of the authors of the manuscript.]

First Name - Middle Name - Surname

Complete Mailing Address

City

State

Country

Postal Code

Contact Phone Number: [Country prefix followed by whole phone number]

Contact Email:

Attachment:

[list of all files attached such as manuscript, cover letter, and any other relevant files as supplementary materials, images, appendix]

On submitting an article, a cover letter is requested in the same email message. In this letter, the emails of all authors and all information regarding the article like the title, name, and address of the authors, must be given. In the case of multiple authors, the corresponding author should be indicated. The corresponding author will be notified of acceptance, rejection, or need for revision.

IMPORTANT INFORMATION:

ALL SUBMISSIONS SHOULD BE MADE THROUGH THE EMAIL (southbchem@gmail.com) of the Journal. This is the only email address applicable to submit a manuscript to this Journal. The Journal does not have or use any other way or electronic system to receive papers;

After the editors have checked the submission, an email will be sent with suitable information;

The reviewing process starts as soon as the Journal receives the paper and sends the author an email confirming the paper and cover letter have been received. The reviewing process may take up to 180 days from the date of receiving the manuscript;

After submitting the manuscript, one of the editors will perform a preliminary review to check some essential topics related to the scope of the Journal, formatting, structure, plagiarism, and so on. If the paper is on the scope, and there are no significant issues, the paper can move forward to the next steps (double-blind peer-review);

Please, before submitting your paper, do not forget to check all relevant information regarding the AIMS and SCOPE and make sure you are submitting to the most suitable Journal;

Please review the Article Processing Charges (APCs);

Make sure your manuscript is accurate and readable;

Asking a colleague who is a native English speaker to review your manuscript for clarity;

If necessary, please hire an Academic and Scientific Proofreading and Editing Services in your country to ensure the meaning and the overall text of your manuscript is clear and with no significant English errors;

Speed of publication: The Southern Brazilian Journal of Chemistry DOES NOT OFFER ANY FAST PUBLICATION SCHEDULE. All papers received by our team will have the same treatment, and the review process will take the standard processing time (up to 180 days from the date of receiving the paper);

Please, check the instructions to the authors. Avoid making incomplete submissions;

Please BE ADVISED THAT THE JOURNAL HAS NO REPRESENTATIVES, and the AUTHORS SHOULD, BY THEMSELVES, SUBMIT MANUSCRIPTS THROUGH THE OFFICIAL email account of the Journal (**southbchem@gmail.com**).